

Synthesis and Structural Investigations of Manganese Carbene Complexes

by

Daniela Ina Bezuidenhout

Submitted in partial fulfilment of the degree

Magister Scientiae

In the Faculty of Natural- and Agricultural Sciences

University of Pretoria
Pretoria

Supervisors: Professor S. Lotz
 Professor P.H. van Rooyen

March 2006

Declaration

I declare that the dissertation, which I hereby submit for the degree Magister Scientiae at the University of Pretoria, is my own work and has not previously been submitted by me for a degree at this or any other tertiary institution.

Results obtained from this study have also been published in:

S. Lotz, M. Landman, D.I. Bezuidenhout, A.J. Olivier, D.C. Liles, P.H. van Rooyen, *Journal of Organometallic Chemistry*, 690, **2005**, 5929-5937.

Signature:

Date:

Acknowledgements

I would like to express my sincere gratitude to the following people and institutions for their individual roles in the completion of this study:

Prof Simon Lotz, my supervisor, for his guidance and support, as well as my co-supervisor, Prof Peet van Rooyen;

Prof Rudi van Eldik for the opportunity to do kinetic research at the Friedrich-Alexander University Erlangen-Nuremberg in Erlangen, Germany;

Mr Eric Palmer for recording of the NMR spectra;

Mr Dave Liles for obtaining the crystal data and some of the crystallographic analyses;

My friends and colleagues, especially Werner Barnard, for their encouragement and camaraderie;

My parents, sister and Sean Kearns for their understanding, support and interest.

The financial assistance of the National Research Foundation (NRF) towards this research is hereby acknowledged. Opinions expressed and conclusions arrived at, are those of the author and are not necessarily to be attributed to the NRF.

Daniela

Table of Contents

Summary	i
List of complexes	iii
List of abbreviations	v
Chapter 1	
Introduction	
1.1 Overview: Carbene Complexes	1
1.2 Schrock Carbene Complexes	2
1.3 Fischer Carbene Complexes	4
1.4 Aim	8
1.5 References	9
Chapter 2	
Dimanganese Monocarbene Complexes	
2.1 Background	11
2.2 Synthesis	16
2.3 Characterization	17
2.4 Conclusions	36
2.5 References	37
Chapter 3	
Cleavage of Metal-Metal Bonds: Monomanganese Monocarbene Complexes	
3.1 Background	40
3.2 Synthesis	45
3.3 Characterization	47
3.4 Conclusions	56

3.5 References	57
----------------	----

Chapter 4 Modification of Carbene Ligands: Aminolysis

4.1 Background	60
4.2 Synthesis	64
4.3 Characterization	65
4.4 Conclusions	88
4.5 References	90

Chapter 5 Kinetic Investigation of Aminolysis Reaction

5.1 Background	92
5.2 Electronic Spectra	95
5.3 Kinetic Investigation	97
5.4 Conclusions	102
5.5 References	104

Chapter 6 Experimental

6.1 Standard operational procedure	106
6.2 Characterization techniques	106
6.3 Preparation of compounds	109
6.4 Analytical Data of Complexes 1 - 15	112
6.5 References	114

Appendices

Appendix 1 Crystallographic data of Complex 2	115
Appendix 2 Crystallographic data of Complex 3	122
Appendix 3 Crystallographic data of Complex 5	128
Appendix 4 Crystallographic data of Complex 7	134

Appendix 5	Crystallographic data of Complex 8	140
Appendix 6	Crystallographic data of Complex 9	146
Appendix 7	Crystallographic data of Complex 11	152

Summary

Synthesis and Structural Investigations of Manganese Carbene Complexes

by

Daniela Ina Bezuidenhout

Supervisor: Prof S Lotz

Co-supervisor: Prof PH van Rooyen

Submitted in partial fulfilment of the requirements for the degree Magister
Scientiae, Department of Chemistry, University of Pretoria

The study involves the synthesis and structural characterization of manganese carbene complexes. The synthesis of dimanganese monocarbene complexes $[\text{Mn}_2(\text{CO})_9\{\text{C}(\text{OEt})(\text{heteroaryl})\}]$ was done via the classical Fischer method, and a range of complexes containing heteroaromatic substituents, e.g. 2,2'-bithiophene, thiophene, furan and N-methyl pyrrole, was isolated. These complexes displayed a novel configuration with the carbene ligand in the axial position, in contrast to the equatorial position found for the analogous rhenium compound and other dimanganese complexes known from the literature.

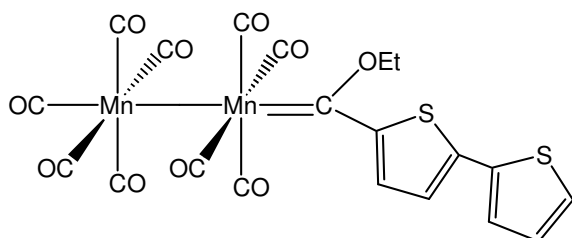
The possibility of manipulating the position of the carbene ligand in the binuclear complexes was investigated by a nucleophilic substitution of the ethoxy substituent with an amine substituent. Only aminolysis with small, primary amines such as ammonia and propylamine, proved successful. The propylaminocarbene ligands retained their axial configuration, but a conversion to the more thermodynamically stable equatorially substituted carbene ligands was observed for the complexes $[\text{Mn}_2(\text{CO})_9\{\text{C}(\text{NH}_2)(\text{heteroaryl})\}]$, while mixtures of the equatorial and axial isomers were observed in solution. Structural X-ray analysis proved that although the equatorial position is more electronically favourable, steric hindrance by the second manganese pentacarbonyl moiety prevented ethoxy- and propylamino-substituted carbene ligands to adopt this configuration. A kinetic study of the

aminolysis reaction was done in an effort to elucidate the reaction mechanism and to explain the axial-equatorial conversion. Due to the competing decomposition reaction of the product and reagent complexes with that of the substitution reaction, no information about reaction intermediates could be obtained.

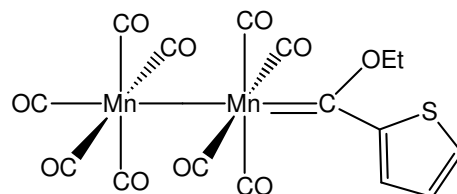
The target mononuclear complexes $[\text{Mn}(\text{CO})_4\{\text{C}(\text{OEt})(\text{heteroaryl})\}\text{X}]$ ($\text{X} = \text{Br}, \text{I}$) was obtained by cleavage of the metal-metal bond of the binuclear precursor complexes. Cleaving of the Mn-Mn bond was done oxidatively by halogens, without affecting the carbene ligand. The product complexes have an assembly resembling that of the Grubbs ruthenium metathesis catalyst. Interestingly, the cleaved complexes were found to have a *cis* configuration of the carbene and halide ligand.

List of Complexes

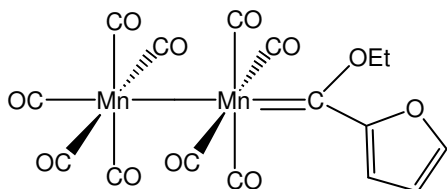
1:



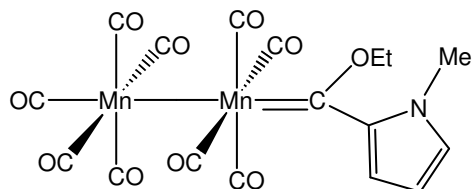
2:



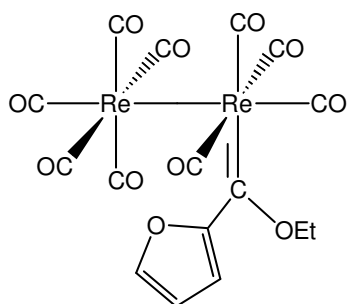
3:



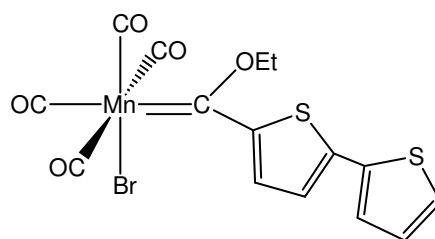
4:



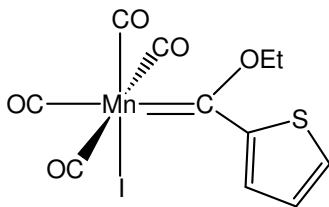
5:



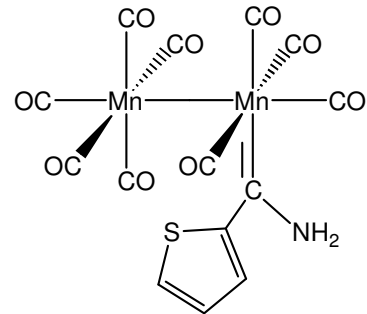
6:



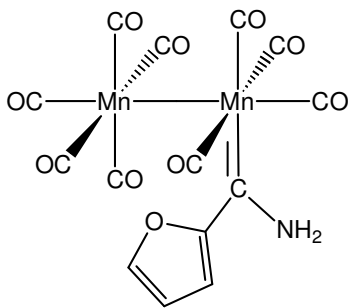
7:



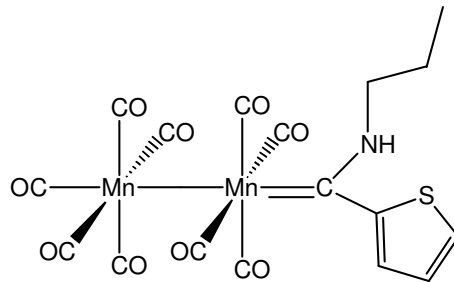
8:



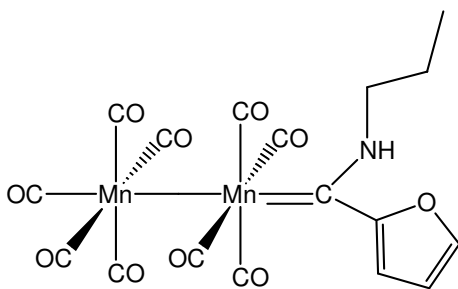
9:



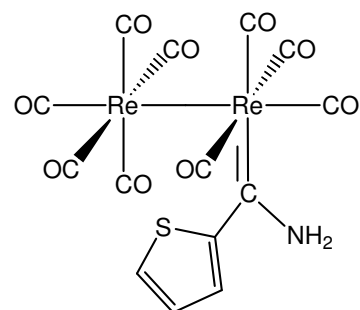
10:



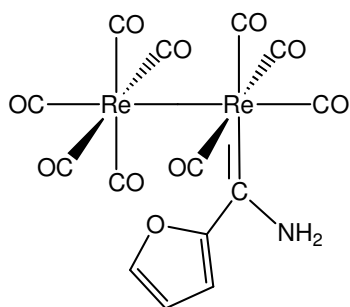
11:



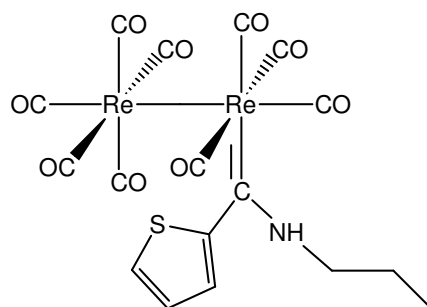
12:



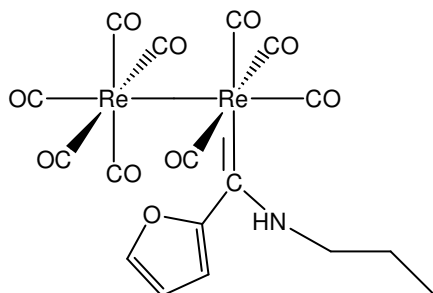
13:



14:



15:



List of Abbreviations

Bu	:	butyl
Cp	:	$\eta^5\text{-C}_5\text{H}_5$
d	:	doublet
DCM	:	dichloromethane
DEE	:	diethyl ether
dd	:	doublet of doublets
ddd	:	doublet of doublets of doublets
Et	:	ethyl
HETCOR	:	Heteronuclear Correlation Spectroscopy
IR	:	Infrared Spectroscopy
<i>J</i>	:	coupling constant
m	:	medium (IR)
Me	:	methyl
MLCT	:	metal-to-ligand charge transfer
NMR	:	Nuclear Magnetic Resonance Spectroscopy
n.o.	:	not observed
Ph	:	Phenyl
R	:	alkyl group
RT	:	room temperature
s	:	singlet (NMR)
s	:	strong (IR)
THF	:	tetrahydrofuran
UV	:	ultraviolet
vs	:	very strong (IR)
vis	:	visible
w	:	weak (IR)
Å	:	angstrom
δ	:	chemical shift
λ	:	wavelength

1 Introduction

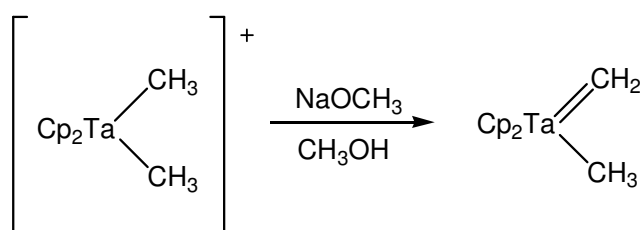
1.1 Overview of carbene complexes

Since the inception of organometallic carbene complexes in the early 1960's, the metal-to-carbon double bond has been extensively studied and numerous examples with different metals and substitution patterns are known. The transition metal carbene complexes are not only chemically versatile^[1;2], but also possess unique physical properties. This is illustrated by the growing search for new materials in nonlinear optics, which stimulated expansive studies of organometallic materials incorporating metal-to-carbon double bonds^[3].

Organometallic carbene complexes as described by Fischer in his Nobel Prize lecture^[4] are highly reactive derivatives of divalent carbon and as such are widely used as organic synthons^[5]. Transition metals stabilize carbenes by coordination yielding two types of complexes with contrasting reactivities, named after their discoverers: the 'Fischer-type' carbenes^[6] where the carbene carbon is electrophilic and the 'Schrock-type' carbene complexes^[7] where the polarity is reversed.

1.2 Schrock carbene complexes

The first nucleophilic carbene complex was prepared by Schrock in an effort to prepare a homoleptic tantalum(V) alkyl^[7]. Schrock carbene complexes are usually characterized by an early transition metal in high oxidation state, with strong donor and weak π -acceptor ligands.



Scheme 1.1 Synthesis of a typical Schrock carbene complex

1.2.1 Theoretical bonding model

The progress in quantum chemical methods for the calculation of electronic structure and theoretical studies gave insight into the nature of the chemical bond in transition metal carbene complexes. Frenking and Frölich^[8] have recently reviewed the state-of-the-art methods of computational chemistry applied to the bonding in transition metal compounds.

Bonding in Schrock complexes are described as a "covalent bond" between a 3B_1 triplet carbene and a triplet metal fragment^[9], implying that the electronic ground state of a carbene ligand can be used to predict binding interactions with a transition metal. Carbene ligands such as methylene and dialkylcarbenes that have a triplet ground state will preferentially form covalent bonds with triplet metal fragments.

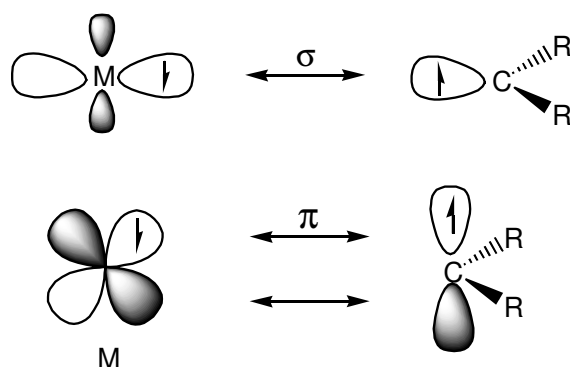


Figure 1.1 Orbital interactions of a Schrock carbene ligand

Besides the neutral resonance form (Figure 1.1) a nucleophilic resonance form $L_nM^+-CR_2^-$ can explain the experimental observations that these compounds react mostly as nucleophiles. A partial negative charge resides on the carbene carbon atom as a result of polarization of shared electrons between an electropositive metal and a more electronegative carbene carbon atom. The carbene ligand is therefore formally considered as an X_2 -type ligand, resulting in electron sharing in a metal-carbon σ - and π -bond.

1.2.2 Applications

Perhaps the most well-known uses of Schrock carbene complexes are their activity in olefin metathesis^[10-12] and their ability to act as substitutes for phosphorous ylides in the Wittig reaction^[13]. Schrock and co-workers developed the popular catalyst, the tungsten and molybdenum alkylidene complexes^[14] while the ruthenium carbene complexes were introduced by Grubbs and co-workers^[15] (Figure 1.2). As a result, Grubbs, Schrock and Chauvin shared the 2005 Nobel Prize in Chemistry, for the "development of the metathesis method in organic synthesis", the citation given by the Royal Swedish Academy of Sciences.

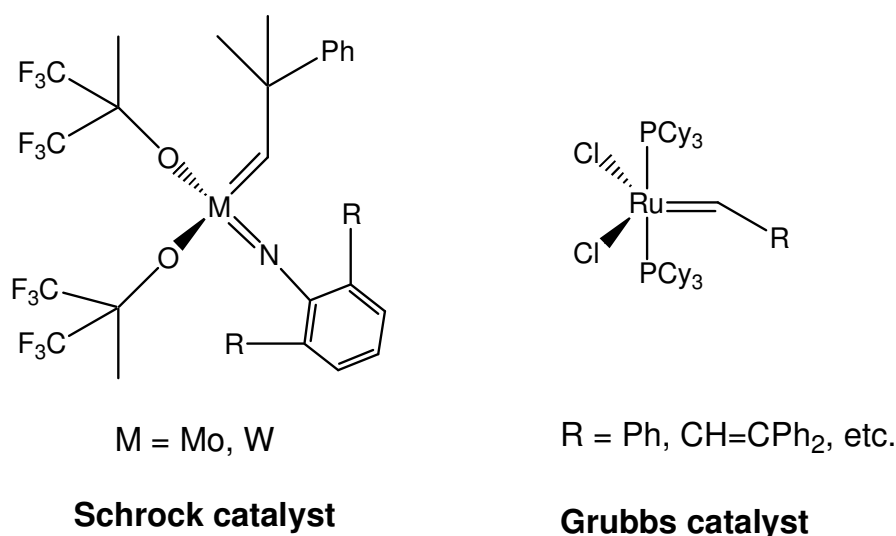
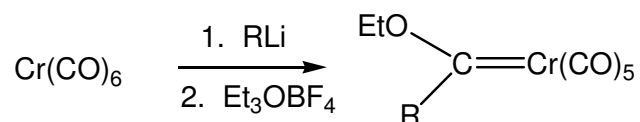


Figure 1.2 Commercially available metathesis catalysts

1.3 Fischer carbene complexes

The first stable transition metal carbene complex was synthesized by Fischer^[6]. Typical Fischer-type carbene complexes contain a low valent Group VI to VIII transition metal stabilized by π -acceptors, and are characterized by an electrophilic carbene carbon atom, the metal-coordinated sp^2 -carbon atom.



Scheme 1.2 Synthesis of a typical Fischer carbene complex

According to Fischer^[16] carbene complexes can be prepared from non-carbene complex precursors and by modification of pre-existing carbene complexes. Carbene complexes that can be obtained from non-carbene (carbonyl, allyl, etc.) complex precursors, can be synthesized from two

different methods: (i) transformation of a non-carbene ligand and (ii) addition of a carbene ligand precursor to a metal complex from pre-existing carbene complexes, of which five reactions are possible. They are (i) the transfer of a carbene ligand from one metal to another, (ii) modification of the carbene ligand, (iii) insertion of an unsaturated organic molecule into the metal carbene bond, (iv) change of the oxidation state of the central metal and (v) modification of the metal-ligand framework.

Due to the ability of Fischer carbene complexes to act as reagents for the synthesis of organic compounds, much interest has been shown in the activity of these carbene complexes. Several review articles and books have addressed this topic^[16-22] which has been explored extensively and applied in various organic syntheses.

1.3.1 Theoretical bonding model

The generally accepted bonding model employs the singlet and triplet states of the fragments CR_2 and L_nM as building blocks for the carbene complexes. For Fischer carbene complexes, the model describes the metal-to-carbon bond in terms of "donor-acceptor interactions" between a (1A_1) singlet carbene and a singlet metal fragment. Carbene ligands with π -donor groups and a singlet ground state will preferentially engage in donor-acceptor interactions with singlet metal fragments^[23]. In particular, dihalocarbenes, which have singlet ground states and large singlet to triplet excitation energies, are considered to be donor-accepting bonding and thus "Fischer type". The resulting electrophilic carbene carbon can be considered as a neutral 2-electron ligand (L-type).

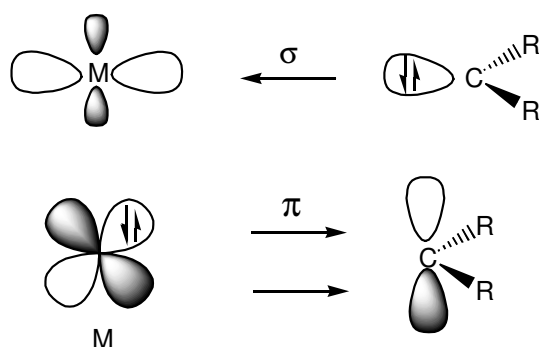


Figure 1.3 Orbital interactions of Fischer type carbene complex ligand

1.3.2 Applications

Many important reactions of Fischer carbene complexes have been recorded, of which nucleophilic attack on the carbene carbon, carbene synthesis and modification of carbene substituents are but a few. The Fischer-type carbene complexes are characterized by an electrophilic carbene carbon atom, the metal-coordinated sp^2 -carbon atom. These carbene complexes can undergo reactions at several sites on the carbene ligand, as outlined in Figure 1.4

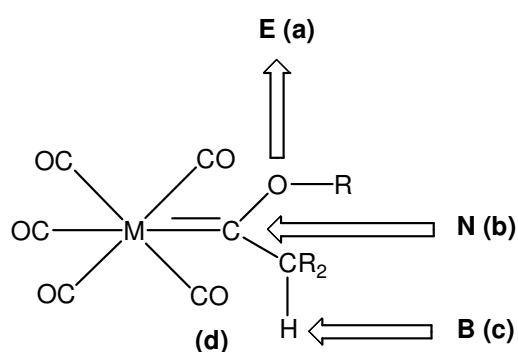


Figure 1.4 Modifications of Fischer carbene complexes

Electrophiles (E), for instance Lewis acids, are coordinated to the alkoxy substituent (route a), leading to the formation of metal-coordinated carbyne complexes. Nucleophilic attack (N) occurs at the electrophilic carbene carbon

atom (route b), e.g. aminolysis. Alkylcarbene complexes are deprotonated by bases (B) to form metal carbene anions (route c), owing to the acidity of the α -CH groups, while carbonyl substitution by other ligands, e.g. phosphine ligands^[24;25], can occur via route d.

Fischer carbene ligands exhibit a wide manifold of reactivity and can be readily modified. A widely applied reaction is the so-called Dötz reaction^[22]. The benzannulation ([3+2+1] carbonylative cycloaddition with alkynes) of alkoxy-carbene complexes with unsaturated substituents (vinyl or aryl) to give cyclohexadienes or phenols, is one of the most unique type of carbene reactions. Chromium complexes are the metal templates of choice, as they allow excellent chemo- and regioselectivity under mild conditions. Benzannulation is an attractive methodology for the synthesis of natural products with hydroquinoid, quinoid or fused phenolic structures.

Other reactions of importance for organic synthesis are [2+2], [3+2] and [4+2] cycloadditions, sigmatropic rearrangements, coupling of anions of the carbene ligand with C-X σ -bonds, coupling of anions of the carbene ligand with C-X π -bonds, Michael additions to α,β -unsaturated carbene complexes and nucleophilic substitutions at and cleavage of the carbene ligand^[26].

The reactions of Fischer carbene complexes are multifaceted and consequently a wide range of products is accessible. One feature often utilised in synthetic strategy is the fact that in these reactions either the metal-carbon bond is retained in the product whilst a ligand is modified or the bond undergoes reaction. Thus, in order to mediate an otherwise difficult transformation, the organic framework is attached to the metal through a carbene carbon, this moiety is modified and then cleaved from the metal to yield the desired product.

1.4 Aim

Carbene chemistry of transition metals such as chromium and tungsten is well developed and can easily be controlled and manipulated^[27], but for transition metals such as manganese and cobalt, discoveries made are still often serendipitous.

The general aim of this project is to investigate aspects of the synthesis, characterization and structural features of Group VII transition metal carbene complexes, specifically manganese, and to a lesser extent, its comparison with the rhenium analogues. The Fischer method will be used to synthesize binuclear ethoxycarbene complexes with a range of heteroaromatic substituents. The structure and properties of such new complexes will address a number of very important aspects in manganese carbene chemistry that will be investigated:

- i) positioning of the carbene ligand with respect to the metal-metal bond,
- ii) the role of the heteroarene ring in stabilizing the carbene ligand of the complex,
- iii) the stability of the metal-metal bond under reaction conditions employing organolithium reagents,
- iv) possible route to the synthesis of mononuclear carbene complexes containing halogen ligands.

The assembly of complexes containing both a carbene and a halide ligand could potentially be used as precursor for carbon-carbon coupling catalysts or templates in organic syntheses, after modification of the carbene ligand. A metal-metal cleaving reaction is to be investigated, where it is planned to use halogens to oxidatively cleave the Mn-Mn bond to yield mononuclear carbene complexes containing a halide ligand.

1.5 References

1. Special edition dedicated to carbene and carbyne complexes and their applications, *J.Organomet.Chem.* 617 - 618, **2001**.
2. Special edition dedicated to carbene complexes and their applications, *Tetrahedron* 56, **2000**, Issue 28.
3. I.R. Whittal, A.M. McDonagh, M.G. Humphrey, M. Samoc, *Adv. Organomet. Chem.* 42, **1998**, 291.
4. E.O. Fischer, *Angew. Chem.* 86, **1974**, 651.
5. J.W. Herndon, *Coord. Chem. Rev.* 206 - 207, **2000**, 237.
6. E.O. Fischer, A. Maasböl, *Angew. Chem. Int. Ed. Engl.* 3, **1964**, 645.
7. R.R. Schrock, *Acc. Chem. Res.* 12, **1979**, 98.
8. G. Frenking, N. Fröhlich, *Chem. Rev.* 100, **2000**, 717.
9. T.R. Cundari, M.S. Gordon, *J. Am. Chem. Soc.* 113, **1991**, 5231.
10. J.S. Murdzek, R.R. Schrock, *Organometallics* 6, **1987**, 1373.
11. R.R. Schrock, S.A. Krouse, K. Knoll, J. Feldman, J.S. Murdzek, D.C. Young, *J. Mol. Catal.* 46, **1988**, 243.
12. A. Furstner, *Angew. Chem. Int. Ed. Engl.* 39, **2000**, 3012.
13. S.H. Pine, G.S. Shen, H. Hoang, *Synthesis* **1991**, 1615.
14. R.R. Schrock, J.S. Murdzek, G.C. Bazan, J. Robbins, M. DiMare, M. O'Regan, *J. Am. Chem. Soc.* 112, **1990**, 3875.
15. R.H. Grubbs, *Tetrahedron* 60, **2004**, 7117.
16. K.H. Dötz, H. Fischer, P. Hofmann, F.R. Kreissl, U. Schubert, K. Weiss, *Transition Metal Carbene Complexes*, VCH Verlag Chemie, Weinheim **1983**.
17. L.S. Hegedus, *Transition Metals in the Synthesis of Complex Organic Molecules*, University Science Books, Mill Valley, California **1994**.
18. W.D. Wulff, *Organometallics* 17, **1998**, 3116.

19. R. Aumann, R. Fröhlich, J. Prigge, O. Meyer, *Organometallics* 18, **1999**, 1369.
20. A. de Meyer, H. Schriver, M. Deutch, *Angew. Chem. Int. Ed. Engl.* **2000**, 3964.
21. J. Barluenga, *Pure Appl. Chem.* 71, **1999**, 1453.
22. K.H. Dötz, P. Tomuschat, *Chem. Soc. Res.* 28, **1999**, 187.
23. A. Marquez, J.F. Sanz, *J. Am. Chem. Soc.* 114, **1992**, 2903.
24. N.J. Coville, A.M. Stolzenberg, E.L. Muetterties, *J. Am. Chem. Soc.* 105, **1983**, 2499.
25. W. Fan, R. Zhang, W.K. Leong, Y.K. Yan, *Inorg. Chim. Acta* 357, **2004**, 2441.
26. W.D. Wulff, *Comprehensive Organic Synthesis*, Trost, Fleming, **1998**, 1065.
27. M.A. Sierra, *Chem. Rev.* 100, **2000**, 3591.

2 Dimanganese Monocarbene Complexes

2.1 Background

2.1.1 Fischer carbene complexes with aromatic substituents

The first reported metal carbene complex $[W(CO)_5C(OMe)Ph]$ prepared by Fischer and Maasböl^[1] contained an aromatic substituent phenyl ring. The structural data of the complexes $[W(CO)_5C(OMe)Ph]$ and $[Cr(CO)_5C(OMe)Ph]$ ^[2] were published shortly thereafter and showed the sp^2 -character of the carbene carbon atom. The role of the heteroatom (X) lone-pair in p_c-p_x π -bonding to stabilize the "singlet" carbene carbon was recognized^[3;4] as well as the transition metals' synergic $d(t_{2g})-p$ π -interaction with the carbene carbon atom.

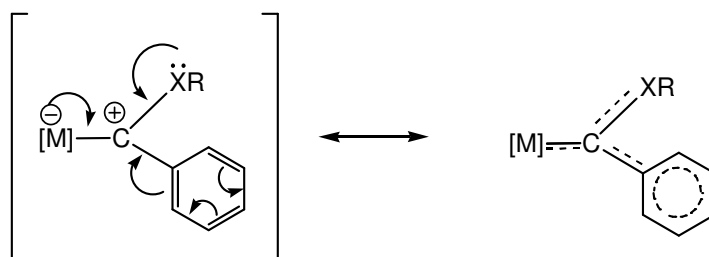


Figure 2.1 π -delocalized network around carbene carbon atom

A phenyl or heteroarene substituent is incorporated into the π -delocalized network surrounding the carbene carbon atom and can act as either an electron withdrawing or electron donating substituent. Casey and Burkhardt^[5] then synthesized the stable $[\text{W}(\text{CO})_5\text{C}(\text{Ph})\text{Ph}]$ carbene complex from $[\text{W}(\text{CO})_5\text{C}(\text{OEt})\text{Ph}]$ where the phenyl substituent donates electron density.

2.1.2 Carbene complexes with heteroaromatic substituents

The first monocarbene complexes of chromium with heteroaromatic substituents were synthesized by Connor and Jones^[6] (Figure 2.2) in order to study the extent to which the heteroatom Y influences the donating of electron-density to the empty carbene carbon p -orbital. It was found that the electron-donation of the heteroaromatic ring increases in the order $\text{Y} = \text{O} < \text{S} < \text{NMe}$. It can be concluded that N-methylpyrrole will stabilize the carbene carbon the most, leading to less back bonding from the metal to the carbene carbon atom.

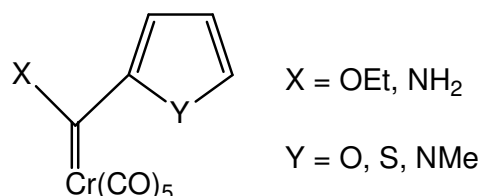


Figure 2.2 Chromium monocarbene complexes with heteroarene substituents

Since these initial discoveries many examples of carbene complexes of arenes and heterocycles have been reported and these compounds have proven to be useful precursors in catalysis^[7]. Monocarbene complexes with 2,2'-bithiophene substituents have also been reported^[8] with the purpose of developing carbene complexes with non-linear optical properties. The general structural motif employing heteroaromatic compounds as conjugated spacer units in mono- and

biscarbene complexes has also been investigated recently in our laboratories^[9-12]. This was done in aid of the design of complexes specifically tailored for electronic transfer processes within the molecule, and to study regioselective reactions.

2.1.3 Binuclear carbene complexes

To determine whether binuclear metal carbonyl complexes can accommodate carbene ligands, Fischer and Offhaus^[13] successfully synthesized the binuclear $[\text{Mn}_2(\text{CO})_9\text{C}(\text{OEt})\text{Ph}]$ and $[\text{Mn}_2(\text{CO})_9\text{C}(\text{OEt})\text{Me}]$ complexes. From the IR spectrum, eight bands were observed for $[\text{Mn}_2(\text{CO})_9\text{C}(\text{OEt})\text{Me}]$, corresponding to the C_s symmetry of an *eq*- $[\text{Mn}_2(\text{CO})_9\text{L}]$ complex. However, for $[\text{Mn}_2(\text{CO})_9\text{C}(\text{OEt})\text{Ph}]$, five ν_{CO} bands, corresponding to C_{4v} symmetry of *ax*- $[\text{Mn}_2(\text{CO})_9\text{L}]$ were seen in the IR spectrum. Shortly after this, Huttner and Regler^[14] reported the crystal structure of $[\text{Mn}_2(\text{CO})_9\text{C}(\text{OEt})\text{Ph}]$, and found the carbene ligand to be in the equatorial position (C_s), and the Et in the *cis* configuration with respect to the C-O bond, in contrast to the *trans* configuration found in the X-ray crystal structure of $[\text{Cr}(\text{CO})_5\{\text{C}(\text{OMe})(\text{Ph})\}]$ ^[14]. This was ascribed to the fact that an equatorially substituted carbene ligand would be too sterically hindered to accommodate the substituents on the carbene ligand in the *trans* configuration, and they explained the appearance of five IR bands instead of eight, as a result of degeneracy and band overlap.

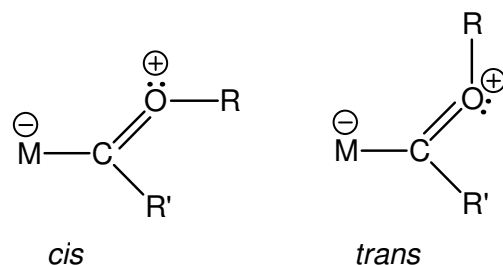
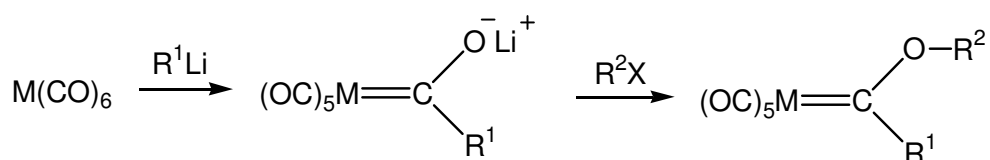


Figure 2.3 *Cis* and *trans* configurations around C-O bond

2.1.4 Preparatory methods

To synthesize alkoxy carbene complexes, the most general route is the addition of an organolithium reagent to a metal carbonyl to give an acyl metallate, which undergoes O-alkylation by strong alkylating reagents such as trialkyloxonium salts, alkyl fluorosulfonates or alkyl trifluoromethanesulfonates. This classical Fischer route^[1] to metal carbene complexes is given in Scheme 2.1. Another widely used alternative approach was developed by Hegedus and Semmelhack^[15;16] (Scheme 2.2) whereby an organoelectrophile is combined with a metal nucleophile.



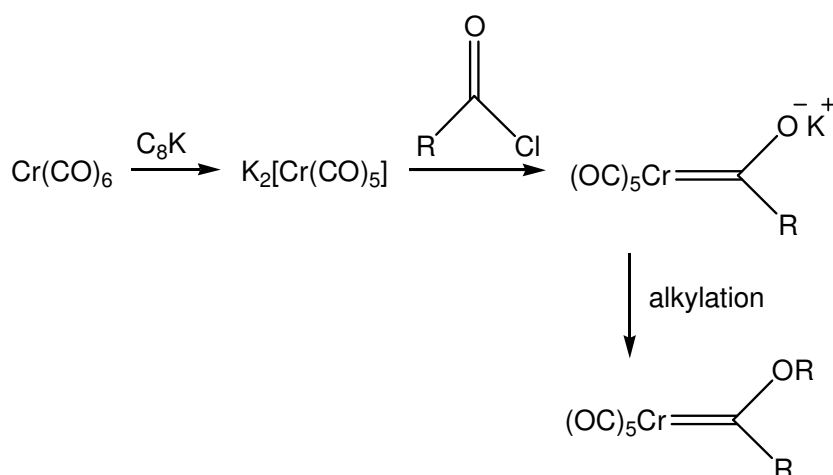
M = Cr, Mo, W

R¹ = alkyl, aryl, vinyl

R²X = R²₃O⁺BF₄⁻, R²OSO₂F

R² = Et, Me

Scheme 2.1 Fischer synthesis of metal carbene complexes



Scheme 2.2 Hegedus-Semmelhack synthesis of alkoxy carbene complexes

C_8K was found to be an efficient reducing agent to convert $Cr(CO)_6$ to $K_2[Cr(CO)_5]$.

For Group VII transition metals, carbene complexes with cyclopentadienyl ligands are readily accessible from $MCp(CO)_3$ and organolithium reagents^[17;18], while binuclear monocarbene complexes can be obtained from $M_2(CO)_{10}$ and organolithium precursors^[13;19;20]. Binuclear monocarbene complexes of manganese were also prepared by the reaction of $Na[Mn(CO)_5]$ and dihaloalkanes or acetyl halides^[21-23], similar to the method employed by Hegedus and Semmelhack (Scheme 2.2).

2.1.5 Focus of this study

The synthesis of novel dinuclear monocarbene complexes of the Group VII transition metal, manganese, containing a range of heteroarene substituents (2,2'-bithiophene, thiophene, furan and N-methylpyrrole) was planned as the first step in this study. The furyl-substituted dirhenium monocarbene was also synthesized in this chapter for comparison with its manganese analogue, to study steric and electronic properties of the carbene ligand in binuclear complexes. Figure 2.4 is a representation of the five complexes synthesized in this chapter.

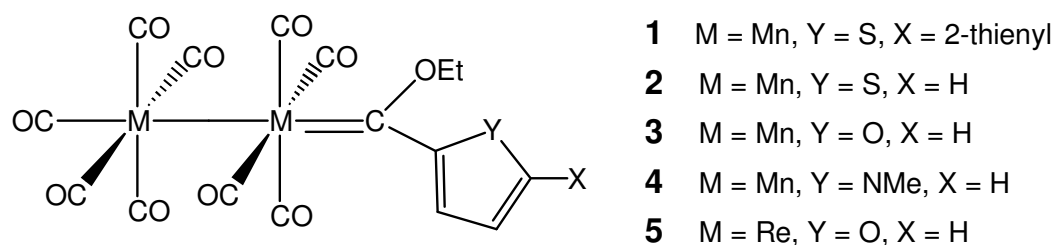
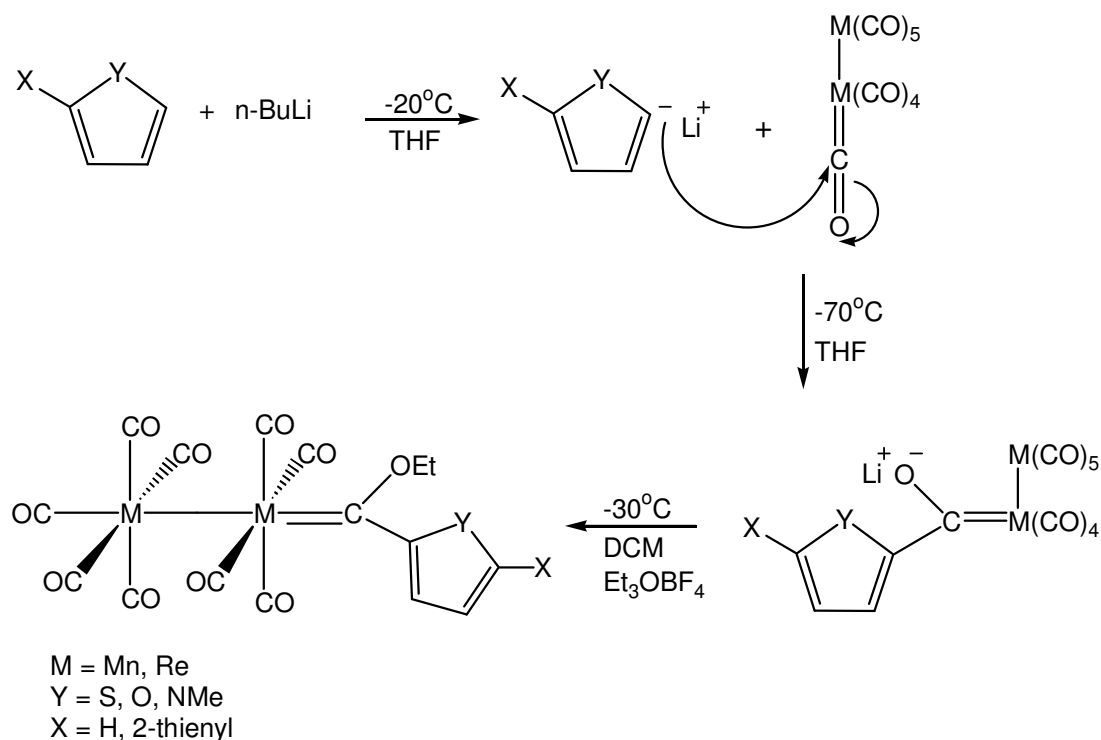


Figure 2.4 Dinuclear monocarbene complexes of manganese and rhenium

2.2 Synthesis

Fischer's classical approach was utilised in the syntheses of the desired binuclear monocarbene complexes $[M_2(CO)_9(\text{carbene})]$ ($M = \text{Mn, Re}$) (Scheme 2.3).



Scheme 2.3 Syntheses of Complexes 1 - 5

Deprotonation of the acidic α -proton of the heteroarenes is accomplished by the use of the strong base $n\text{-BuLi}$ in THF at -20°C . After addition of the bimetallic decacarbonyl to the reaction mixture at -70°C , the resulting nucleophilic α -carbon of the heteroarene ring attacks an electron-deficient carbon of the bimetal decacarbonyl to form a metal acylate. After removing the THF under reduced pressure, the residue is dissolved in dichloromethane. Alkylation is then carried out by adding triethyloxonium salt to the metal acylate at -30°C and purification of the product to remove unreacted metal decacarbonyl is achieved by column chromatography. The desired neutral carbene complexes are formed in yields ranging from 63 - 74%. The monocarbene complexes **2**, **3** and **5** were

crystallized from a hexane:dichloromethane (1:1) solution and afforded orange-red crystals. Complexes **1** and **4** were isolated and characterized spectroscopically, but no high quality crystals could be obtained.

2.3 Characterisation

The binuclear monocarbene complexes **1** - **5** were characterized in solution using NMR and infrared spectroscopy, as well as FAB mass spectrometry and in the solid state by molecular crystal structure determinations.

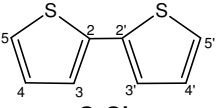
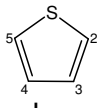
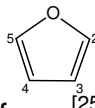
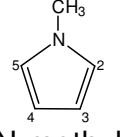
2.3.1 NMR Spectroscopy

2.3.1.1 ¹H NMR Spectroscopy

The chemical shifts in the ¹H NMR spectrum of the uncoordinated heteroarene rings are given in Table 2.1. The assignment of the chemical shifts of the protons of these uncoordinated ligands was based on the assignments made by the references given in the table for each heteroarene.

The NMR spectra of complexes **1**, **4** and **5** were recorded in deuterated chloroform as solvent but spectra of high resolution could only be obtained for complexes **2** and **3** in d₆-acetone. Slow decomposition of products with time was observed in the spectra, and broadening of the signals in the case of the N-methyl pyrrole-substituted carbene complex **4**. Chemical shifts are given in Table 2.2.

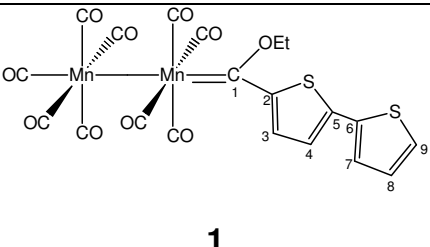
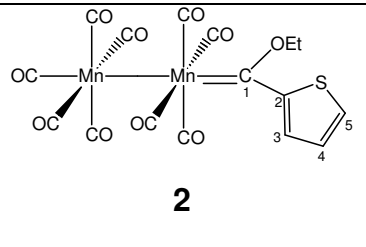
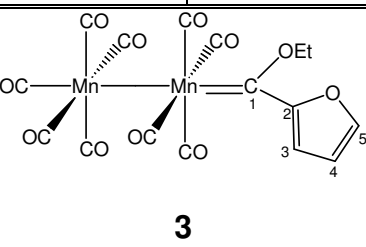
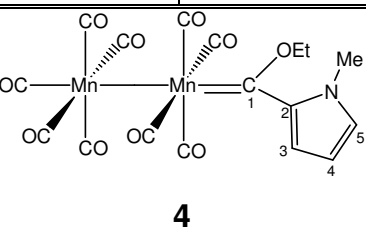
Table 2.1 ^1H NMR data of uncoordinated heteroarenes

Assignment	 2,2'- bithiophene ^[11]	Assignment	 thiophene ^[24]	 furan ^[25]	 N-methyl pyrrole ^[26]
Proton	Chemical shift (δ , ppm)	Proton	Chemical shift (δ , ppm)		
H3, H3'	7.18	H2, H5	7.20	7.38	6.60
H4, H4'	7.02	H3, H4	6.96	6.30	6.13
H5, H5'	7.21	N-CH ₃	-	-	3.66

On comparing the literature chemical shift values of the uncoordinated heteroarenes with the corresponding values of the complexes, it is clear that the coordination to a metal fragment has a marked influence on the chemical shifts of the protons. Upon coordination to the metal, the carbene moiety causes draining of electron density from the double bonds of the heteroarene ring to the electrophilic carbene moiety, resulting in a downfield shift of the protons of the coordinated rings compared to the uncoordinated heteroarenes. Assignments of the ring protons of the 2,2'-bithienyl, thienyl and N-methyl pyrrolyl substituents are based on the assignments made by Gronowitz^[27].

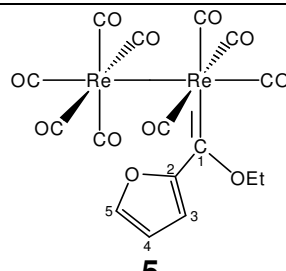
The more downfield shifts of H3 and H5 compared to H4 can be explained by considering the resonance structures of the complexes as shown in Figure 2.5. Deshielding of protons H3 and H5 are effected by the positive charges afforded on these two protons caused by the π -resonance effect. Proton H4 is not affected by the resonance effect and therefore its chemical shift is comparable to that of the free heteroarene.

Table 2.2 ^1H NMR data of complexes **1** - **5**

Assignment	Complexes			
	Chemical shifts (δ , ppm) and coupling constants (J , Hz)			
	 1		 2	
Proton	δ^a	J	δ^b	J
H3	8.33 (d)	4.4	8.35 (dd)	4.1, 0.8
H4	7.61 (d)	4.4	7.42 (dd)	4.9, 4.1
H5	-	-	8.07 (dd)	5.0, 0.8
H7	7.65 (dd)	3.6, 0.8	-	-
H8	7.23 (dd)	5.0, 3.6	-	-
H9	7.76 (dd)	4.1, 0.8	-	-
-OCH ₂ CH ₃	5.31 (q)	7.0	5.32 (q)	7.0
-OCH ₂ CH ₃	1.79 (t)	7.0	1.80 (t)	7.0
Assignment	 3		 4	
Proton	δ^b	J	δ^a	J
H3	7.19 (dd)	3.9, 1.9	7.90	-
H4	6.85 (dd)	3.9, 0.7	6.58	-
H5	7.46 (dd)	3.9, 0.7	7.40	-
-OCH ₂ CH ₃	5.28 (q)	7.0	5.25 (q)	7.0
-OCH ₂ CH ₃	1.76 (t)	7.0	1.81 (t)	7.0
-NCH ₃	-	-	3.93 (s)	-

 a) Spectra recorded in CDCl₃ b) Spectra recorded in acetone-d₆

Table 2.2 contd. ^1H NMR data of complex **5**

Assignment	Complex	
	Chemical shifts (δ , ppm) and coupling constants (J , Hz)	
	 <p style="text-align: center;">5</p>	
Proton	δ^a	J
H3	7.09 (dd)	3.6, 0.8
H4	6.58 (dd)	3.6, 1.8
H5	7.77 (dd)	1.6, 0.8
-OCH ₂ CH ₃	4.58 (q)	7.0
-OCH ₂ CH ₃	1.60 (t)	7.0

a) Spectra recorded in CDCl₃

The atypical assignment of the furyl ring proton chemical shifts of complexes **3** and **5** is based on the assignments made by Crause^[11] for chromium complexes, which agrees well with the predicted shifts for an ester derivative^[25].

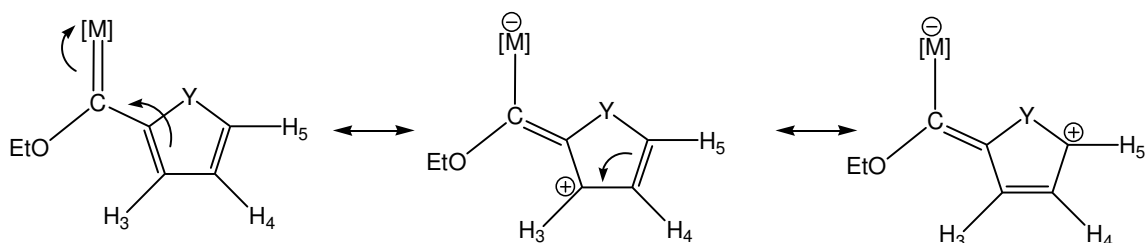


Figure 2.5 π -resonance effect in monocarbene complex

The heteroarene resonances, the methylene quartet and the methyl triplet of the ethoxy group, with relative intensities of 1:2:3, were clearly evident in all spectra (Figure 2.6). The large downfield shift of the methylene protons of the ethoxy-group is consistent with the strong electron withdrawing character of the $M(\text{CO})_5\{\text{C}(\text{C}_4\text{H}_3\text{Y})\}$ ($\text{Y} = \text{S}, \text{O}, \text{N-Me}$) groups, compared to the signal of approximately 3.6 ppm observed for normal $-\text{CH}_2\text{OR}$ protons. The chemical shifts of these methylene protons are characteristic for a specific metal, as shown by the difference in methylene, methyl chemical shifts for complex **3** (5.28 ppm, 1.76 ppm) and complex **5** (4.58 ppm, 1.60 ppm), the 2-furyl substituted dimanganese and dirhenium carbene complexes, respectively, and insensitive to the number and type of carbene substituents (compare complexes **1** - **4**). On the other hand, the number of carbene ligands as well as the nature of the transition metal involved determines the chemical shifts of the ring protons of the heterocycle.

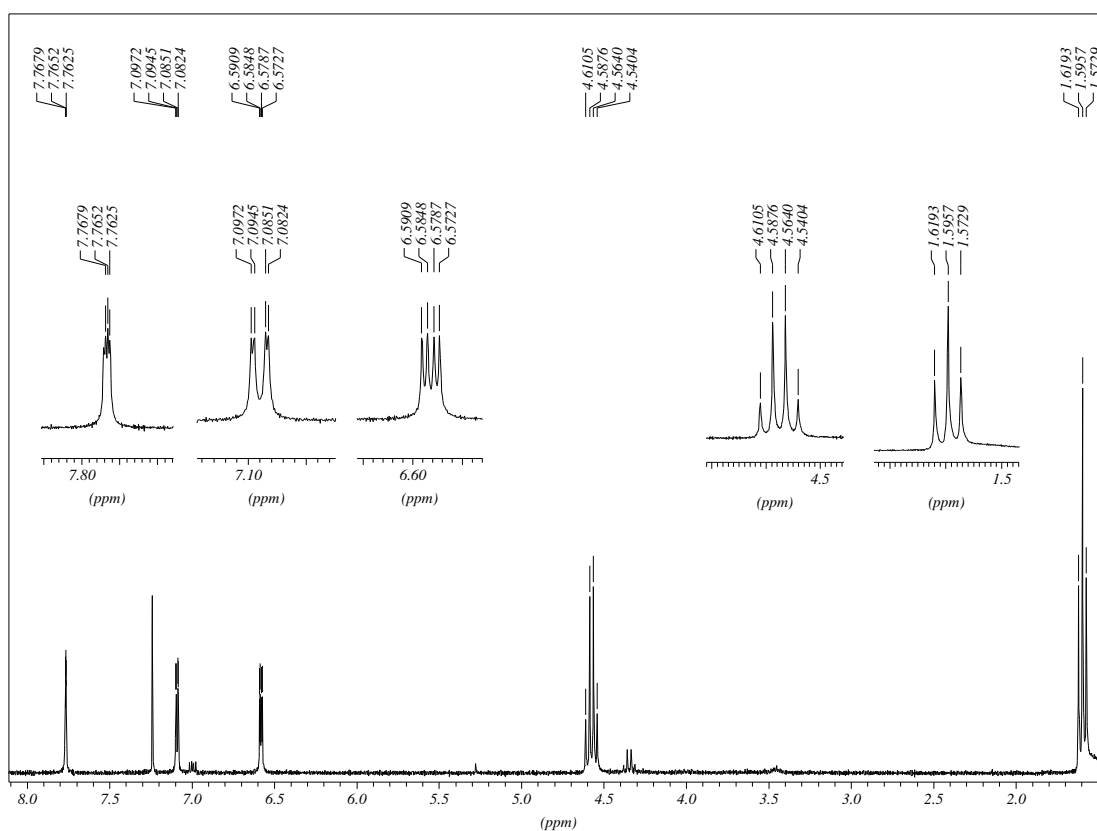
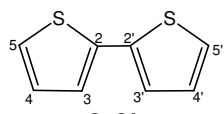
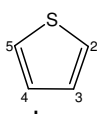
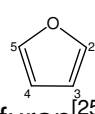
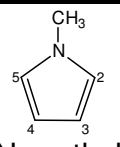


Figure 2.6 ^1H NMR spectrum of complex **5** in CDCl_3 , with expansion of ring and methylene proton signals

2.3.1.2 ^{13}C NMR Spectroscopy

The chemical shifts in the ^{13}C NMR spectra for the free heterocycles are known from literature^[11;24-26] and are given in Table 2.3. The ^{13}C NMR data for the binuclear monocarbene complexes **1** - **3** and **5** are summarized in Table 2.4, although no ^{13}C NMR data could be obtained for **4**, as this complex decomposed during data collection. The chemical shift assignments (C3 - C9) of the 2,2'-bithienyl monocarbene complex are based on the assignments made and corroborated by 2D HETCOR NMR spectra for chromium and tungsten carbene complexes synthesized by Crause^[11].

Table 2.3 ^{13}C NMR data of uncoordinated heteroarenes

Assignment	 2,2'- bithiophene ^[11]	Assignment	 thiophene ^[24]	 furan ^[25]	 N-methyl pyrrole ^[26]
Carbon	Chemical shift (δ , ppm)	Carbon	Chemical shift (δ , ppm)		
C2, C2'	137.4	C2, C5	127.6	143.0	124.3
C3, C3'	123.7	C3, C4	125.8	109.9	111.2
C4, C4'	127.7	N-CH ₃	-	-	38.1
C5, C5'	124.3	-	-	-	-

Fischer carbene carbon atoms are defined as being electron-deficient sp^2 -hybridized carbons stabilized by dative π -bonding from the heteroatom in the alkoxy substituent and from the metal combined with inductive release from the heteroaromatic substituent. Spectroscopic data supports this model as metal carbene carbon shifts can be found very downfield in a broad range of 200^[28] to 400^[29] ppm and the chemical shift of the carbene ligands decrease as a function of the donor properties of the heterocyclic substituent^[6] as follows:

2,2'-bithienyl > 2-thienyl > 2-furyl. This trend was observed on comparing the spectra of complexes **1**, **2** and **3**.

The carbene carbon resonances depend both on the carbene substituents and on the metal, and are more sensitive to changes in the electronic environment than the carbonyl ligands.

Table 2.4 ^{13}C NMR data of complexes **1** - **5** recorded in CDCl_3

Assignment	Complexes			
	1	2	3	5
Carbon*	δ (ppm)	δ (ppm)	δ (ppm)	δ (ppm)
C1	309.9	306.5	301.0	283.2
C2	162.1	155.4	163.9	165.5
C3	140.9	133.9	112.8	114.7
C4	125.3	128.9	110.1	113.9
C5	146.8	138.9	149.5	151.6
C6	134.4	-	-	-
C7	127.8	-	-	-
C8	128.8	-	-	-
C9	126.6	-	-	-
$\text{M}(\text{CO})_4$	222.7	224.6	223.9	193.9
$\text{M}(\text{CO})_5$	211.0, n.o.	221.0, 208.9	219.5, 221.4	190.4, 188.5
$-\text{OCH}_2\text{CH}_3$	74.4	74.6	74.2	77.6
$-\text{OCH}_2\text{CH}_3$	15.5	15.1	15.1	14.7

* See Table 2.2 for numbering of carbons

Chemical shifts for terminal metal carbonyls lie in the range of 150 to 240 ppm^[30] with shielding of the carbonyl nucleus increasing with increasing atomic number of the metal, as shown by the carbonyl resonances of complex **3** (223.9, 221.4 and 219.5 ppm), the manganese analogue of the dirhenium complex **5** (193.9, 190.4 and 188.5 ppm). On the other hand, the carbonyl groups are fairly insensitive to changes of substituents on ligands, e.g. replacing a 2,2'-bithienyl substituent with either a 2-thienyl or a 2-furyl substituent. Three carbonyl signals are observed in each spectrum. The most downfield shift can be assigned to the

M(CO)₄-fragment, while the other two signals can be attributed to the *cis* and *trans* carbonyl ligands of the M(CO)₅-fragment.

As in the case of the ¹H NMR spectra, slow decomposition of the complexes were observed in the ¹³C NMR spectra, as indicated by the repetition of the heteroarene signals. The decomposition products could be the ester analogues^[31] of the carbene complexes, although no further investigation into these decomposition products were carried out.

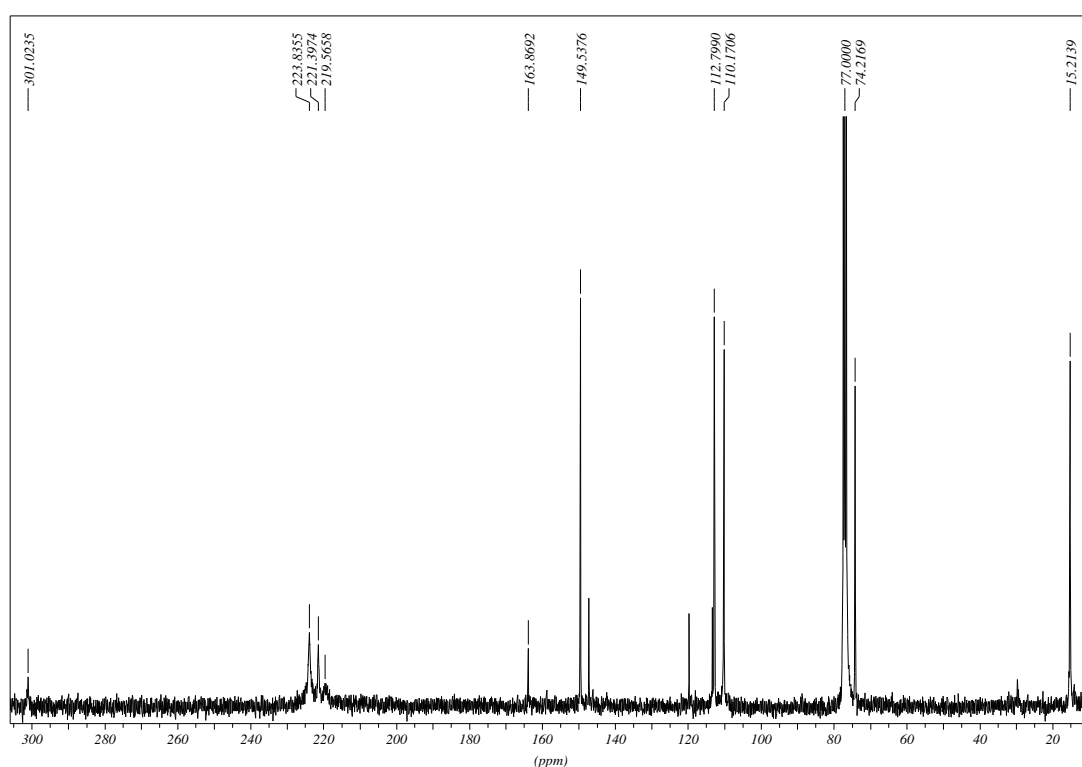


Figure 2.7 ¹³C NMR spectrum of complex 3

2.3.2 IR Spectroscopy

The stretching vibrational frequency of a free CO group is 2143 cm⁻¹, but lies between 1850 and 2120 cm⁻¹ for terminal carbonyl ligands^[32]. In contrast to M-C stretching frequencies, the C-O stretching vibrational frequencies can be seen as being independent from other vibrations in the molecule, thus a qualitative

correlation between CO stretching vibrational frequencies and the bond order of the C-O bond can be made.

As backbonding from the metal to the carbonyl ligand increases, the M-C bond becomes stronger and thus shorter. The C-O bond weakens accordingly and becomes longer, and the carbonyl stretching frequency shifts to a lower wave number on the IR spectrum. Carbene ligands have weaker π -acceptor properties compared to carbonyl groups, which means back bonding from the metal to the carbonyl ligand increases. This is shown by the lower wave numbers of the bands caused by ν_{CO} vibrations in carbene carbonyl complexes compared to the corresponding metal carbonyl complexes.

The number and intensities of carbonyl stretching frequencies are dependent on the local symmetry of the carbonyl ligands around the central atom. The carbonyl stretching modes of equatorially and axially substituted bimetal nonacarbonyl complexes were summarized by Ziegler *et al*^[33]. The *eq*-[M₂(CO)₉L] displays a nine band pattern in the IR spectrum, corresponding to C_s symmetry (Figure 2.8). These bands include six A' bands and three degenerate A'' bands. On the other hand, the IR spectrum of *ax*-[M₂(CO)₉L] is observed to have only five bands: the three A' bands and two E bands which corresponds with C_{4v} symmetry (Figure 2.9).

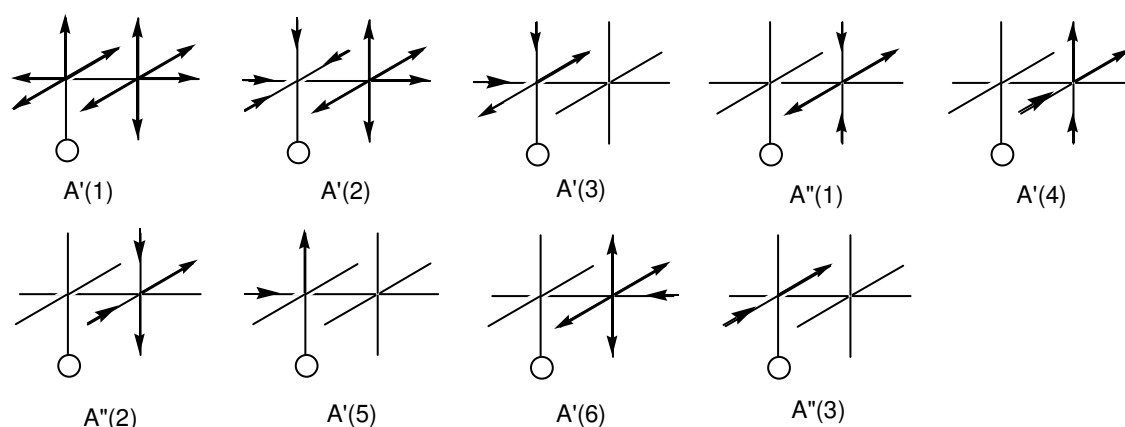


Figure 2.8 IR-active normal modes observed for *eq*-[M₂(CO)₉L]

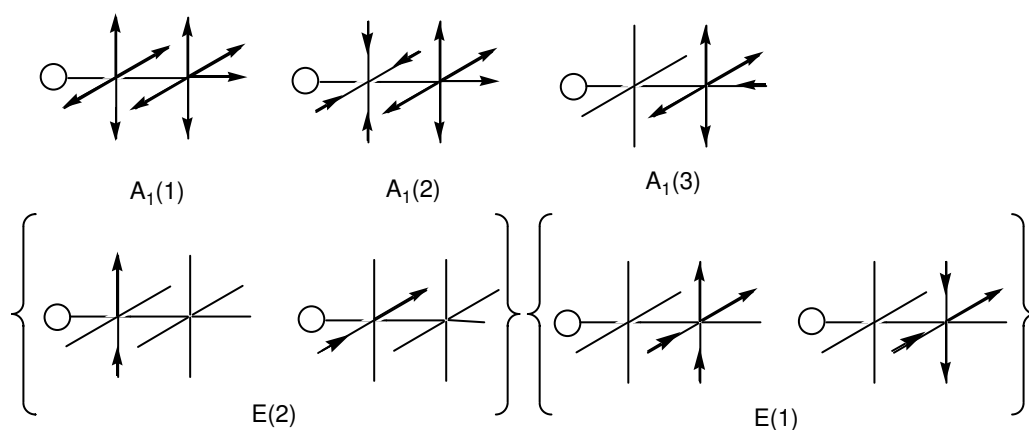


Figure 2.9 IR-active normal modes observed for $ax-[M_2(CO)_9L]$

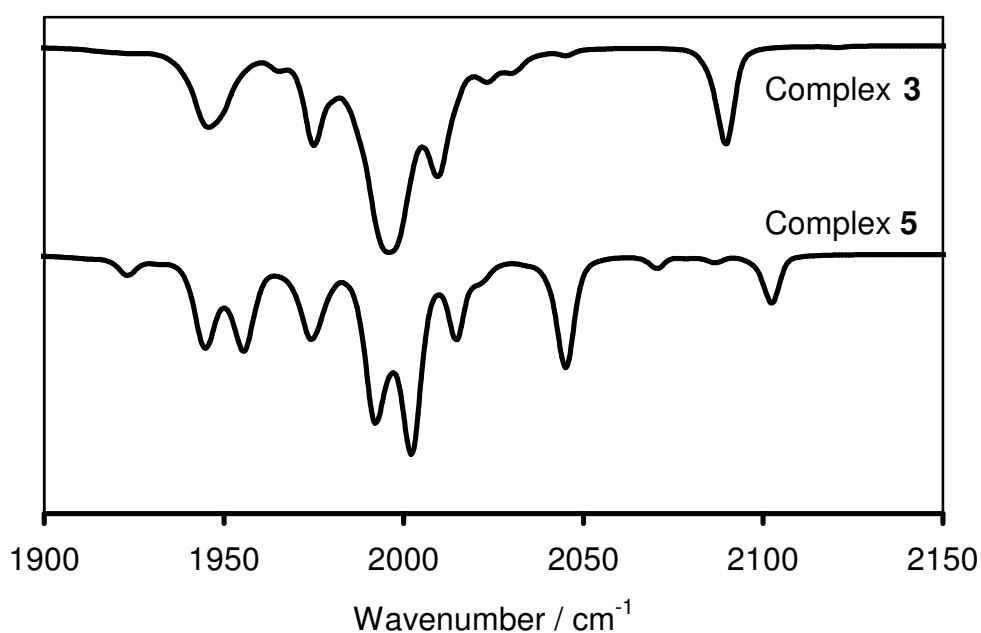


Figure 2.10 Stacked IR spectra of complexes **3** and **5** in the carbonyl region

The $[Re_2(CO)_9\{C(OEt)(2-furyl)\}]$ complex **5** displayed the expected typical nine band pattern for an equatorially substituted bimetal nonacarbonyl complex with C_s symmetry^[33] (Table 2.6, Figure 2.10). However, the IR spectra of all the dimanganese monocarbene complexes **1** - **4** displayed only five carbonyl stretching bands in the carbonyl region (Table 2.5, Figure 2.10). This five band

pattern indicates C_{4v} symmetry, but needs to be examined carefully as the number of bands in $eq\text{-}[\text{Mn}_2(\text{CO})_9\text{L}]$ may be less than nine because of band overlap. C_{4v} symmetry places the carbene ligand in an axial position relative to the Mn-Mn bond. A search of the Cambridge Structural Database revealed that only one other axially substituted carbene complex of dimanganese nonacarbonyl has been structurally characterized. This complex has the unusual carbene ligand, $(\text{M})=\text{C}(\text{NMe}_2)\text{OAl}_2(\text{NMe}_2)_5$ ^[34].

Table 2.5 IR data in the carbonyl region of complex **1** - **4**^a

Complex	Carbonyl stretching frequencies (ν_{CO} , cm^{-1}) for pseudo- C_{4v} symmetry of $ax\text{-}[\text{Mn}_2(\text{CO})_9(\text{carbene})]$				
	A ₁ (1)	A ₁ (2)	E (1)	A ₁ (3)	E (2)
1	2089 (m)	2009 (m)	1996 (vs)	1975 (m)	1945 (m)
2	2090 (m)	2010 (m)	1996 (vs)	1975 (m)	1946 (m)
3	2087 (m)	2006 (m)	1992 (vs)	1971 (m)	1936 (m)
4	2089 (m)	2009 (m)	1996 (vs)	1975 (m)	1944 (m)

a) Hexane as solvent

Table 2.6 IR data in the carbonyl region of complex **5**^a

Complex	Carbonyl stretching frequencies (ν_{CO} , cm^{-1}) for C_s - symmetry of $eq\text{-}[\text{Re}_2(\text{CO})_9(\text{carbene})]$								
	A'(1)	A'(2)	A'(3)	A''(1)	A'(4)	A''(2)	A'(5)	A'(6)	A''(3)
5	2102 (w)	2045 (m)	2016 (s)	2002 (vs)	1992 (s)	1974 (m)	1955 (m)	1945 (m)	1923 (w)

a) Hexane as solvent

2.3.3 Mass Spectrometry

A molecular ion peak, M^+ , was observed in the mass spectra for complexes **1**, **2**, **3** and **5**, although with a low intensity.

Table 2.7 Mass spectral data of binuclear monocarbene complexes

Complex	m/z	Intensity (%)	Fragment ion
1	584	7	$[M]^+$
	556	4	$[M - CO]^+$
	511	12	$[M - CO - OEt]^+$
	500	4	$[M - 3CO]^+$
	472	13	$[M - 4CO]^+$
	195	9	$[Mn(CO)_5]^+$
2	502	2	$[M]^+$
	390	15	$[M - 4CO]^+$
	279	2	$[M - Mn - 6CO]^+$
3	486	9	$[M]^+$
	413	8	$[M - CO - OEt]^+$
	374	7	$[M - 4CO]^+$
	263	35	$[M - Mn - 6CO]^+$
	235	45	$[M - Mn - 7CO]^+$
	207	30	$[M - Mn - 8CO]^+$
5	749	28	$[M]^+$
	721	5	$[M - CO]^+$
	681	5	$[M - (2-furyl)]^+$
	423	19	$[M - Re - 5CO]^+$

The identified fragment ions (m/z) are summarized in Table 2.7. The general initial fragmentation pattern in which the carbonyl ligands were lost sequentially, followed by the loss of an ethyl/methyl group and carbene ligand were observed, although not as consistently as reported by Crause^[11] and Landman^[12] for

monocarbene complexes with similar ligands, but with chromium, tungsten and molybdenum metal centres. This fact could be ascribed due to interaction of the compounds with the FAB matrix of nitrobenzyl alcohol.

2.3.4 X-Ray Crystallography

Single crystal X-ray diffraction studies confirmed the molecular structure of complexes **2**, **3** and **5**, but no suitable diffraction quality crystals of complex **1** and **4** were obtained. The crystal structures supported the information obtained from the infrared data that the dimanganese monocarbene complexes have an axially substituted carbene ligand while the dirhenium monocarbene has the expected equatorial configuration. The complexes crystallized from a dichloromethane:hexane (1:1) solution by layering of the solvents, yielding orange-red crystals for **2** and **3** and red crystals for **5** of good quality. Figures 2.11, 2.12 and 2.13 represent the ORTEP^[35] + POV-Ray^[36] plots of the geometry of the structures **2**, **3** and **5**, and also indicate the atom numbering system used for the structural data.

The crystal structure of free thiophene was determined by Harshbarger and Bauer^[37] while Liescheski and Rankin^[38] determined the molecular structure of furan by using various combinations of data from gas-phase electron diffraction, rotational spectroscopy and liquid crystal NMR spectroscopy. The geometrical parameters of these two free heteroarenes are summarized in Table 2.8.

Both complex **2** and **3** crystallized in the monoclinic system, space group $P2_1/c$ with four molecules in the unit cell. Complex **5** crystallized in the orthorhombic system, space group $Pbca$ with eight molecules in the unit cell. Selected bond lengths and angles determined for the complexes are tabulated in Table 2.9, whilst the most important torsion angles are listed in Table 2.10. The complete set of crystallographic data of **2**, **3** and **5** are listed in Appendices 1, 2 and 3 respectively.

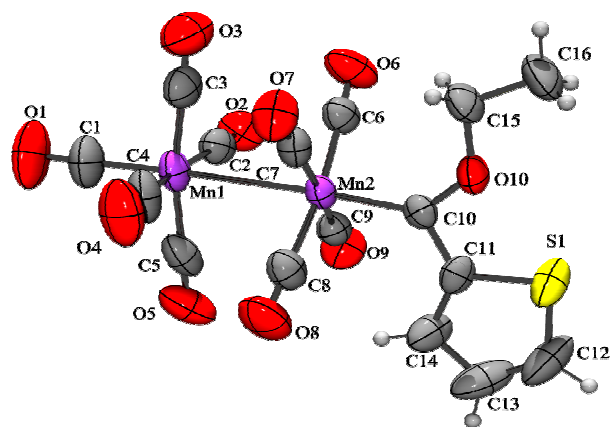


Figure 2.11 ORTEP + POV-Ray plot of the geometry of complex 2

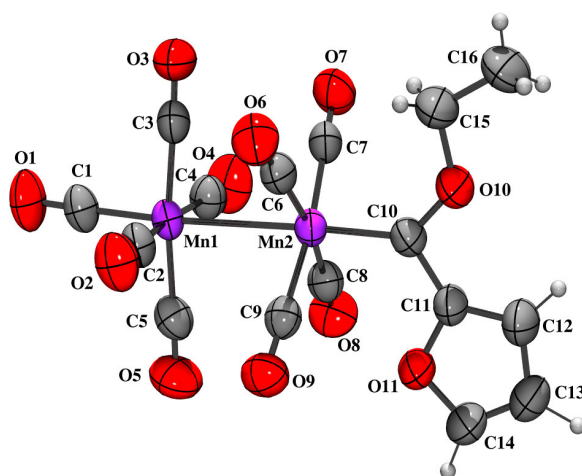


Figure 2.12 ORTEP + POV-Ray plot of the geometry of complex 3

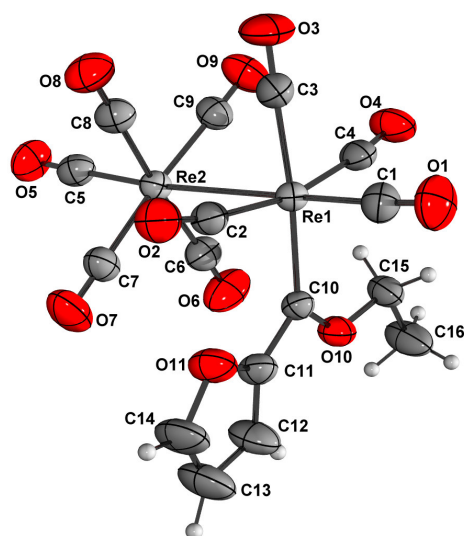


Figure 2.13 ORTEP + POV-Ray plot of the geometry of complex **5**

Table 2.8 Geometrical parameters of free thiophene and furan

Thiophene			
Atoms	Bond Lengths (Å)	Atoms	Bond Angles (°)
S-C(2)	1.718(4)	C(2)-S-C(5)	92.0(3)
C(2)-C(3)	1.370(4)	S-C(2)-C(3)	111.2(3)
C(3)-C(4)	1.442(2)	C(2)-C(3)-C(4)	112.5(3)
Furan			
Atoms	Bond Lengths (Å)	Atoms	Bond Angles (°)
O-C(2)	1.3641(7)	C(2)-O-C(5)	106.74(7)
C(2)-C(3)	1.3640(9)	O-C(2)-C(3)	110.49(7)
C(3)-C(4)	1.4303(19)	C(2)-C(3)-C(4)	106.14(6)

For complexes **2** and **3**, the coordination of each manganese atom is approximately octahedral with the two sets of the equatorial carbonyl ligands being staggered. The carbene ligand is in the axial position and is therefore

trans to the metal-metal bond. Both the thienyl and the furyl rings are close to being coplanar with the plane of the bonding geometry about the carbene carbon. For **2**, the dihedral angle between the least-squares planes through {S(1), C(11), C(12), C(13) and C(14)} and through {C(10), C(11), O(10) and Mn(2)} is 7.6(9)°. The plane of the carbene carbon, thienyl/furyl ring and oxygen is approximately perpendicular to the equatorial plane of carbonyl ligands {C(10)-Mn(2)-CO (91 - 96°)} and is in an intermediate position between the carbonyl ligands around Mn(2), as is evident from the torsion angles of 45.5(10)° and -44.9(10)° (complex **2**) and -41.0(2)° and 48.7(2)° (complex **3**) for C(6)-Mn(2)-C(10)-O(10) and C(7)-Mn(2)-C(10)-O(10) respectively.

Table 2.9 Selected bond lengths and angles of **2**, **3** and **5**

Atoms	Bond Lengths (Å)		Atoms	Bond Angles (°)	
	2 (Y = S)	3 (Y = O)		2 (Y = S)	3 (Y = O)
Mn(1)-C(1)	1.798(7)	1.813(2)	Mn(2)-C(10)-O(10)	131.1(6)	131.79(16)
Mean Mn(1)-C(x) (x=2,3,4,5)	1.841(9)	1.846(3)	O(10)-C(10)-C(11)	103.8(5)	103.25(18)
Mn(1)-Mn(2)	2.9238 (14)	2.9316(5)	C(11)-C(10)-Mn(2)	125.1(6)	124.96(15)
Mean Mn(2)-C(x) (x=6,7,8,9)	1.833(7)	1.858(2)	C(11)-Y-C(14)	92.3(5)	107.0(2)
Mn(2)-C(10)	1.933(7)	1.932(2)	Y-C(11)-C(12)	109.0(6)	107.4(2)
C(10)-O(10)	1.312(7)	1.332(3)			
C(10)-C(11)	1.470(11)	1.446(3)	Y-C(14)-C(13)	112.3(8)	110.8(3)
C(11)-C(12)	1.384(10)	1.352(3)			
C(12)-C(13)	1.390(12)	1.403(4)	C(12)-C(13)-C(14)	114.0(9)	106.6(2)
C(13)-C(14)	1.313(19)	1.317(4)			
C(11)-Y	1.715(10)	1.379(3)	C(11)-C(12)-C(13)	112.3(9)	108.2(2)

Table 2.9 contd. Selected bond lengths and angles of **5**

Atoms	Bond Lengths (Å)	Atoms	Bond Angles (°)
Re(2)-C(5)	1.934(4)	Re(1)-C(10)-O(10)	130.2(3)
Mean Re(2)-C(x) (x=6,7,8,9)	1.989(5)	O(10)-C(10)-C(11)	103.1(3)
Re(1)-Re(2)	3.0809(3)	C(11)-C(10)-Re(1)	126.6(3)
Re(1)-C(1)	1.923(5)		
Re(1)-C(3)	1.992(5)	C(11)-O(11)-C(14)	106.6(4)
Mean Re(1)-C(x) (x=2,4)	1.990(4)		
Re(1)-C(10)	2.129(4)	O(11)-C(11)-C(12)	108.9(4)
C(10)-O(10)	1.323(5)		
C(10)-C(11)	1.457(5)	O(11)-C(14)-C(13)	111.2(4)
C(11)-C(12)	1.355(6)		
C(12)-C(13)	1.418(7)	C(12)-C(13)-C(14)	105.9(5)
C(13)-C(14)	1.331(8)		

Some disorder of the ethoxy-thien-2-yl-methylidene ligand was observed with a minor component rotated approximately 180° about the Mn-C(carbene) bond with respect to the orientation of the major component, such that the C(11)A, C(12)A and C(13)A atoms of the thienyl ring of the minor component nearly coincide with the O(10), C(15) and C(16) atoms, respectively, of the ethoxy group of the major component (O(10)A, C(15)A and C(16)A also nearly coincide with C(11), C(12) and C(13) respectively). This disorder is shown in Figure 2.14. Figure 2.11 shows the major orientation (88.2(4)%).

The carbene ligand is in the *trans*-configuration about the C-O bond (C(11)-C(10)-O(10)-C(15) 177.2(8)° (complex **2**) and -178.9(3)° (complex **3**). The metal-carbon(carbonyl) bond distance *trans* to the Mn-Mn bond is significantly shorter than the mean distance of the Mn-C(carbonyl) bond lengths in the equatorial planes (Table 2.9) to compensate for the weaker π -acceptor properties of the

carbene carbon compared to a carbonyl carbon on the other side of the metal-metal bond.

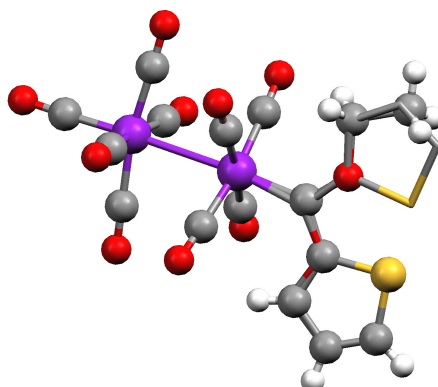


Figure 2.14 The major (88.3(5)%) and minor (11.7(5)%) orientations of the disordered (C₄H₃S)-C-OEt ligand of **2**

The Mn(1)-Mn(2) distance is longer and the *trans* Mn-C(carbonyl) distance is of the same order magnitude when comparing the corresponding Mn-Mn (2.90381(6)Å) and *trans* Mn-C(carbonyl) (1.811(3)Å) distances reported for [Mn₂(CO)₁₀]^[39]. The Mn-C(carbene), Mn-Mn and M-C(carbonyl) distances are similar in the dimanganese nonacarbonyl carbene complex *eq*-[Mn₂(CO)₉{C(OEt)Ph}] where the carbene ligand is in an equatorial position and the carbene substituents are in the *cis*-configuration about the carbene C-O bond. The Mn-C(carbene)-C angles are identical for the axial and equatorial carbene ligands, however, the other bond angles about the carbene carbon are significantly different with Mn-C(carbene)-O 119.4(3)° and C-C(carbene)-O 115.5(3)° in [Mn₂(CO)₉{C(OEt)Ph}]^[14]. The large Mn(2)-C(10)-O(10) angle in **2** and **3** (131.1(6)° and 131.79(16)° respectively) can be ascribed to the steric interactions between the -CH₂ of the ethyl group and the adjacent equatorial carbonyl ligands.

The bond C(11)-C(12) (1.384(10) and 1.352(3) Å for **2** and **3**, respectively) is slightly longer than a double C=C bond, and than the corresponding C(2)-C(3) bonds (1.370(4)Å for thiophene, 1.3640(9)Å for furan) of the free heteroarenes. The C(12)-C(13) bond (1.390(12) and 1.403(4) Å for **2** and **3**, respectively), on

the other hand, is significantly shorter than a single C-C bond, and the same bond (1.442(2)Å for thiophene, 1.4303(19)Å for furan) in the free heteroarene, indicating more electron delocalization in the ring. For all three complexes, the bond angles of the thienyl or furyl rings differ from the angles in uncoordinated thiophene and furan (Table 2.8), indicating ring involvement in stabilizing the carbene carbon.

Table 2.10 Selected torsion angles of **2**, **3** and **5**

Bond	Torsion Angle (°)	
	2 (Y = S)	3 (Y = O)
C(6)-Mn(2)-C(10)-O(10)	45.5(10)	139.0(2)
C(7)-Mn(2)-C(10)-O(10)	135.1(10)	48.7(2)
Mn(2)-C(10)-C(11)-Y	171.0(10)	174.4(2)
Mn(2)-C(10)-C(11)-C(12)	-6.4(11)	173.3(3)
C(3)-Mn(1)-Mn(2)-C(6)	-46.0(3)	45.97(10)
Bond	Torsion Angle (°)	
	5	
C(4)-Re(1)-C(10)-O(10)	3.5(4)	
C(2)-Re(1)-C(10)-O(10)	177.7(3)	
Re(1)-C(10)-C(11)-O(11)	-5.4(5)	
Re(1)-C(10)-C(11)-C(12)	175.6(4)	
Re(2)-Re(1)-C(10)-C(11)	-87.2(3)	
C(3)-Re(1)-Re(2)-C(8)	-30.93(19)	

The staggered conformation of the carbonyls are shown by the dihedral angle C(3)-Mn(1)-Mn(2)-C(6) of -46.0(3)° for **2**, and 45.97(10)° for **3** (Table 2.10). The rhenium complex shows a smaller dihedral angle (C(3)-Re(1)-Re(2)-C(8) - 30.93(19)°) which indicates a less symmetric staggered conformation, due to the longer Re-Re bond length.

For complex **5**, the Re(1)-Re(2) bond distance (3.0809(3)Å) is longer than the Re-Re bond (3.0413(11)Å) reported for Re₂(CO)₁₀^[39] and is considerably longer than the Mn-Mn bond distance of **2** and **3** by approximately 0.15 Å. The bulky carbene ligand can therefore be accommodated in the equatorial position. Most *eq*-[Mn₂(CO)₉(carbene)] complexes studied crystallographically have cyclic carbene ligands that display less steric hindrance compared to carbene complexes with two separate substituents^[40;41].

2.4 Conclusions

This study indicated that there may still be a lot to be discovered in the area of carbene complexes of manganese and rhenium; an area that has been neglected. The bulkiness of an Mn(CO)₅-fragment can affect the coordination site of a carbene ligand. It is clear that although the equatorial position is the electronically favoured position for the carbene ligand, steric effects can force the carbene ligand to occupy an axial position. It was assumed that the carbene would have taken up an equatorial position based on the many reported studies of cyclic carbene ligands which are not very bulky^[40-45]. The steric constraints are much more pronounced for the manganese complexes compared to the rhenium complexes, because of the much shorter Mn-Mn bond length compared to the Re-Re bond length. Complex **5** has its carbene ligand in the electronically favourable equatorial position.

It is possible to use infrared spectra to deduce the site of coordination of the carbene ligand, provided the spectra are carefully examined and possible band overlap is taken into account. This is useful if X-ray crystallography cannot be utilized for structure elucidation.

The possible manipulation of the position of the carbene ligand is planned in future work. This could be attempted by substitution of carbonyl ligands with bulky phosphine ligands^[46], known to substitute axially, to force the carbene ligand to adopt an equatorial position for the dimanganese complexes.

2.5 References

1. E.O. Fischer, A. Maasböl, *Angew. Chem. Int. Ed. Engl.* 3, **1964**, 645.
2. O.S. Mills, A.D. Redhouse, *J. Chem. Soc. A*, **1968**, 642.
3. E.O. Fischer, *Angew. Chem.* 86, **1974**, 651.
4. F.A. Cotton, C.M. Lukehart, *Prog. Inorg. Chem.* 16, **1972**, 487.
5. C.P. Casey, T.J. Burkhardt, *J. Am. Chem. Soc.* 95, **1973**, 5833.
6. J.A. Connor, E.M. Jones, *J. Chem. Soc. A*, **1971**, 1974.
7. W.A. Hermann, *Kontakte* 3, **1991**, 29.
8. S. Maiorana, A. Papagni, E. Licandro, A. Persoons, K. Clay, S. Houbrechts, W. Porzio, *Gazz. Chim. Ital.* 125, **1995**, 377.
9. M.M. Moeng, *Terthienyl Carbene Complexes*, University of Pretoria, **2001**.
10. A.J. Olivier, *Novel Carbene Complexes with Pyrrole Ligands*, University of Pretoria, **2001**.
11. C. Crause, *Synthesis and Application of Carbene Complexes with Heteroaromatic Substituents*, University of Pretoria, **2004**.
12. M. Landman, *Synthesis of Metal Complexes with Thiophene Ligands*, University of Pretoria, **2000**.
13. E.O. Fischer, E. Offhaus, *Chem. Ber.* 102, **1969**, 2449.
14. G. Huttner, D. Regler, *Chem. Ber.* 105, **1972**, 1230.
15. M.A. Schwindt, T. Lejon, L.S. Hegedus, *Organometallics* 9, **1990**, 2814.
16. M.F. Semmelhack, G.R. Lee, *Organometallics* 6, **1987**, 1839.
17. A. Rabier, N. Lugan, R. Mathieu, *J. Organomet. Chem.* 617-618, **2001**, 681.
18. C.P. Casey, S. Kraft, D.R. Powell, M. Kavana, *J. Organomet. Chem.* 617-618, **2001**, 723.
19. E.O. Fischer, P. Rustemeyer, *J. Organomet. Chem.* 225, **1982**, 265.
20. U. Schubert, K. Ackermann, P. Rustemeyer, *J. Organomet. Chem.* 231, **1982**, 323.

21. C.P. Casey, C.R. Cyr, R.L. Anderson, D.F. Marten, *J. Am. Chem. Soc.* 97, **1975**, 3053.
22. C.P. Casey, R.L. Anderson, *J. Am. Chem. Soc.* 93, **1971**, 3554.
23. C.P. Casey, C.R. Cyr, *J. Organomet. Chem.* 37, **1973**, C69.
24. R.J. Abrahams, J. Fischer, P. Loftus, *Introduction to NMR Spectroscopy*, John Wiley and Sons, **1988**.
25. E. Pretch, J. Seibl, T. Clerc, W. Simon, *Tables for Spectral Data for Structure Determination of Organic Compounds*, 2nd Ed. Springer-Verlag, Berlin/Heidelberg **1989**.
26. R.J. Cushley, R.J. Sykes, C.-K. Shaw, H.H. Wasserman, *Can. J. Chem.* 53, **1975**, 148.
27. S. Gronowitz, *Adv. Heterocycl. Chem.* 1, **1963**, 1.
28. B.A. Anderson, W.D. Wulff, A. Rahm, *J. Am. Chem. Soc.* 115, **1993**, 4602.
29. E.O. Fischer, T. Selmayr, F.R. Kreissl, U. Schubert, *Chem. Ber.* 110, **1977**, 574.
30. B.E. Mann, *Adv. Organomet. Chem.* 12, **1974**, 135.
31. Y.M. Terblans, H.M. Roos, S. Lotz, *J. Organomet. Chem.* 566, **1998**, 133.
32. P.S. Braterman, *Metal Carbonyl Spectra*, Academic Press Inc., London **1975**.
33. M.L. Ziegler, H. Haas, R.K. Sheline, *Chem. Ber.* 98, **1965**, 2454.
34. J.Fr. Janik, E.N. Duesler, R.T. Paine, *J. Organomet. Chem.* 323, **1987**, 149.
35. L.J. Farrugia, *J. Appl. Crystallogr.* 30, **1997**, 565.
36. The POV-Ray Team, POV-Ray **2004**, URL: <http://www.povray.org/download/>.
37. W.R. Harshbarger, S.H. Bauer, *Acta Crystallogr.* B26, **1970**, 1010.
38. P.B. Liecheski, D.W.H. Rankin, *J. Mol. Struct.* 196, **1989**, 1.
39. M.R. Churchill, K.N. Amoh, H.J. Wasserman, *Inorg. Chem.* 20, **1981**, 1609.
40. J.-A.M. Garner, A. Irving, J.R. Moss, *Organometallics*, 9, **1990**, 2836.
41. J.-A.M. Anderson, S.J. Archer, J.R. Moss, M.L. Niven, *Inorg. Chim. Acta* 206, **1993**, 187.

42. P.J. Fraser, W.R. Roper, F.G.A. Stone, *J. Chem. Soc., Dalton Trans.* **1974**, 760.
43. C.H. Game, M. Green, J.R. Moss, F.G.A. Stone, *J. Chem. Soc., Dalton Trans.* **1974**, 351.
44. C.H. Game, M. Green, F.G.A. Stone, *J. Chem. Soc., Dalton Trans.* **1975**, 2280.
45. D.H. Bowen, M. Green, D.M. Grove, J.R. Moss, F.G.A. Stone, *J. Chem. Soc., Dalton Trans.* **1974**, 1189.
46. N.J. Coville, A.M. Stolzenberg, E. L. Muetterties, *J. Am. Chem. Soc.* **1983**, 105, 2499.

Cleaving of Metal-Metal

3 Bonds: Monomanganese

Monocarbene Complexes

3.1 Background

3.1.1 Overview

In 1998, the Schrock-type carbene complex, the so-called Grubbs carbene $[\text{Ru}(\text{PR}_3)_2(\text{carbene})\text{Cl}_2]$ was awarded the title "reagent of the year" for the success it exhibited as ring-closing metathesis catalyst^[1]. Such was the impact of this work that Schrock, Grubbs and Chauvin were awarded the Nobel Prize for Chemistry in 2005.

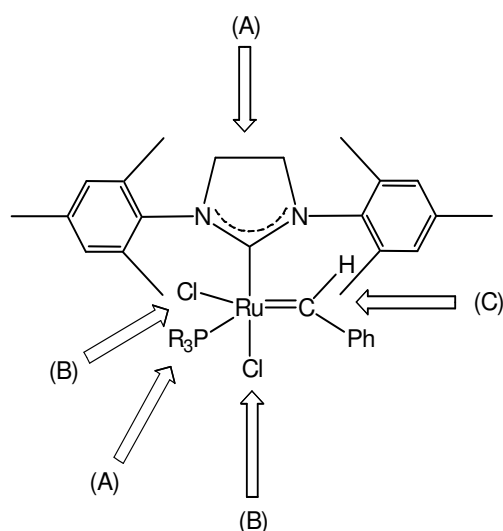


Figure 3.1 Assembly of the second generation Grubbs ruthenium catalyst

The catalyst system (Figure 3.1) consists of a ruthenium metal centre, bulky ligands to protect the reaction centre (A), X-type halide ligands to support alkyl binding (B), and the carbene ligand (C) to initiate metathesis.

For Group VII transition metals, specifically manganese, low oxidation state catalysts are fairly unknown. Perhaps the best known example of this transition metal as high-valent catalyst is the Mn(III)-salen complexes catalysing epoxidation reactions^[2].

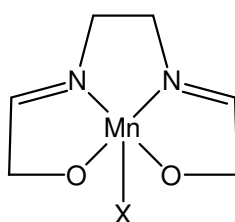
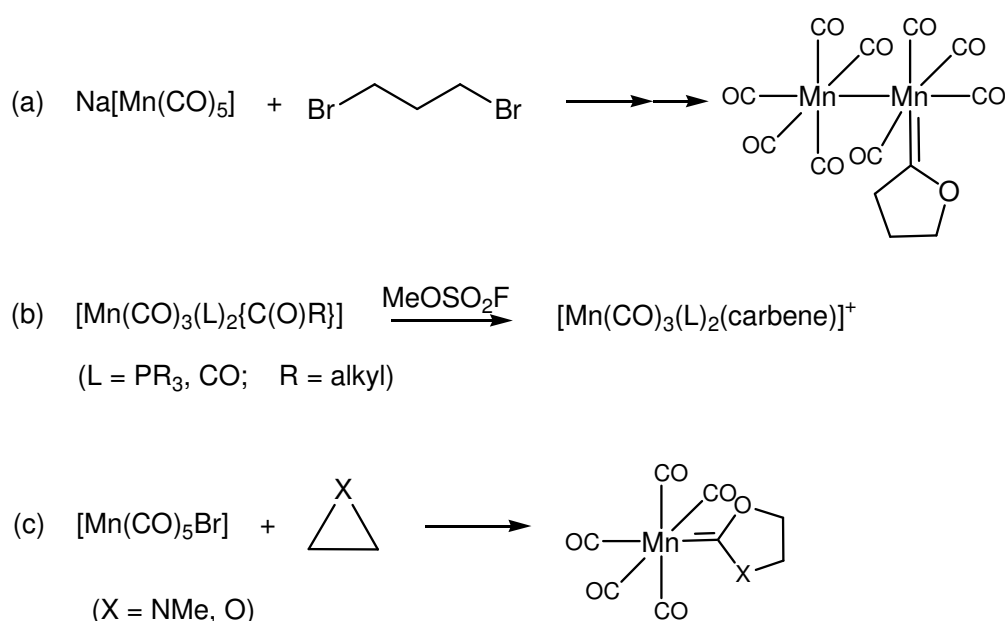


Figure 3.2 General structure of the Mn(III)-salen complexes

The chemistry of Group VII transition metal carbonyl complexes containing both Fischer carbene and halogen ligands, $[\text{Mn}(\text{CO})_4(\text{carbene})\text{X}]$ (X = halogens), has been neglected due to the difficulties associated with the synthesis of such compounds^[3-6].

The King compound, $[\text{Mn}_2(\text{CO})_9(\overline{\text{COCH}_2\text{CH}_2\text{CH}_2})]$, that was initially assigned an incorrect structure without a carbene ligand $[\text{Mn}_2(\text{CO})_{10}(\text{CH}_2)_3]$ ^[7], sparked interest in the challenges associated with the synthesis of $[\text{M}(\text{CO})_4(\text{carbene})\text{X}]$ (M = Mn, Re; X = halogens) complexes. The isolation of binuclear monocarbene complexes of Group VII transition metals, $[\text{Mn}_2(\text{CO})_9\{\text{C}(\text{OR})\text{R}\}]$, (R = alkyl) prepared from $\text{Na}[\text{Mn}(\text{CO})_5]$ and 1,3-dihaloalkanes was reinvestigated and resulted in detailed mechanistic studies of the reactions of $\text{Na}[\text{M}(\text{CO})_5]$ (M = Mn, Re) with dihaloalkanes^[8-11]. By using different dihaloalkanes, a number of complexes similar to the King compound containing a cyclic carbene ligand were synthesized and characterized^[12;13]. In a few instances, with more sophisticated chloro precursors, cationic

mononuclear carbene complexes $[\text{Mn}(\text{CO})_3(\text{L})_2(\text{carbene})]^+$ ($\text{L} = \text{phosphine or CO}$) could be obtained, which after subsequent treatment with halides, afforded the desired neutral halo-carbene complexes $[\text{M}(\text{CO})_4(\text{carbene})\text{X}]^{[14-19]}$ (Scheme 3.1, (a)). However, the complexes $[\text{Mn}(\text{CO})_3(\text{L})_2(\text{carbene})]^+$ ($\text{L} = \text{PR}_3$ or CO) could be afforded by employing the alkylation of $[\text{Mn}(\text{CO})_3(\text{L})_2\{\text{C}(\text{O})\text{R}\}]$ with the strong alkylating agent $\text{MeOSO}_2\text{F}^{[20]}$ (Scheme 3.1, (b)). These contributions to this field of the carbene chemistry of Group VII transition metals are illustrated in Scheme 3.1.

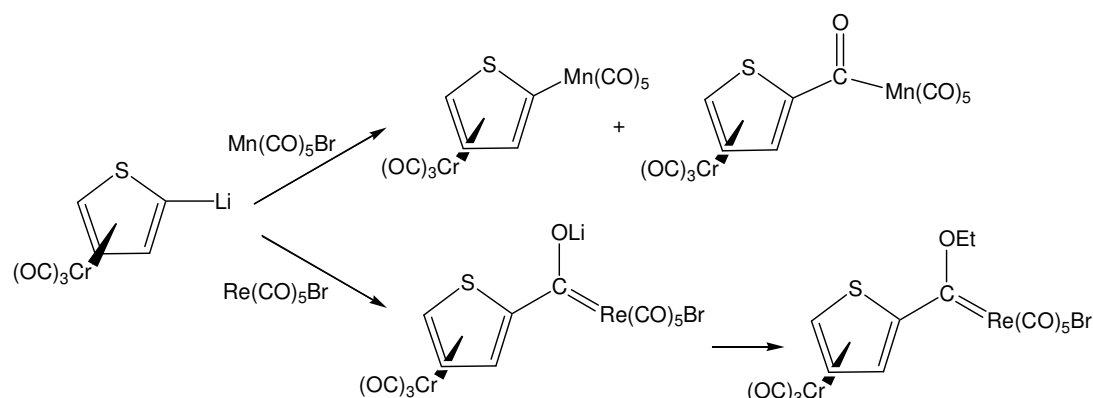


Scheme 3.1 Preparatory pathways of manganese carbene complexes

A major contribution came from the work done by Angelici and his group^[21-23]. Strained 3-membered heterocyclic substrates (oxirane, aziridine) with $[\text{M}(\text{CO})_5\text{X}]$ ($\text{M} = \text{Mn}, \text{Re}; \text{X} = \text{Br}, \text{Cl}$) afforded neutral cyclic aminoxy and dioxy carbene complexes also containing a halogen ligand (Scheme 3.1, (c)). This reaction could also be applied to $[\text{M}_2(\text{CO})_{10}]$ ($\text{M} = \text{Mn}, \text{Re}$) for oxirane^[22].

Reaction of the lithiated $[(\eta^5\text{-thiophene})\text{Cr}(\text{CO})_3]$ or the analogous lithiated $[(\eta^6\text{-benzene})\text{Cr}(\text{CO})_3]$ with $[\text{Mn}(\text{CO})_5\text{Br}]$ involved attack either on the metal centre or on a carbonyl ligand with elimination of bromide and yielded for the thiophene precursor the binuclear complexes $[(\eta^1, \eta^5\text{-thienyl-}$

$\text{Mn}(\text{CO})_5\text{Cr}(\text{CO})_3$ and $[\{\eta^1, \eta^5\text{-thienyl-C}(\text{O})\text{Mn}(\text{CO})_5\}\text{Cr}(\text{CO})_3]$ (Scheme 3.2)^[24-28].



Scheme 3.2 Different reaction routes of $[\text{M}(\text{CO})_5\text{Br}]$ with lithiated $[\{\eta^5\text{-thiophene}\}\text{Cr}(\text{CO})_3]$ ($\text{M} = \text{Mn}, \text{Re}$)

By contrast, the corresponding reaction with $[\text{Re}(\text{CO})_5\text{Br}]$ involved attack on a carbonyl ligand without the elimination of bromide. Subsequent alkylation of the latter with $[\text{Et}_3\text{OBF}_4]$ yielded the binuclear carbene complex $[\{\eta^1, \eta^5\text{-thienyl-C}(\text{OEt})\text{Re}(\text{CO})_4\text{Br}\}\text{Cr}(\text{CO})_3]$ (Scheme 3.2).

This prompted the investigation of the reaction of $[\text{Re}(\text{CO})_5\text{Br}]$ with lithiated thiophene to assess the role, if any, of the $\text{Cr}(\text{CO})_3$ -fragment. Although not reacting smoothly, it was possible, after subsequent alkylation with $[\text{Et}_3\text{OBF}_4]$, to isolate and characterize the monocarbene dirhenium nonacarbonyl complex, $[\text{Re}_2(\text{CO})_9\{\text{C}(\text{OEt})\text{thienyl}\}]$ ^[29]. This reaction showed that it was possible to eliminate a bromide from $[\text{Re}(\text{CO})_5\text{Br}]$ during a Fischer carbene synthesis procedure ($\text{Li-thienyl}/\text{Et}_3\text{OBF}_4$) and replace it with the isolobal fragment $\text{Re}(\text{CO})_5$ to give $[\text{Re}_2(\text{CO})_9\{\text{C}(\text{OEt})\text{thienyl}\}]$.

In contrast, reactions of lithiated thiophene with $[\text{Mn}(\text{CO})_5\text{Br}]$ afforded a number of unstable compounds that could not be characterized unambiguously^[29].

We envisaged that the reverse reaction of cleaving the manganese-manganese bond in the binuclear carbene complexes could be applied, provided the carbene ligand would not be affected by the oxidant.

3.1.2 Cleaving of metal-metal bonds

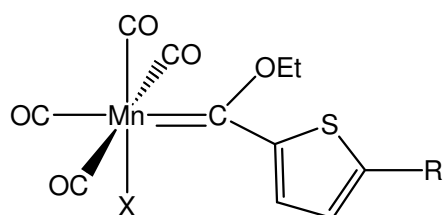
The metal-metal bond in $[\text{Mn}_2(\text{CO})_{10}]$ can easily be cleaved reductively by sodium, affording the anionic sodium salt $\text{Na}[\text{Mn}(\text{CO})_5]^{[30]}$. On the other hand the metal-metal bond can also be cleaved oxidatively with halogens to give neutral metal carbonyl halides, $[\text{Mn}(\text{CO})_5\text{X}]$ ($\text{X} = \text{halogens}$)^[31]. The reductive cleavage of the Mn-Mn bond of $[\text{Mn}_2(\text{CO})_9\{\text{C}(\text{OR})\text{Me}\}]$ with sodium in THF was attempted by Fischer and co-workers, but only $\text{Mn}_2(\text{CO})_{10}$ and $\text{Na}[\text{Mn}(\text{CO})_5\text{X}]$ were observed to have formed^[32].

Oxidation of the metal results either in the loss of the carbene ligand or the coordination of the products of the oxidizing agent to the metal. Biscarbene complexes of Group VII transition metals are readily oxidized by trace amounts of oxygen to give monocarbene-ester products^[33;34], while diaminecarbene complexes of tungsten could be oxidized with iodine to yield $[\text{W}(\text{CO})_4(\text{I})_2(\text{carbene})]^{[35]}$. Although largely unnoticed in later work, the cleavage of the metal-metal bond of the dioxy carbene by bromine was reported by Angelici^[22]. Nevertheless, very few examples exist where the ligand in $[\text{M}(\text{CO})_4(\text{carbene})\text{X}]$ ($\text{M} = \text{Mn}$, $\text{X} = \text{halogen}$) complexes is not a cyclic alkoxy carbene.

3.1.3 Focus of this study

The object of this chapter was to synthesize low valent mononuclear manganese carbene complexes. After some modification these complexes could serve as precursors with potential catalytic properties. The assembly of the complexes should contain both an X-type ligand to support alkyl-binding,

bulky ligands to protect the reaction site, and carbene ligands, which could initiate carbon-carbon coupling and carbonyl insertion reactions.



6 X = Br, R = thienyl

7 X = I, R = H

Figure 3.3 Mononuclear manganese carbene complexes

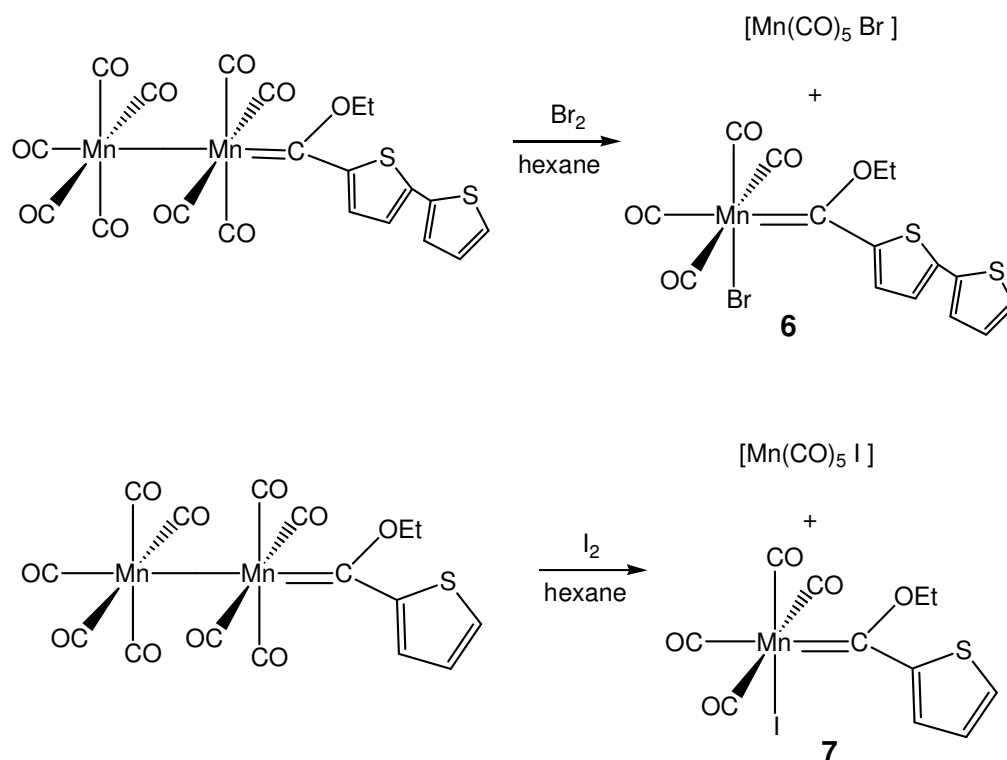
The synthesis of these complexes was afforded by the oxidative metal-metal bond cleavage by halogens of the binuclear monocarbene precursor complexes synthesized in Chapter 2.

3.2 Synthesis

The bimetallic carbene complex is dissolved in a small volume hexane and a stoichiometric amount of halogen, also dissolved in a minimum volume of hexane, was added dropwise under vigorous stirring. A red-orange precipitate immediately started forming and stirring was continued until the solution became clear. The solvent and unreacted halogen were removed under reduced pressure and the products were purified by column chromatography on silica gel for **6** and aluminium oxide for **7**.

The reaction of the bithiophene monocarbene complex and bromine did not proceed smoothly and only 21% of complex **6** (dark red) and 41% of $[\text{Mn}(\text{CO})_5\text{Br}]$ could be isolated. By changing the solvent to CS_2 , a solvent generally used to cleave $[\text{Mn}_2(\text{CO})_{10}]$ ^[28], only reactions leading to the

decomposition of the complex and elimination of the carbene ligand with the formation of $\text{Mn}_2(\text{CO})_{10}$ were observed. Replacing the bromine with iodine and using the minimum amount of hexane as solvent, gave 43% of complex **7** (red) after purification.

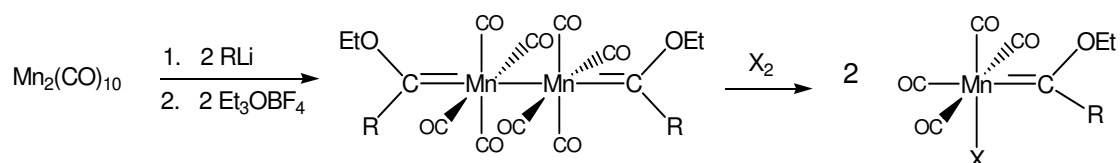


Scheme 3.3 Synthesis of **6** and **7**

Substitution kinetics of carbonyl ligands in $[\text{Mn}(\text{CO})_5\text{halides}]$ revealed that rates increased with decreasing atomic number for the halides^[36]. Based on this result it can be concluded that the bromo-carbene complex of manganese is less stable in the reaction medium compared to the analogous iodo-carbene complex of manganese.

During the synthesis of the $[\text{Mn}(\text{CO})_4(\text{carbene})\text{X}]$ complexes, 50% of the transition metal manganese is lost as $[\text{Mn}(\text{CO})_5\text{X}]$. In an effort to increase the yields of the desired mononuclear manganese carbene complexes with halide ligands, the synthesis of binuclear biscarbenes were attempted as illustrated in Scheme 3.4. If synthesis of biscarbene complexes proved possible, then subsequent cleaving of the Mn-Mn bond would double yields of the halo-

carbene complex. The synthesis of biscarbene was attempted by addition of two equivalents of lithiated heteroarene in a one-pot Fischer reaction, as well as the stepwise addition of two equivalents of lithiated reagent as described by Brandsma^[37]. However, it was not possible to isolate biscarbene complexes prepared by either method.



Scheme 3.4 Proposed synthesis of biscarbene complexes

3.3 Characterisation

Compositions of products were established by spectroscopic methods and mass spectrometry and final confirmation of the structures came from a single crystal X-ray diffraction study of **7**.

3.3.1 NMR Spectroscopy

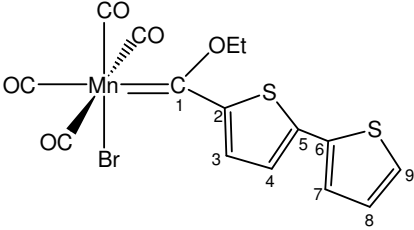
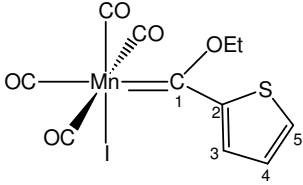
The NMR spectra of complex **6** were recorded in CDCl₃, but better resolution was achieved by recording the spectra of **7** in deuterated acetone. The same system of numbering of the carbon atoms and protons of the heteroarene substituents used in Chapter 2 was applied.

3.3.1.1 ¹H NMR Spectroscopy

The ¹H NMR data of **6** and **7** are summarized in Table 3.1. When comparing chemical shift values of **6** and **7** with that of **1** and **2** in Chapter 2, a downfield

shift of $\Delta\delta > 0.2$ ppm is observed for the methylene protons, and the ring protons show a downfield shift varying between $\Delta\delta = 0.1 - 0.3$ ppm. This can be ascribed to the change of oxidation state of the manganese metal centre: the oxidative cleavage causes the binuclear Mn(0) carbene complexes to be oxidized to the monocuclear Mn(I) carbene complexes containing a halide ligand. The manganese atom therefore has less electron density for back donation to the electrophilic carbene carbon. The electrophilic carbene carbon then has to be stabilized by even more electron donation from the ethoxy and heteroarene substituents, as illustrated in Figure 3.4.

Table 3.1 ^1H NMR data of complexes **6** and **7**

Assignment	Complexes			
	Chemical shifts (δ , ppm) and coupling constants (J , Hz)			
	 6		 7	
Proton	δ^a	J	δ^b	J
H3	8.53	n.o.	8.74 (dd)	4.1, 1.1
H4	7.72	n.o.	7.49 (dd)	4.9, 4.1
H5	-	-	8.29 (dd)	4.9, 1.1
H7	7.80	n.o.	-	-
H8	7.49	n.o.	-	-
H9	7.90	n.o.	-	-
-OCH ₂ CH ₃	5.53 (q)	7.0	5.67 (q)	7.0
-OCH ₂ CH ₃	2.02 (t)	7.0	1.72 (t)	7.0

a) Spectrum recorded in CDCl₃

b) Spectrum recorded in acetone-d₆

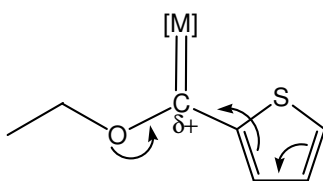


Figure 3.4 Electron donation by carbene substituents

3.3.1.2 ^{13}C NMR Spectroscopy

The ^{13}C NMR data of **6** and **7** are reported in Table 3.2. In the spectrum of **6** recorded in CDCl_3 , the signals of the carbene carbon and the carbonyl ligands were not observed. An improved spectrum was obtained for **7** in acetone- d_6 . In contrast with the data obtained for ^1H NMR, no consistent downfield shift of the signals was observed in the ^{13}C NMR spectra.

Table 3.2 ^{13}C NMR data of complexes **6** and **7**

Assignment	Complexes	
	6	7
Carbon	δ^a (ppm)	δ^b (ppm)
C1	n.o.	296.4
C2	162.3	144.9
C3	134.4	138.0
C4	124.4	129.4
C5	134.6	143.6
C6	133.5	-
C7	127.3	-
C8	131.3	-
C9	125.6	-
CO (trans)	n.o.	217.6
CO (<i>cis</i>)	n.o.	211.9
-OCH ₂ CH ₃	76.2	79.6
-OCH ₂ CH ₃	14.7	14.9

a) Spectrum recorded in CDCl_3

b) Spectrum recorded in acetone- d_6

3.3.2 Infrared Spectroscopy

For an octahedral $[M(\text{CO})_4\text{L}_2]$ complex, the two non-carbonyl ligands, L, can either be *cis* or *trans* substituted. To distinguish between these two possibilities, the infrared spectrum of the carbonyl stretching region can be inspected. For a *trans*- $[M(\text{CO})_4\text{L}_2]$ complex, a single intense band can be observed, which is assigned to the IR-active E_u -mode^[38]. In some cases, much weaker high-frequency satellites have been observed which could be assigned to the Raman-active A_{1g} and B_{1g} modes (Figure 3.5). The order of the frequencies for this symmetry must be $A_{1g} > B_{1g} > E_u$.

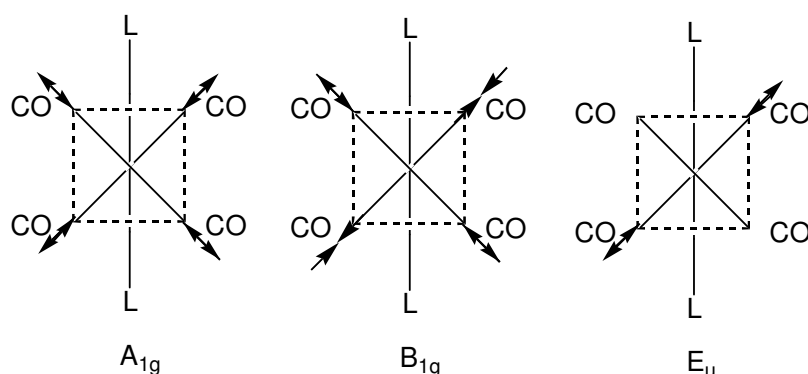


Figure 3.5 IR- and Raman -active modes observed for *trans*- $[M(\text{CO})_4\text{L}_2]$

On the other hand, there are four IR-active normal modes (Figure 3.6) for the *cis*-substituted $[M(\text{CO})_4\text{L}_2]$ complexes, with the following order: $A_1(1) > A_1(2) > B_1 > B_2$ ^[38]. The characteristic $\nu(\text{CO})$ pattern is a sharp $A_1(1)$ mode of medium intensity followed by the intense $A_1(2)$ band, and then the B_1 and B_2 bands.

When the infrared spectra of **6** and **7** were recorded in hexane, four bands were seen in the carbonyl region, as seen in Figure 3.7. The infrared data is summarized and the assignments of the observed bands are given in Table 3.4. It was therefore concluded that the cleaved product is *cis*-substituted, even although the binuclear precursor was axially substituted. When comparing these manganese complexes with their rhenium analogues recently synthesized in our laboratories^[29], it is clear that the cleaved product

is always *cis*-[M(CO)₄(carbene)X], regardless of whether or not the starting material was the equatorially coordinated dirhenium monocarbene or the axially coordinated dimanganese monocarbene. This information would suggest a dissociative reaction mechanism, although no further studies were done in this project on the reaction mechanism of the cleaving of the binuclear monocarbene complexes with halogens.

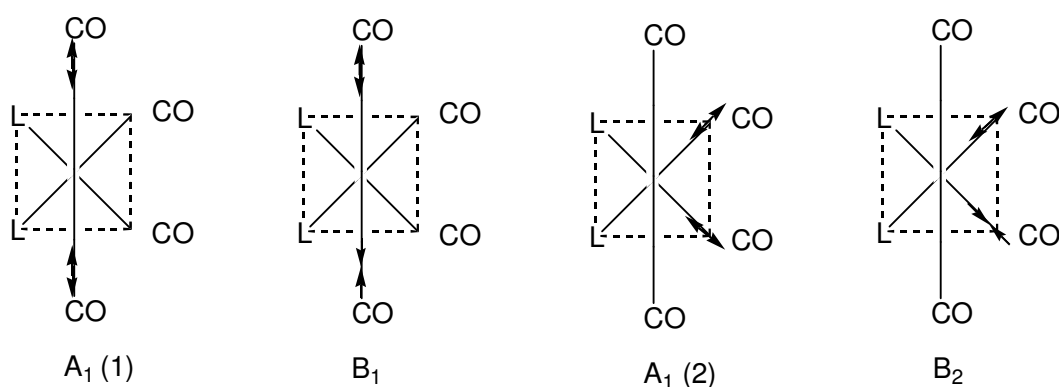


Figure 3.6 IR-active normal modes for *cis*-[M(CO)₄L₂]

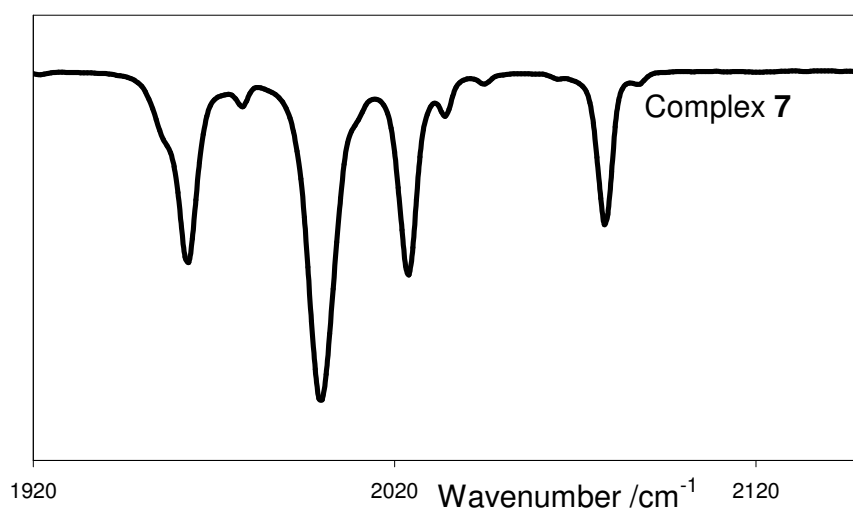


Figure 3.7 Infrared spectrum of **7** in the carbonyl region

Table 3.3 IR-data in the carbonyl region of complex **6** and **7**^a

Complex	Carbonyl stretching frequencies (ν_{CO} , cm^{-1}) for <i>cis</i> -[Mn(CO) ₄ (carbene)(halogen)]			
	A ₁ (1)	A ₁ (2)	B ₁	B ₂
6	2089 (m)	2009 (m)	1996 (vs)	1975 (m)
7	2090 (m)	2010 (m)	1996 (vs)	1975 (m)

a) Spectra recorded in hexane

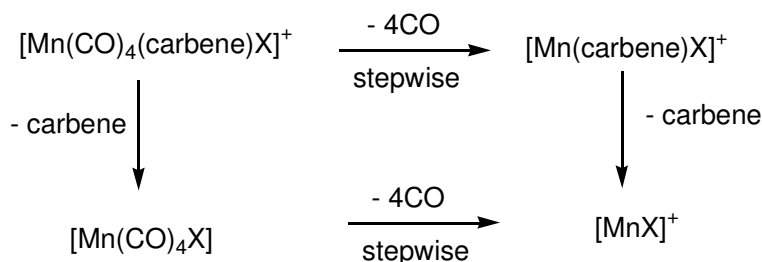
3.3.3 Mass Spectrometry

A molecular ion peak, M^+ , was observed in the mass spectra for complexes **6** and **7**, and in contrast to the mass spectral data observed for complexes **1** - **5** in Chapter 2, a more consistent fragmentation pattern was observed. The identified fragment ions are summarized in Table 3.4.

Table 3.4 Mass spectral data of cleaved monocarbene halide complexes

Complex	m/z	Intensity (%)	Fragment ion
6	469	2	$[M]^+$
	441	9	$[M - \text{CO}]^+$
	385	15	$[M - 3\text{CO}]^+$
	357	4	$[M - 4\text{CO}]^+$
	247	11	$[M - (\text{carbene})]^+$
7	434	36	$[M]^+$
	350	4	$[M - 3\text{CO}]^+$
	322	21	$[M - 4\text{CO}]^+$
	294	7	$[M - (\text{carbene})]^+$
	138	69	$[M - \text{CO} - (\text{carbene}) - \text{I}]^+$

The fragmentation pattern deduced from the fragment ions observed (and tabulated in Table 3.4) indicates that two routes exist (Scheme 3.4). In the first, the carbonyl ligands were lost sequentially, followed by the loss of the carbene ligand and then the halide ligand. In the second unexpected route, the carbene ligand is fragmented before stepwise loss of carbonyl ligands.



Scheme 3.4 Fragmentation routes for $[\text{Mn}(\text{CO})_4(\text{carbene})\text{X}]^+$

3.3.4 X-Ray Crystallography

No suitable crystals could be obtained for complex **6**, but solvent layering of hexane:dichloromethane (3:1) yielded dark-red crystals of good quality for complex **7**, and final confirmation of the molecular structure of this complex was obtained using X-ray crystallography. Figure 3.8 represents the ORTEP^[39] + POV-Ray^[40] plot of the geometry of **7**, while Table 3.5 gives a summation of the most important bond lengths, angles and torsion angles. The complete set of crystallographic information of **7** is given in Appendix 4.

Complex **7** crystallized in the tetragonal system, space group $I4_1/a$ with sixteen molecules in the unit cell. The coordination of the manganese atom is octahedral and a *cis*-arrangement of non-carbonyl ligands, already deduced from the infrared spectrum of the molecule, was confirmed.

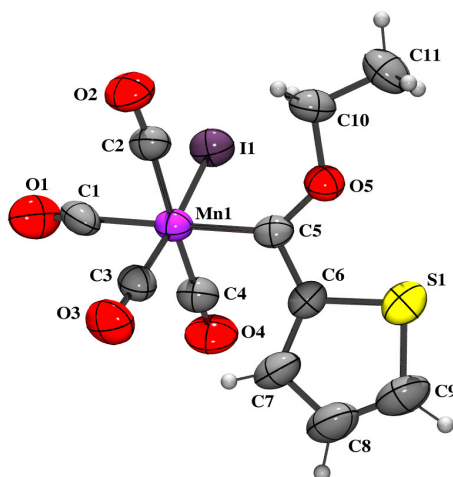


Figure 3.8 ORTEP + POV-Ray plot of the geometry of complex **7** with atom numbering

The dihedral angle between the least-squares planes through (S(1), C(6), C(7), C(8) and C(9)) and through (C(5), C(6), O(5) and Mn(1)) is 8.0(6)°. The plane of the carbene carbon, thienyl ring and oxygen atom is again approximately perpendicular to the equatorial plane of the *cis* carbonyl; this is demonstrated by the angles (C(5)-Mn(1)-C(carbonyl) 90 - 93°, C(5)-Mn(1)-I(1) 95.4(3)°) and is positioned approximately intermediately between the equatorial ligands around Mn(1), as is evident from the torsion angles of -38.9(7)° and 51.4(7)° for C(2)-Mn(1)-C(5)-O(5) and I(1)-Mn(1)-C(5)-O(5), respectively (Table 3.5).

The same disorder of the ethoxy-thien-2-yl-methylidene ligand as that described for **2** (Chapter 2) was also observed in **7**. Figure 3.8 shows the major orientation (85.9(5)%).

The carbene ligand is again in the *trans*-configuration about the C-O bond (C(6)-C(5)-O(5)-C(10) -173.8(6)°) - as expected when the thienyl ring is close to being coplanar with the plane of the bonding geometry about the carbene carbon as this prevents a *cis*-configuration being adopted. The metal carbon bond distance *trans* to the iodide ligand is significantly shorter than the Mn-CO

distances opposite carbonyl ligands, reflecting the poor π -acceptor properties of an iodide ligand. The Mn-carbon distances observed for the carbene and the carbonyl ligand *trans* to the carbene are almost the same corresponding to a very long metal-carbonyl bond distance.

The bond angles of the thienyl ring (Table 3.5) are distorted even more severely than that of **2** compared to the bond angles of free thiophene^[41], indicating an even greater ring involvement in stabilizing the carbene carbon atom of the oxidized manganese carbene complex than was exhibited by **2** (Chapter 2).

Table 3.5 Selected bond lengths, bond angles and torsion angles of **7**

Atoms	Bond Lengths (Å)	Atoms	Bond Angles (°)
Mn(1)-C(1)	1.949(10)	Mn(1)-C(5)-O(5)	132.8(6)
Mean Mn(1)-C(x) (x=2,4)	1.857(6)	O(5)-C(5)-C(6)	105.2(6)
Mn(1)-C(5)	1.986(8)	C(6)-C(5)-Mn(1)	122.0(6)
C(5)-O(5)	1.318(8)	S(1)-C(6)-C(7)	130.7(7)
C(5)-C(6)	1.437(9)	C(6)-S(1)-C(9)	92.5(5)
C(6)-C(7)	1.411(10)	C(7)-C(8)-C(9)	116.0(9)
C(7)-C(8)	1.414(13)	Atoms	Torsion Angles (°)
C(8)-C(9)	1.364(15)		
Mn(1)-C(3)	1.784(6)	I(1)-Mn(1)-C(5)-O(5)	51.4(7)
Mn(1)-I(1)	2.709(1)	C(2)-Mn(1)-C(5)-O(5)	-38.9(7)

A comparison of the structure of **7** with the complex *cis*-[Mn(CO)₄(COCH₂CH₂O)Cl], synthesized by Moss and co-workers^[16], can be done. For both these complexes, the manganese atom is in a slightly distorted

octahedral environment (angles at Mn 87 - 93°), although the angle (49°) between the mean plane of the carbene carbon atom and the two oxygen atoms in the ring, and which encompassed Mn(1), C(1), C(5), C(4) and C(2) is distinctly different from the almost planar arrangement found for **7** (8.0(6)°). The Mn-C(carbene) bond lengths are very similar (1.986(8)Å for **7** and 1.96Å for the chloro-carbene). The arrangement around the central manganese atom is therefore similar in both cases, but the cyclic carbene of the chloro-carbene complex is not co-planar as is found for the carbene ligand of **7** with the ethoxy- and thienyl-substituents.

3.4 Conclusions

The oxidative cleavage of the manganese-manganese bond in binuclear monocarbene complexes with halogens, without affecting the carbene ligand, proved successful. The resulting products had manganese metal centres in oxidation state +1, which means that less back bonding from the metal to the electrophilic carbene carbon atom is evident. The change in oxidation state is compensated for by the electron donation of the ethoxy and heteroarene substituents on the carbene ligand, as seen by the downfield shift of these protons in the ¹H NMR spectra and the distortion of the thienyl ring in the crystal structure obtained for **7**. The cleaved products exhibit a *cis*-configuration, even although the binuclear carbene precursors were axially substituted.

Future work would include investigating the modification of the carbene by replacing the alkoxy substituent. This would transform the Fischer carbene complexes to Schrock carbenes. A possible route to achieve this is by reacting the carbene ligand with a Lewis acid such as a BX₃ reagent to form a carbyne with elimination of the ethoxy group, followed by an attack of a hydride to insert a hydrogen as substituent on the carbene ligand^[42]. Schrock carbene complexes show higher reactivity as catalysts towards carbon-carbon coupling reactions.

3.5 References

1. R.H. Grubbs, *Tetrahedron* 60, **2004**, 7117.
2. B. Cornils, W.A. Hermann, *Applied Homogeneous Catalysis with Organometallic Compounds: A Comprehensive Handbook in Two Volumes*, VCH Publishers, **1996**.
3. M.A. Sierra, *Chem. Rev.* 100, **2000**, 3591.
4. P.M. Treichel, *Comprehensive Organometallic Chemistry II*. E.W. Abel, F.G.A. Stone, and G. Wilkinson, Pergamon, **1995**.
5. J.M. O'Connor, *Comprehensive Organometallic Chemistry II*. E.W. Abel, F.G.A. Stone, and G. Wilkinson, Pergamon, **1995**, 167.
6. T.C. Flood. *Comprehensive Organometallic Chemistry II*. E.W. Abel, F.G.A. Stone, and G. Wilkinson, Pergamon, **1995**, 21.
7. R.B. King, *J. Am. Chem. Soc.* 85, **1963**, 1922.
8. C.P. Casey, *J. Chem. Soc., Chem. Commun.* **1970**, 1220.
9. C.P. Casey, C.R. Cyr, R.L. Anderson, D.F. Marten, *J. Am. Chem. Soc.* 97, **1975**, 3053.
10. C.P. Casey, R.L. Anderson, *J. Am. Chem. Soc.* 93, **1971**, 3554.
11. C.P. Casey, C.R. Cyr, *J. Organomet. Chem.* 37, **1973**, C69.
12. J.-A.M. Garner, A. Irving, J.R. Moss, *Organometallics* 9, **1990**, 2836.
13. J.-A.M. Anderson, S.J. Archer, J.R. Moss, M.L. Niven, *Inorg. Chim. Acta* 206, **1993**, 187.
14. P.J. Fraser, W.R. Roper, F.G.A. Stone, *J. Chem. Soc., Dalton Trans.* **1974**, 760.
15. C.H. Game, M. Green, F.G.A. Stone, *J. Chem. Soc., Dalton Trans.* **1975**, 2280.
16. M. Green, J.R. Moss, I.W. Nowell, F.G.A. Stone, *J. Chem. Soc., Chem. Commun.* **1972**, 1339.
17. C.H. Game, M. Green, J.R. Moss, F.G.A. Stone, *J. Chem. Soc., Dalton Trans.* **1974**, 351.

18. D.H. Bowen, M. Green, D.M. Grove, J.R. Moss, F.G.A. Stone, *J. Chem. Soc., Dalton Trans.* **1974**, 1189.
19. A.J. Hartshorn, M.F. Lappert, K. Turner, *J. Chem. Soc., Dalton Trans.* **1978**, 348.
20. P.M. Treichel, K.P. Wagner, *J. Organomet. Chem.* **88**, **1975**, 199.
21. M.M. Singh, R.J. Angelici, *Inorg. Chem.* **23**, **1984**, 2699.
22. M.M. Singh, R.J. Angelici, *Inorg. Chim. Acta* **100**, **1985**, 57.
23. G.L. Miessler, S. Kim, R.A. Jacobson, R.J. Angelici, *Inorg. Chem.* **26**, **1987**, 1690.
24. S. Lotz, M. Schindehutte, P.H. van Rooyen, *Organometallics* **11**, **1992**, 629.
25. P.H. van Rooyen, M. Schindehutte, S. Lotz, *Inorg. Chim. Acta* **208**, **1993**, 207.
26. T.A. Waldbach, P.H. van Rooyen, S. Lotz, *Organometallics* **12**, **1993**, 4250.
27. T.A. Waldbach, R. van Eldik, P.H. van Rooyen, S. Lotz, *Organometallics* **16**, **1997**, 4056.
28. T.A. Waldbach, P.H. van Rooyen, S. Lotz, *Angew. Chem. Int. Ed. Engl.* **32**, **1993**, 710.
29. S. Lotz, M. Landman, D.I. Bezuidenhout, A.J. Olivier, D.C. Liles, P.H. van Rooyen, *J. Organomet. Chem.* **690**, **2005**, 5929.
30. C.M. Lukehart, G. Paull Torrence, *Inorg. Synth.* **28**, **1990**, 199, USA, John Wiley & Sons, Inc.
31. M.H. Quick, R.J. Angelici, *Inorg. Synth.* **28**, **1990**, 156, USA, John Wiley & Sons, Inc.
32. E.O. Fischer, E. Offhaus, *Chem. Ber.* **102**, **1969**, 2449.
33. Y.M. Terblans, H.M. Roos, S. Lotz, *J. Organomet. Chem.* **566**, **1998**, 133.
34. M. Landman, H. Görls, S. Lotz, *J. Organomet. Chem.* **617-618**, **2001**, 280.
35. M.F. Lappert, P.L. Pye, *J. Chem. Soc., Dalton Trans.* **1977**, 1283.
36. R.J. Angelici, F. Basolo, *J. Am. Chem. Soc.* **84**, **1962**, 2495.

37. L. Brandsma, H. Verkruijse, *Preparative Polar Organometallic Chemistry 1*, Springer-Verlag, Berlin **1987**, 125.
38. D.M. Adams, *Metal-Ligand and Related Vibrations: A Critical Survey of the Infrared and Raman Spectra of Metallic and Organometallic Compounds*, Edward Arnold Publishers Ltd, London **1998**.
39. L.J. Farrugia, *J. Appl. Crystallogr.* 30, **1997**, 565.
40. The POV-Ray Team, POV-Ray **2004**, URL: <http://www.pov-ray.org/download/>.
41. W.R. Harshbarger, S.H. Bauer, *Acta Crystallogr. B*26, **1970**, 1010.
42. H. Fischer, P. Hofmann, F.R. Kreissl, R.R. Schrock, U. Schubert, K. Weiss, *Carbyne Complexes*, VCH Publishers, New York **1988**.

4 Modification of Carbene Ligands: Aminolysis

4.1 Background

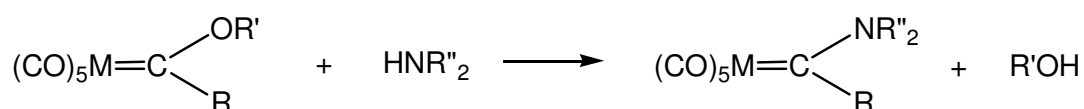
4.1.1 Overview

Aminocarbene complexes of transition metals are being increasingly seen as versatile starting materials for the synthesis of nitrogen-containing heterocycles^[1-10]. Their behaviour has been found to be fundamentally different from that of related alkoxy carbene complexes since nitrogen ylides, derived from ketene intermediates, have been isolated and shown to rearrange upon thermolysis to give pyrrolinones by 1,2 and 1,4 nitrogen to carbon migrations of alkyl groups.

4.1.2 Synthesis of aminocarbene complexes

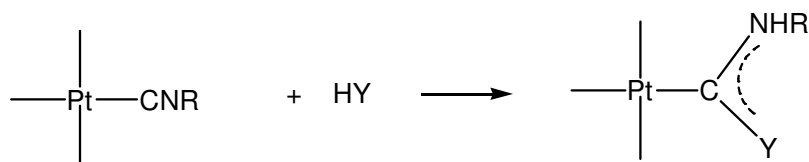
Due to the electrophilic nature of the carbene carbon of Fischer carbene complexes, nucleophilic attack on the carbene carbon is possible. Connor and Fischer first investigated the nucleophilic substitution reactions of Fischer carbene complexes with amines^[11], after the synthesis of the first aminocarbene complexes by Klabunde^[12]. It was found that the nucleophilic attack of the nitrogen lone pair on the carbene carbon atom leads to the elimination of alcohol and the formation of the aminocarbene product. This

outcome was rationalised by the view that the $M(CO)_5$ -moiety is electronically similar to a carbonyl oxygen atom, so that the reaction is similar to the aminolysis of esters to form amides.



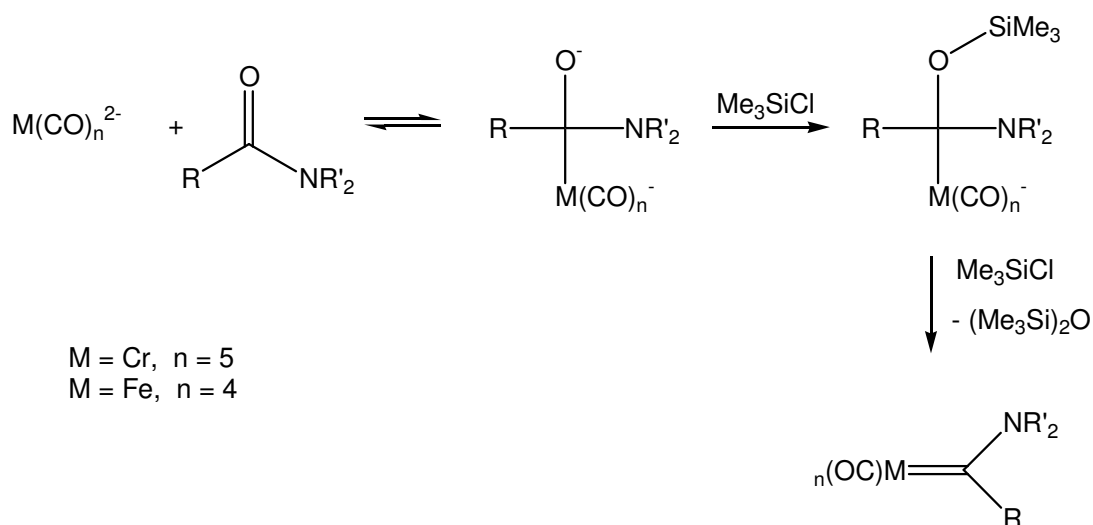
Scheme 4.1 Aminolysis of Fischer carbene complexes

As with the synthesis of alkoxy-carbene complexes, alternative synthetic methods were developed. Platinum complexes containing an isocyanide ligand easily undergo attack by protic nucleophiles such as amines or alcohols to yield metal-carbene derivatives (Scheme 4.2) through attack at the terminal carbon atom ^[13;14].



Scheme 4.2 Nucleophilic attack on isocyanide ligand of platinum complexes

Another example is the very efficient method for the preparation of chromium aminocarbene complexes introduced by Hegedus^[15] (Scheme 4.3). It involves the reaction of $Cr(CO)_5^{2-}$ with tertiary amides in the presence of chlorotrimethylsilane. The reaction proceeds via nucleophilic addition of $Cr(CO)_5^{2-}$ to the carbonyl group of an amide followed by the O-silylation of the adduct. Addition of excess chlorotrimethylsilane then affords the elimination of hexamethyldisiloxane and the formation of product aminocarbene ensues.



Scheme 4.3 Hedgedus synthesis of aminocarbene complexes

Since the synthesis of the first aminocarbene complexes, it was recognized that these complexes are more stable than their alkoxy analogues. This was ascribed to greater participation of the nitrogen lone pair compared to oxygen in stabilizing the electrophilic carbene carbon atom. The observations of Kreissl that $[\text{W}(\equiv\text{CC}_6\text{H}_4\text{Me-4})\text{Cp}(\text{CO})_2]$ reacts with hydrogen chloride to form the acyl complex $[\text{W}(\eta^2\text{-C}(\text{O})\text{CH}_2\text{C}_6\text{H}_4\text{Me-4})\text{Cp}(\text{CO})\text{Cl}_2]$ ^[16], but the same reagent with $[\text{W}(\equiv\text{CNEt}_2)\text{Cp}(\text{CO})_2]$ affords the aminomethylene complex $[\text{W}(=\text{CHNEt}_2)\text{CpCl}(\text{CO})_2]$ ^[17] confirmed the indications that amino substituents could stabilize carbene ligands bound to mid-valent Group VI metal centres.

4.1.3 Binuclear aminocarbene complexes

After Fischer's first paper^[18] reporting the synthesis of several binuclear alkoxy-carbenes of the type $[\text{M}_2(\text{CO})_9\{\text{C}(\text{OR}')\text{R}\}]$ ($\text{M} = \text{Mn}, \text{Tc}, \text{Re}$; $\text{R} = \text{alkyl or aryl}$; $\text{R}' = \text{alkyl}$)^[19], there was some uncertainty as to whether the carbene ligand was in the equatorial or the axial position (C_s or C_{4v} symmetry) relative to the Mn-Mn bond when the carbene was bulky. X-ray crystal structure determination of $[\text{Mn}_2(\text{CO})_9\{\text{C}(\text{OCH}_3)\text{C}_6\text{H}_5\}]$ proved the carbene occupies the equatorial position^[20].

Post and Watters were the first to report the preparation and characterization of methylaminocarbene of binuclear metal carbonyl complexes^[21]. From the infrared and Raman data they obtained, they concluded that both complexes $[\text{Mn}_2(\text{CO})_9\{\text{C}(\text{NHCH}_3)\text{CH}_3\}]$ and $[\text{Re}_2(\text{CO})_9\{\text{C}(\text{NHCH}_3)\text{CH}_3\}]$ were equatorially substituted. While the dirhenium aminocarbene could be isomerized into a *cis-trans* mixture about the C-N bond, no *trans* dimanganese aminocarbene complex could be isolated.

4.1.4 Focus of this study

In order to investigate the possibility of manipulating the orientation of carbene ligands of the dimanganese carbene complexes synthesized in Chapter 2, the aminolysis of these compounds were carried out.

After successful aminolysis with ammonia gas, the reactions were repeated with the more bulky secondary amines, diethylamine and diisopropylamine. These attempts did not prove possible, and could be explained by the observation made by Werner^[22]. The mechanism proposed by Werner for aminolysis involves more than one amine to activate the carbene carbon atom. This implies that only small amines will affect this type of reaction in already hindered carbene complexes. The reaction of the primary amine, propylamine, more bulky than ammonia but small enough to be accommodated as substituent on the carbene ligand of the binuclear complexes, was then attempted and proved successful.

Once again, the rhenium analogues of the dimanganese monocarbene complexes were also synthesized and characterized for comparison of the steric and electronic properties of the amino-substituted carbene ligands. Figure 4.1 illustrates the complexes synthesized in this chapter.

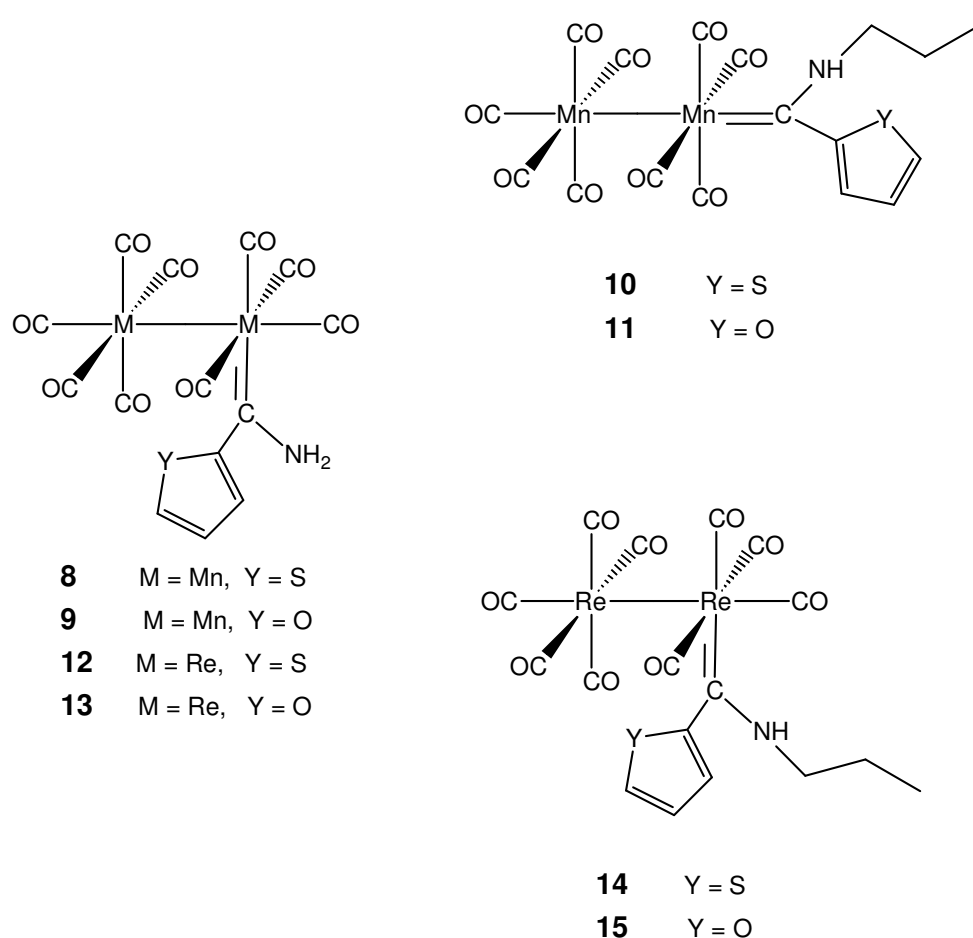
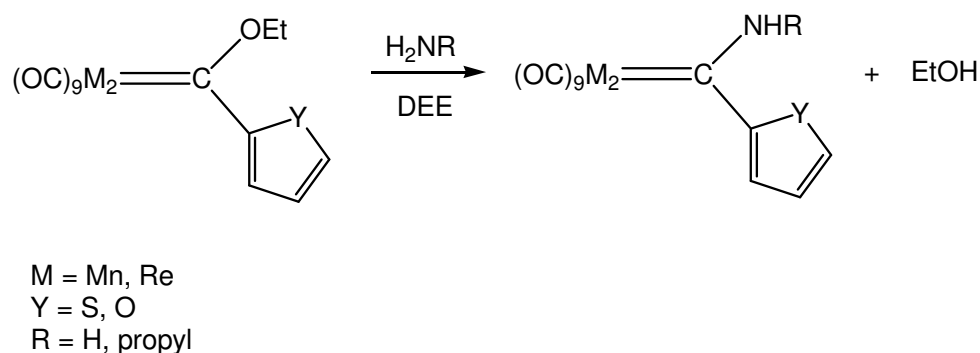


Figure 4.1 Binuclear aminocarbene complexes synthesized

4.2 Synthesis

Synthesis of the aminocarbene complexes was carried out as described by Klabunde and Fischer^[12]. A slow stream of ammonia was bubbled through a solution of the binuclear ethoxycarbene complexes dissolved in diethyl ether at room temperature. The colour of the solution changed rapidly from red to orange. After thin layer chromatography confirmed that all the ethoxycarbene complex had been converted, the solvent was removed and the aminocarbene complexes were purified by column chromatography on aluminium oxide, and complexes **8**, **9**, **12** and **13** were obtained in yields greater than 85%.



Scheme 4.4 Aminolysis of binuclear ethoxycarbene complexes

The procedure was repeated, but instead of bubbling ammonia gas through the solution, excess propylamine was added to the reaction mixture in ether, to obtain the propylamine-substituted carbene complexes **10**, **11**, **14** and **15** in yields ranging from 75 to 87%.

4.3 Characterisation

The aminocarbene complexes **8** - **15** were characterized spectroscopically in solution and in the solid state by mass spectrometry and X-ray crystallography.

4.3.1 NMR Spectroscopy

In the 1H NMR spectra of the manganese complexes **8** - **11**, the heteroarene and amine protons are duplicated in a major and minor isomer. The same duplication of carbon resonances was observed in the ^{13}C NMR spectra for these four complexes. We suspect that in solution, a mixture of the equatorial

and axial isomers exists. However, it is unclear which set of signals belongs to which isomer.

Both the ^1H and ^{13}C NMR spectra of complex **8** and **9** were recorded in acetone- d_6 , as no clearly resolved spectra could be obtained in CDCl_3 . The rest of the complexes were analysed in the deuterated chloroform, and better resolution was achieved than for **8** and **9**. The same numbering system of the carbon atoms and protons of the heteroarene substituents was used as before.

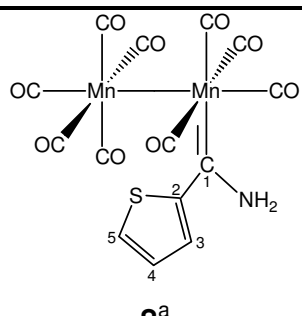
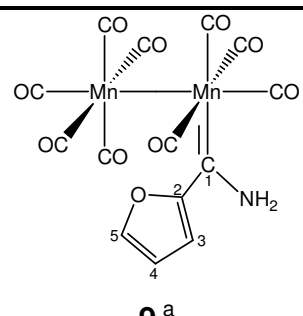
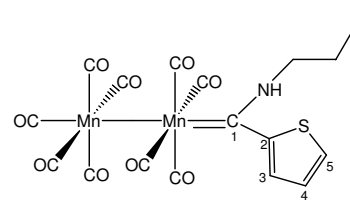
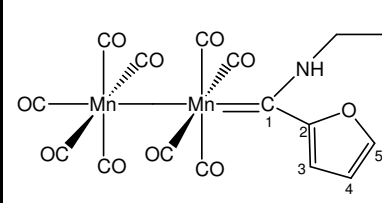
4.3.1.1 ^1H NMR Spectroscopy

The ^1H NMR data of **8** - **15** are summarized in Table 4.1. For **8** and **9**, the major and minor isomers (duplication of signals) were easily distinguishable, but the signals in the spectrum of **10** and **11** respectively were too broadened, so that no J couplings, nor the duplication of the proton resonances of the isomers were observed.

Figure 4.2 is an expansion of the aromatic region in the ^1H NMR spectrum recorded for **8**, showing the duplication of the thienyl ring protons, the major and minor isomer having different signal intensities. The N-H proton signals overlap, so that assignment of the N-H protons of both isomers cannot be done.

The broadening of signals in the spectra of **8** - **11** might be due to the paramagnetic nature of $\text{Mn}(0)$, possibly present as a decomposition product. No consistent upfield or downfield shift of the chemical shift values of the ring protons could be observed.

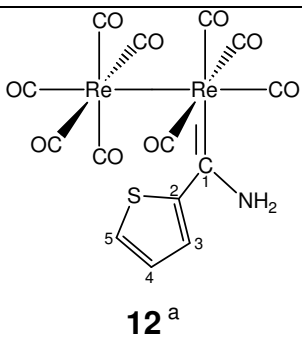
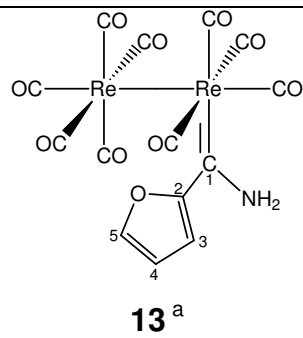
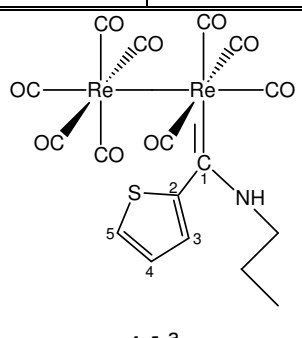
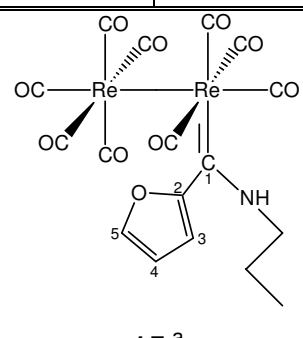
Table 4.1 ^1H NMR data of complexes **8** - **15**

Assignment	Complexes			
	Chemical shifts (δ , ppm) and coupling constants (J , Hz)			
	 8^a		 9^a	
Proton	<i>Isomer a</i>	<i>Isomer b</i>	<i>Isomer a</i>	<i>Isomer b</i>
H3	7.81 d (4.2)	7.95	7.50	6.79
H4	7.24 d (4.4)	7.31	6.78	n.o.
H5	7.59 d (2.1)	7.74	7.96	7.54
-NH ₂	10.57, 9.78	9.95, n.o. signal overlap	10.49, 9.90	9.48, n.o. signal overlap
Assignment	 10^b		 11^b	
Proton	<i>Peaks too broad to distinguish between isomers</i>			
H3	7.47		7.41	
H4	6.82		6.75	
H5	7.05		7.64	
-NCH ₂ CH ₂ CH ₃	1.67		1.74	
-NCH ₂ CH ₂ CH ₃	1.24		1.00	
-NCH ₂ CH ₂ CH ₃	0.96		0.84	
-NH	n.o.		n.o.	

 a) Spectra recorded in acetone- d_6

 b) Spectra recorded in CDCl_3

Table 4.1 contd. ^1H NMR data of complexes **8 - 15**

Assignment	Complexes			
	Chemical shifts (δ , ppm) and coupling constants (J , Hz)			
	 12^a		 13^a	
Proton	δ	J	δ	J
H3	7.60 (dd)	5.2, 0.9	7.53 (dd)	5.0, 1.6
H4	7.19 (dd)	5.0, 3.9	6.62 (dd)	5.0, 3.9
H5	7.58 (dd)	4.0, 1.0	7.62 (dd)	3.8, 1.8
-NH ₂	8.32, 8.14 (s, s)	-	8.87, 8.03 (s, s)	-
Assignment	 14^a		 15^a	
Proton	δ	J	δ	J
H3	7.64 (dd)	5.0, 1.0	7.65	n.o.
H4	6.90 (dd)	5.0, 3.7	6.89	n.o.
H5	7.07 (dd)	3.6, 1.1	7.65	n.o.
-NCH ₂ CH ₂ CH ₃	1.18 (t)	7.0	1.24	n.o.
-NCH ₂ CH ₂ CH ₃	1.66 (tt)	7.2, 7.5	1.08	n.o.
-NCH ₂ CH ₂ CH ₃	0.94 (t)	7.4	0.99	n.o.
-NH	8.52 (s)	-	8.60	n.o.

 a) Spectra recorded in CDCl₃

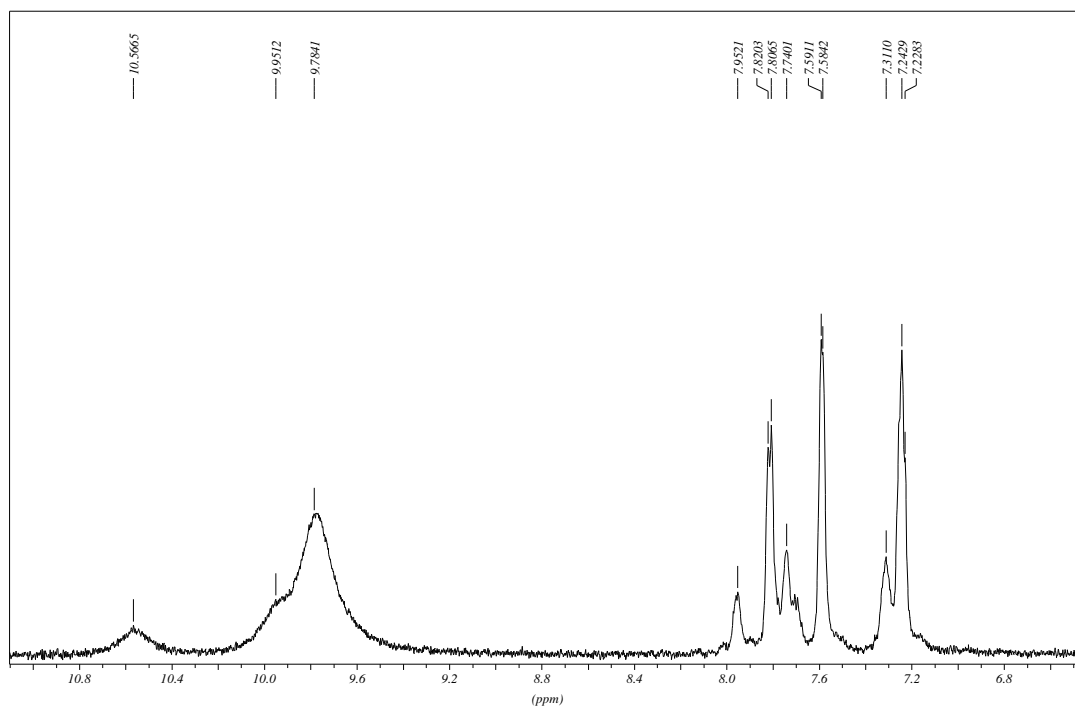


Figure 4.2 Expansion of the ^1H NMR spectrum of **8** in acetone- d_6 illustrating the presence of a major and minor isomer

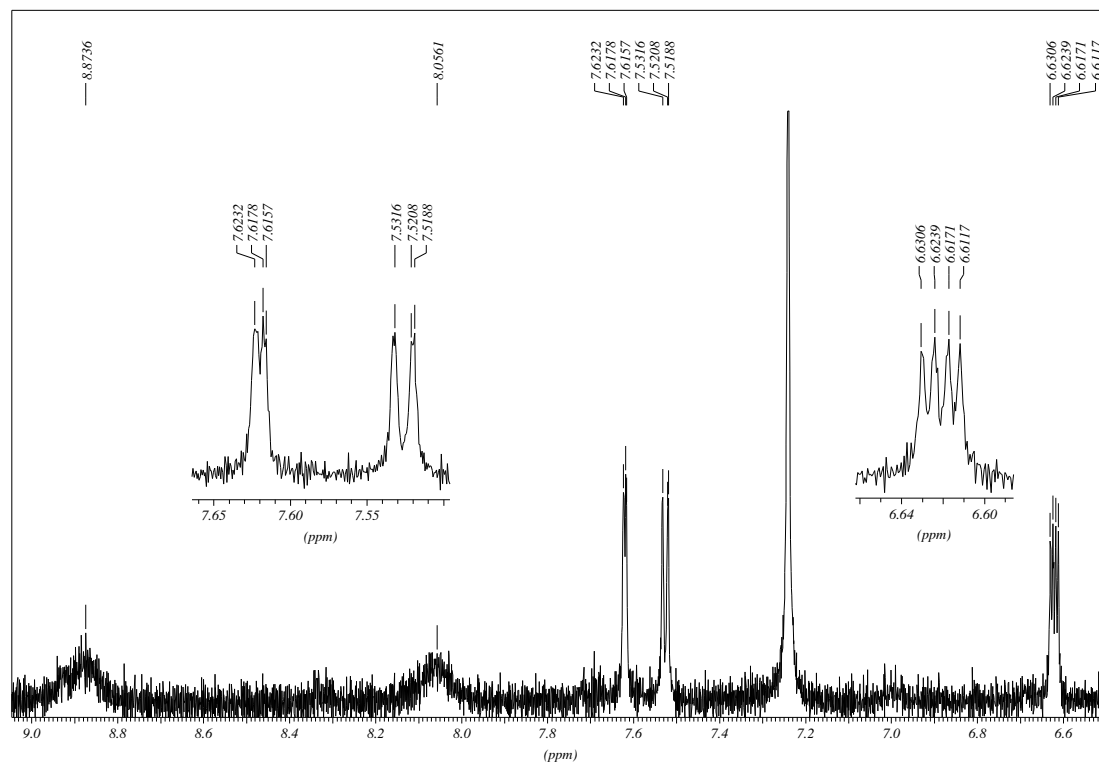


Figure 4.3 An expansion of the ^1H NMR spectrum of **13** in CDCl_3

4.3.1.1 ^{13}C NMR Spectroscopy

The ^{13}C NMR data of **8** - **15** are reported in Table 4.2 and 4.3. Better resolution of the signals was attained than for the ^1H NMR spectra, with the presence of a major and a minor isomer of the manganese complexes in solution clearly visible in the spectra. No ^{13}C NMR spectra could be obtained for **10** and **15** due to the decomposition of these complexes during spectrum recording.

Figure 4.4 shows the mixture of isomers present in solution for **11**, while the absence of a duplicated set of signals is apparent when looking at Figure 4.5, the ^{13}C NMR spectrum of the dirhenium aminocarbene **14**.

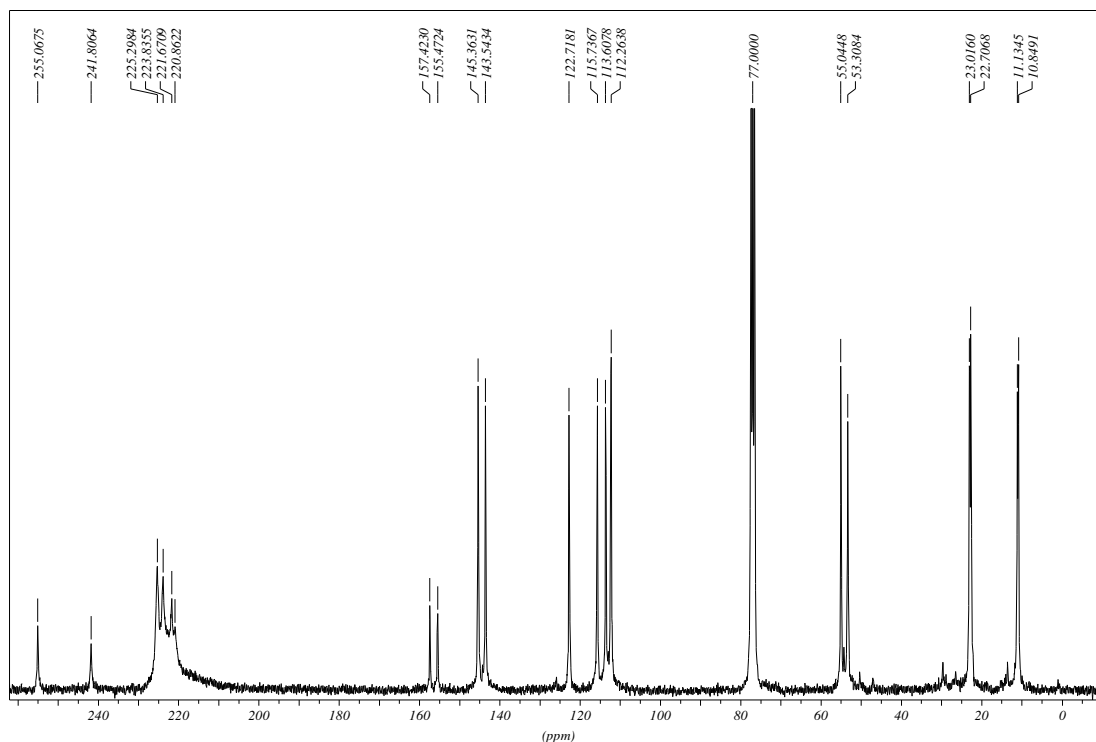


Figure 4.4 ^{13}C NMR spectrum of **11** in CDCl_3 , displaying duplication of carbon resonances for the two isomers

Table 4.2 ^{13}C NMR data of complexes **8**, **9**, **11** and **14**

Assignment	Complexes			
	8^a		9^a	
	<i>Isomer a</i>	<i>Isomer b</i>	<i>Isomer a</i>	<i>Isomer b</i>
Carbon	δ (ppm)	δ (ppm)	δ (ppm)	δ (ppm)
C1	269.6	262.6	275.4	267.6
C2	157.5	156.3	150.8	150.2
C3	133.8	135.9	121.0	117.3
C4	132.0	131.1	117.1	116.9
C5	132.1	131.1	123.5	120.9
M(CO) ₄	227.8	226.4	233.6	229.1
M(CO) ₅	225.7, 223.9	224.7, 222.8	228.4, 226.2	224.2, n.o. signal overlap
Assignment	11^b		14^b	
	<i>Isomer a</i>	<i>Isomer b</i>		
C1	255.1	241.8	239.3	
C2	157.4	155.5	150.4	
C3	122.7	115.7	127.0	
C4	113.6	112.3	124.2	
C5	145.4	143.5	128.2	
M(CO) ₄	225.3	223.8	199.9	
M(CO) ₅	221.7, n.o. signal overlap	220.9, n.o. signal overlap	193.9, 190.2	
-NCH ₂ CH ₂ CH ₃	55.0	53.3	56.5	
-NCH ₂ CH ₂ CH ₃	23.0	22.7	29.7	
-NCH ₂ CH ₂ CH ₃	11.1	10.8	10.9	

 a) Spectra recorded in acetone-d₆

 b) Spectra recorded in CDCl₃

Table 4.3 ^{13}C NMR data of complexes **12** and **13**

Assignment	Complexes ^a	
	12	13
Carbon	δ (ppm)	δ (ppm)
C1	268.8	238.0
C2	166.7	n.o.
C3	131.6	126.0
C4	128.9	114.3
C5	130.8	145.8
M(CO) ₄	198.8	200.5
M(CO) ₅	196.2, 184.0	197.9, 184.8

a) Spectra recorded in CDCl_3

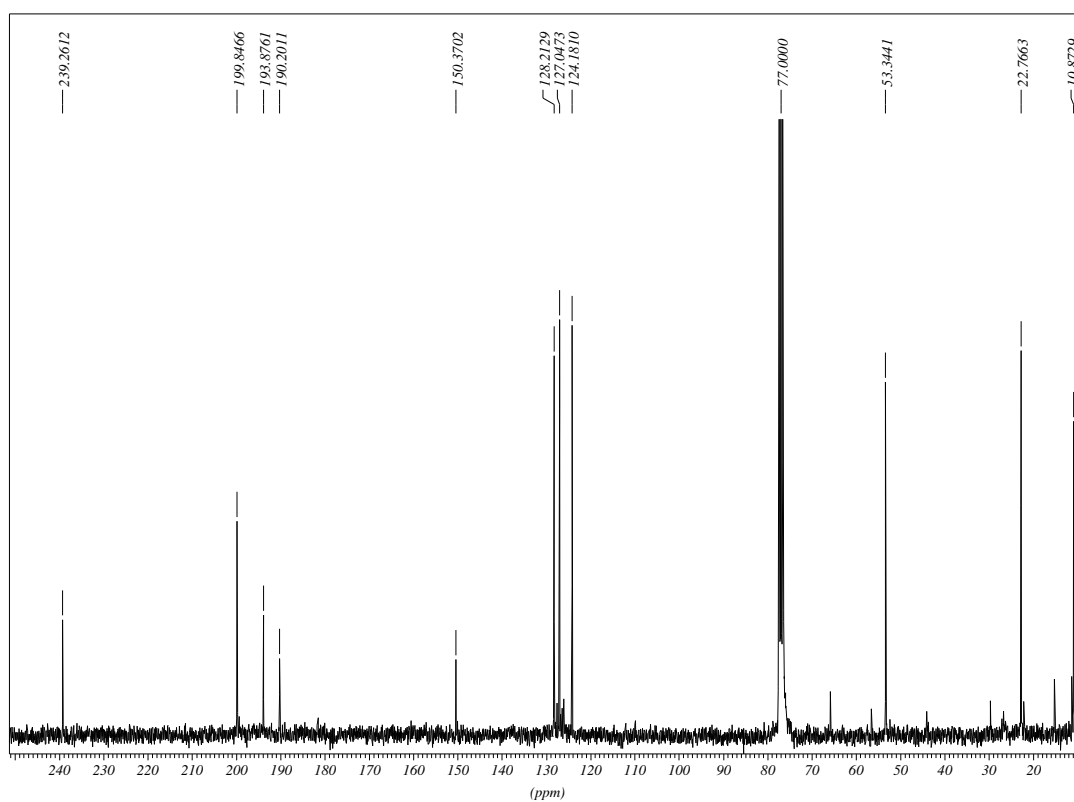


Figure 4.5 ^{13}C NMR spectrum of **14** in CDCl_3

A significant upfield shift of the chemical shift value of the C1 carbene carbon atom resonance of $\Delta\delta = 20 - 50$ ppm is observed in all recorded spectra (Table 4.2, 4.3), when compared to the ethoxycarbene analogues, although a smaller upfield shift for the arene carbon atoms are seen. This is ascribed to the greater ability of the nitrogen lone pair (compared to oxygen as heteroatom in these Fischer carbene complexes) to donate electron density to the electrophilic carbene carbon atom, stabilizing and shielding the nucleus.

On the other hand, a downfield shift of the terminal carbonyls is observed in the case of **8** and **9**, but for **10 - 14** the chemical shift values for the metal carbonyls are comparable with their ethoxy analogues characterized in Chapter 2, or previously reported in the case of the dirhenium compounds^[23]. A possible explanation could be found when looking at the X-ray structures of **8** and **9**: the configuration of these complexes changed from axial ethoxycarbenes to equatorial aminocarbene complexes. Complexes **10 - 15** retain the configuration shown originally in the ethoxy precursors, and their carbonyl groups are fairly insensitive to changes of substituents on ligands.

4.3.2 IR Spectroscopy

The infrared spectra of **8 - 15** were recorded in dichloromethane, instead of the usual hexane, due to the insolubility of these aminocarbene complexes in hexane. The theory of the ν_{CO} vibrations of bimetal nonacarbonyl compounds was discussed in Chapter 2. For the *eq*-[M₂(CO)₉L] complexes with C_s symmetry, a nine band pattern is expected in the IR spectrum, while five bands are expected for the *ax*-[M₂(CO)₉L] displaying C_{4v} symmetry. The five band pattern was observed for both **10** and **11**, the propylamine-substituted carbene complexes of dimanganese (Table 4.4). This indicated that the complexes retained their axial configuration during the nucleophilic substitution reaction.

Table 4.4 IR data in the carbonyl region of **10**, **11**^a

Complex	Carbonyl stretching frequencies (ν_{CO} , cm^{-1}) for pseudo- C_{4v} symmetry of $ax\text{-}[\text{Mn}_2(\text{CO})_9(\text{carbene})]$				
	A_1 (1)	A_1 (2)	E (1)	A_1 (3)	E (2)
10	2083 (w)	2029 (m)	1985 (vs)	1975 (s)	1926 (m)
11	2082 (m)	2012 (s)	1984 (vs)	1957 (s)	1928 (m)

a) DCM as solvent

In the case of **8**, **9**, **12** - **15**, the IR spectrum displayed only six bands, two of which are strong (Table 4.5). The observation of only six bands instead of the expected nine pattern for the C_s symmetry of an equatorially substituted $[\text{M}_2(\text{CO})_9\text{L}]$, can be explained by the following factors. In the first case, band overlap of the bands could have occurred due to solvent interaction. The assignments of the carbonyl stretching frequencies made in Table 4.5 are done as if this was the case. On the other hand, the solvent hexane is more inert towards the vibrational modes of the compounds and displays a greater resolution power in the spectra. In a non-polar hexane solution, the degeneracy of the band can be lifted, leading to the splitting of bands into two separate bands of different vibrational frequencies^[24]. Therefore, in the polar dichloromethane solvent fewer bands will be seen as when the spectrum is recorded in hexane. According to the rules specified by Nakamoto, if the A' and A'' vibrational modes become degenerate in dichloromethane, the resulting band can be assigned as an A'' mode. The same scenario was observed recently in our laboratories^[25], when the IR spectrum of a $[\text{M}(\text{CO})_5\text{L}]$ complex was recorded in dichloromethane. Recording the spectrum of the same compound in hexane led to the splitting of the E-band observed in dichloromethane into two separate bands as the degeneracy associated with the E-band was lifted.

Table 4.5 IR data in the carbonyl region of **8**, **9**, **12** - **15**^a

Complex	Carbonyl stretching frequencies (ν_{CO} , cm^{-1}) for C_s - symmetry of $eq\text{-}[M_2(\text{CO})_9(\text{carbene})]$					
	A'(1)	A'(2) and A'(3)	A''(1) and A'(4)	A''(2)	A'(5)	A'(6) and A''(3)
8	2084 (s)	2013 (s)	1987 (s)	1979 (s)	1960 (m)	1937 (m)
9	2082 (m)	2012 (s)	1984 (vs)	1977 (s)	1956 (m)	1935 (s)
12	2099 (w)	2035 (m)	1992 (vs)	1984 (s)	1961 (m)	1932 (s)
13	2098 (w)	2034 (m)	1990 (vs)	1983 (s)	1958 (m)	1931 (s)
14	2098 (w)	2034 (m)	1992 (vs)	1982 (s)	1959 (m)	1928 (m)
15	2098 (w)	2033 (m)	1990 (s)	1982 (s)	1958 (m)	1930 (s)

a) DCM as solvent

In the case of the dirhenium monocarbenes, all complexes show an equatorial configuration, but the amino-substituted dimanganese monocarbenes display equatorial configuration while the propylamine-substituted complexes are seen to be axially substituted.

Post and Watters reported the N-H vibrational frequencies obtained in the solid state^[21]. For their dimanganese and dirhenium aminomonocarbene complexes, two N-H stretch bands were observed in the region 3330 - 3405 cm^{-1} , assigned to a *cis* and *trans* configuration respectively, with the *cis* N-H stretch occurring at a higher wavenumber. Also observed were the N-H bend vibrational frequencies in the region 1530 - 1575 cm^{-1} . When inspecting the IR spectra recorded in solution for **8** - **15**, very weak N-H stretch bands were seen for **8**, **9**, **11** and **13** as listed in Table 4.6, but the N-H bands of the rest of the synthesized compounds were too weak to be observed in solution. No signal for the N-H bend was observed.

Table 4.6 N-H vibrational frequencies in the IR spectra of binuclear aminocarbene complexes^a

N-H stretch (cm ⁻¹)	8	9	11	13
<i>cis</i> N-H	3453	3473	3393	3479
<i>trans</i> N-H	3328	3348	3316	3351

a) DCM as solvent

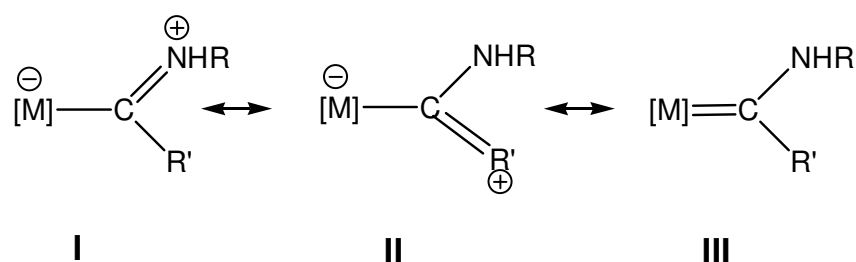


Figure 4.6 Limiting structures for carbene complexes

The structure of carbene complexes may be understood in terms of three limiting forms (I, II and III) that contribute to the stabilization of the formally electron-deficient carbene carbon (Figure 4.6). In limiting structure I the substituent R serves as a π -donor, while in limiting structure II substituent Y serves as a π -donor. Limiting structure III is stabilized by π -donation from the metal. Structural evidence^[26;27] led to the assumption that amine substituents are better π -donors than ethoxy substituents. Therefore the contribution of limiting structure I becomes more important where amine substituents are concerned, while metal π -donation is a larger contributing factor in the case of ethoxy substituents. Aryl substituents are generally poor π -donors to the carbene carbon and as a result carbene complexes with aryl substituents must either have substantial π -donation from the other substituent or a substantial contribution from limiting form III. Carbene complexes with π -

donor substituents (structures **I** and **II**) will have low M-C(carbene) bond orders and longer M-C(carbene) bond distances. The opposite is true for complexes with poor π -donor substituents (structure **III**).

Transition metal carbonyl bonds can be described as two resonance structures (Figure 4.7). In the case of the ethoxycarbene complex, metal π -donation is necessary to stabilize the electrophilic carbene carbon. Backbonding from the metal to the carbonyl carbon decreases, hence decreasing the M-C(carbonyl) bond order and simultaneously increasing the C(carbonyl)-O bond order. For aminocarbene complexes, less metal π -donation to the carbene carbon is necessary since the amine substituent stabilizes the carbene carbon. Backbonding from the metal to the carbonyl carbon increases resulting in a higher M-C(carbonyl) bond order and a decrease in the C(carbonyl)-O bond order. This explains the lower stretching frequencies observed on the spectra of complexes **10** and **11** compared to those of the ethoxycarbene complexes **2** and **3**, which is especially pronounced in the vibration wave number for the E(1) and E(2) bands.

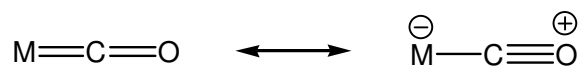


Figure 4.7 Resonance structures for M-C-O bonds

4.3.3 Mass Spectrometry

The mass spectral data of the aminocarbenes are summarized in Table 4.7 for the dirhenium compounds, and in Table 4.8 for the dimanganese complexes. In the case of **14** and **15**, no molecular ion peak was observed, and little information about the fragmentation pattern could be obtained. For the rest of the complexes, however, clear fragmentation patterns can be distinguished (Scheme 4.5, 4.6).

Table 4.7 Mass spectral data of the dirhenium aminocarbene complexes^a

Complex	m/z	Intensity (%)	Fragment ion
12	736	7	[M] ⁺
	409	52	[M – Re(CO) ₅] ⁺⁺
	381	13	[M – Re – 6CO] ⁺⁺
13	719	19	[M] ⁺
	664	7	[M – 2CO] ⁺
	636	6	[M – 3CO] ⁺
	393	94	[M – Re(CO) ₅] ⁺⁺
	365	24	[M – Re – 6CO] ⁺⁺
	337	6	[M – Re – 7CO] ⁺⁺

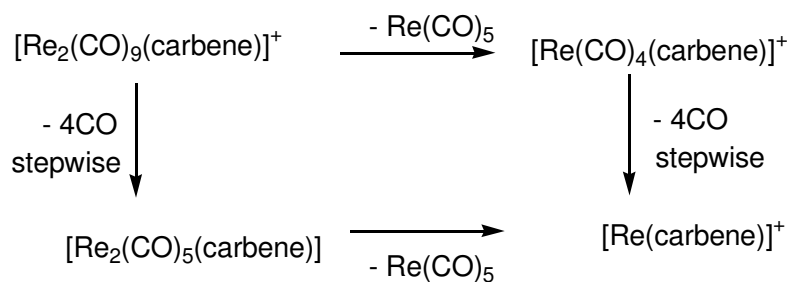
a) No [M⁺] was observed for **14** and **15**

The dirhenium aminocarbene complexes (**12**, **13**) lose the [Re(CO)₅]⁺-fragment by Re-Re bond cleavage first, followed by the loss of two further carbonyl ligands. This is the preferred fragmentation route, as seen by the intensities of the [M – Re(CO)₅]⁺⁺ fragment ion observed. The second route is the stepwise loss of carbonyl ligands after which the [Re(CO)₅]⁺-fragment is lost. The unusual fragmentation of the carbene ligand was not observed for the manganese analogues.

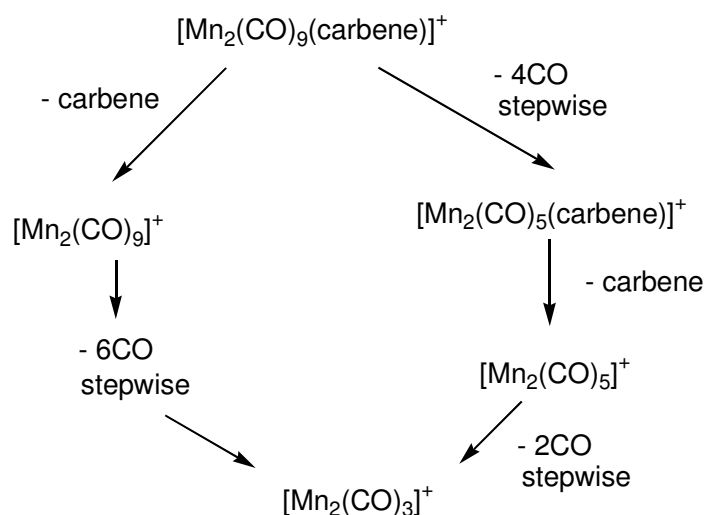
For the dimanganese aminocarbene complexes, no Mn-Mn bond breaking and loss of the Mn(CO)₅⁺-fragment ion can be seen. This can be ascribed to the much shorter Mn-Mn bondlength due to the smaller atomic radii of the manganese atoms when compared to rhenium. Instead, carbonyl ligands are lost first, followed by the carbene ligand. Subsequent loss of carbonyl ligands then continue until only a Mn₂(CO)₃-fragment remains. The other possible route is the fragmentation of the carbene ligand first, and then the stepwise fragmentation of carbonyl ligands. This early loss of the complete carbene ligand is an unusual feature in the mass spectrometry of carbene complexes.

Table 4.8 Mass spectral data of the dimanganese aminocarbene complexes

Complex	m/z	Intensity (%)	Fragment ion
8	473	4	$[M]^+$
	429	29	$[M - CO - NH_2]^+$
	362	12	$[M - (\text{carbene})]^+$
	278	44	$[M - 3CO - (\text{carbene})]^+$
	222	9	$[M - 5CO - (\text{carbene})]^+$
9	457	22	$[M]^+$
	401	14	$[M - 2CO]^+$
	345	10	$[M - 4CO]^+$
	306	15	$[M - 2CO - (\text{carbene})]^+$
	278	27	$[M - 3CO - (\text{carbene})]^+$
	250	37	$[M - 4CO - (\text{carbene})]^+$
	222	26	$[M - 5CO - (\text{carbene})]^+$
	194	26	$[M - 6CO - (\text{carbene})]^+$
10	515	-	$[M]^+$ n.o.
	459	38	$[M - 2CO]^+$
	306	19	$[M - 2CO - (\text{carbene})]^+$
11	499	12	$[M]^+$
	304	100	$[M - 2CO - (\text{carbene})]^+$
	278	32	$[M - 3CO - (\text{carbene})]^+$
	250	42	$[M - 4CO - (\text{carbene})]^+$
	222	29	$[M - 5CO - (\text{carbene})]^+$
	194	31	$[M - 6CO - (\text{carbene})]^+$



Scheme 4.5 Fragmentation routes for $[\text{Re}_2(\text{CO})_9(\text{carbene})]$



Scheme 4.6 Fragmentation pattern for $[\text{Mn}_2(\text{CO})_9(\text{carbene})]$

4.3.4 X-Ray Crystallography

Single crystal X-ray diffraction studies confirmed the molecular structure of complexes **8**, **9** and **11**. The X-ray structures corroborated the observations made from the infrared data: the dimanganese propylaminocarbene complexes have an axially substituted carbene ligand, while the dimanganese aminocarbene has an equatorial configuration. The complexes crystallized from a dichloromethane:hexane (1:1) solution by layering of the solvents,

yielding light orange crystals for **8**, **9** and **11** of good quality. Figures 4.8, 4.9 and 4.10 represent the ORTEP^[28] + POV-Ray^[29] plots of the geometry of these complexes. Once again, the same atom numbering system is used as employed in the previous chapters.

All three complexes crystallize in the monoclinic system, space group $P2_1/c$ with four molecules in the unit cell. Selected bond lengths and angles determined for the complexes are tabulated in Table 4.9 and 4.10 respectively, whilst the most important torsion angles are listed in Table 4.11. The complete crystallographic data of **8**, **9** and **11** are listed in Appendices 5, 6 and 7 respectively.

The average Mn-CO and Mn-Mn bond lengths of all three complexes are very similar to that of the ethoxycarbene precursors (Table 4.9). The Mn-C(carbene) bond length for **8** (2.019(3)Å), **9** (2.0275(16)Å) and **11** (1.994(5)Å) is significantly longer than the corresponding distance in **2** (1.933(7)Å) and **3** (1.932(2)Å), indicating a weaker Mn-C(carbene) bond due to less back bonding from the Mn metal centre to the carbene carbon. A very short C(carbene)-N bond length [**8** (1.315(4)Å); **9** (1.310(2)Å; **11** (1.351(12)Å)] indicates double bond character and implies a high degree of electron donation from the nitrogen lone pair to the electrophilic carbene carbon^[30]. This is also evident from the chemical shift of the carbene carbon atom at 269 ppm for **8**, 275 ppm for **9** and 255 ppm for **11** compared to 307 ppm for **2** and 301 ppm for **3**.

The Mn-C(carbene) bond is also slightly shorter for the axial carbene ligand in **11** compared to the equatorial carbene ligands of **8** and **9**. This means that the carbene carbon in the axial position must participate more in π -backbonding, due to the metal-metal bond *trans* to it, compared to when carbonyl ligands are *trans* to the carbene ligand in the equatorial position. As a result of this, the nitrogen atom in the axial carbene ligand shows less participation in the stabilization of the carbene carbon, as indicated by the slightly longer C(carbene)-N bond length of **11** than for **8** or **9**.

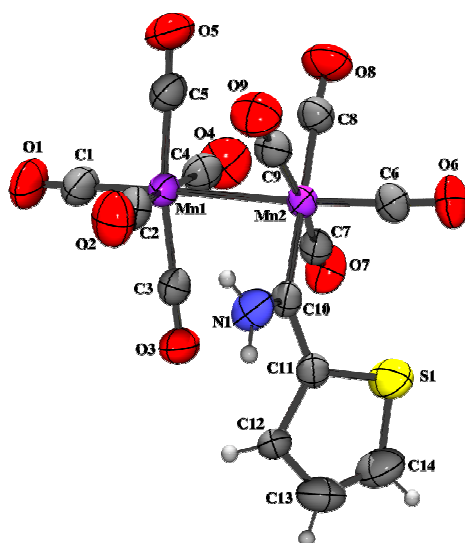


Figure 4.8 ORTEP + POV-Ray plot of the geometry of complex **8**

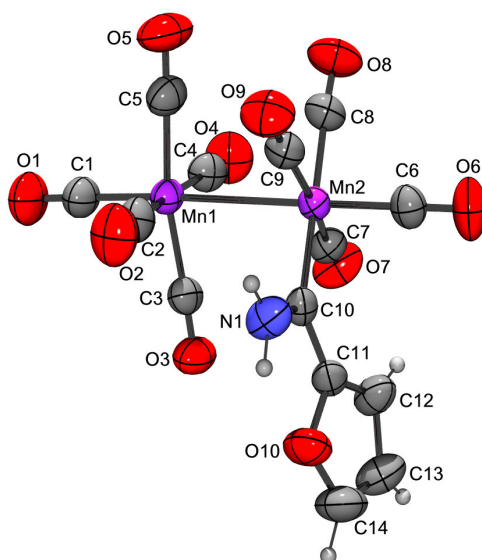


Figure 4.9 ORTEP + POV-Ray plot of the geometry of complex **9**

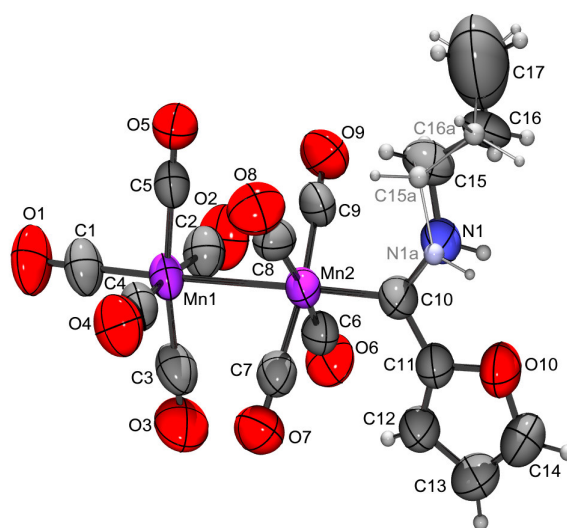


Figure 4.10 ORTEP + POV-Ray plot of the geometry of complex **11**

In contrast to the dimanganese ethoxycarbene **2** and the cleaved iodo-monomanganese carbene complex **7**, the thienyl ring of **8** is not close to being coplanar with the plane of the bonding geometry about the carbene carbon. The dihedral angle between the least-squares planes through (S(1), C(11), C(12), C(13) and C(14)) and through (C(10), C(11), N(1) and Mn(2)) is $39.7(1)^\circ$. The carbene ligand is in the preferred equatorial position, but to occupy this position, a deviation out of the plane is necessary to fit the thienyl S between the two closest carbonyl ligands C(6)-O(6) and C(7)-O(7). This deviation was also seen for the phenyl ring reported by Huttner and Regler for the *eq*-[Mn₂(CO)₉[C(OMe)Ph]] complex^[20]. The same is true for the furyl ring of complex **9**, but not **11**. The axial carbene ligand of the latter complex has enough space to adopt the preferred planar conformation.

From the X-ray crystal structure of **11**, a major and minor component was observed due to rotation of the propylamino-substituent around the N(1)-C(15) bond, such that the torsion angles of {C(9)-Mn(2)-C(10)-N(1) and C(8)-Mn(2)-C(10)-N(1)} for the two components are { $26.5(11)$ and $-64.8(11)^\circ$ } and { $67.2(11)$ and $-24.1(11)^\circ$ } respectively. The dihedral angles between the least-squares plane through (O(10), C(11), C(12), C(13) and C(14)), through (C(10), C(11), N(1), or Mn(2)) and (C(10), C(11), N(1a) and Mn(2)) are $12.9(5)^\circ$ and $9.5(6)^\circ$ respectively. This means that the furyl ring is close to

being coplanar with the plane of the bonding geometry about the carbene carbon, similar to the axial complexes **2** and **3**. The plane of the carbene carbon, furyl ring and nitrogen is approximately perpendicular to the equatorial plane of carbonyl ligands [C(10)-Mn(2)-CO (92 - 95°)] and is in an intermediate position between the carbonyl ligands around Mn(2), as is evident from the torsion angles of -47.3(5)° and 42.5(5)° for C(6)-Mn(2)-C(10)-C(11) and C(7)-Mn(2)-C(10)-C(11) respectively. As seen for the other axial binuclear carbene complexes (Chapter 2), the carbene ligand is in the *cis* configuration about the C(carbene)-N bond in **11**.

Table 4.9 Selected bond lengths of **8**, **9** and **11**

Atoms	Bond Lengths (Å)		
	8 (Y = S)	9 (Y = O)	11 (Y = O)
Mn(1)-C(1)	1.820(4)	1.8106(9)	1.798(5)
Mean Mn(1)-C(x) (x=2,3,4,5)	1.843(4)	1.847(2)	1.844(6)
Mn(1)-Mn(2)	2.9280(6)	2.9331(4)	2.9190(9)
Mean Mn(2)-C(x) (x=7,9) for 8,9 (x=6,7,8,9) for 11	1.845(3)	1.8435(18)	1.834(6)
Mn(2)-C(10)	2.019(3)	2.0275(16)	1.994(5)
C(10)-N(1)	1.315(4)	1.310(2)	1.351(12)
C(10)-C(11)	1.464(4)	1.452(2)	1.454(6)
C(11)-C(12)	1.496(4)	1.344(3)	1.329(7)
C(12)-C(13)	1.431(5)	1.414(3)	1.424(8)
C(13)-C(14)	1.321(7)	1.304(4)	1.312(9)
Mn(2)-C(6)	1.790(3)	1.7928(19)	-
Mn(2)-C(8)	1.836(3)	1.8355(19)	-
Y-C(11)	1.690(3)	1.376(2)	1.376(6)

Table 4.10 Selected bond angles of **8**, **9** and **11**

Atoms	Bond Angles (°)		
	8 (Y = S)	9 (Y = O)	11 (Y = O)
Mn(2)-C(10)-N(1)	125.7(2)	124.59(14)	124.1(7)
N(1)-C(10)-C(11)	109.8(3)	111.20(15)	111.9(6)
C(11)-C(10)-Mn(2)	124.4(2)	124.10(11)	122.2(3)
C(11)-Y-C(14)	93.09(19)	106.72(17)	107.0(5)
Y-C(11)-C(12)	111.5(2)	107.91(16)	108.2(4)
Y-C(14)-C(13)	113.2(3)	111.0(2)	110.3(6)
Y-C(11)-C(10)	122.8(2)	116.64(15)	118.0(4)
C(12)-C(13)-C(14)	116.8(4)	106.7(2)	106.4(6)
C(11)-C(12)-C(13)	105.4(3)	107.7(2)	108.0(5)

Complex **8** did not display major and minor components with the carbene ligand differing in orientation, unlike the disorder observed for **2** and **7**. This can be ascribed to the fact that the spatial similarity between the nearly coplanar ethoxy group and thienyl ring in the carbene ligand in both **2** and **7** is not present in the carbene ligand of **8**. The small NH₂-group of **8** and **9** can be accommodated adjacent to the carbonyl ligands C(2)-O(2), C(3)-O(3) and C(9)-O(9) in the equatorial plane. In **2** and **3**, with the carbene ligand adopting a *trans*-configuration about the C-O bond, the ethoxy group is too bulky to be accommodated and the carbene ligand is forced to occupy the axial position. This is also true in the case of **11**: the steric hindrance caused by the bulkier propylamine group forces the carbene ligand in the axial position, as it cannot be accommodated between the carbonyl ligands of the neighbouring metal centre. This is illustrated by the space-filling model of **9** in Figure 4.11 and **11** in Figure 4.12. Figure 4.11 shows the NH₂ group (N(1), H(1a), H(1b)) in relation to the adjacent carbonyl (C(9), O(9)) on Mn(2) and the adjacent carbonyl (C(2), O(2)) on Mn(1).

Table 4.11 Selected torsion angles of **8**, **9** and **11**

Atoms	Torsion Angles (°)	
	8 (Y = S)	9 (Y = O)
Mn(2)-C(10)-C(11)	- 142.7(2)	12.3(3)
Mn(2)-C(10)-C(11)-Y	38.8(3)	- 171.13(12)
C(9)-Mn(2)-C(10)-N(1)	10.4(3)	9.92(16)
C(7)-Mn(2)-C(10)-N(1)	- 160.4(3)	- 161.13(16)
Mn(1)-Mn(2)-C(10)-C(11)	106.7(2)	- 70.79(14)
C(8)-Mn(2)-Mn(1)-C(5)	- 40.16(16)	- 40.64(9)
C(9)-Mn(2)-Mn(1)-C(5)	49.18(15)	47.46(9)
Atoms	11 (Y = O)	
C(9)-Mn(2)-C(10)-N(1)	26.5(11)	
C(8)-Mn(2)-C(10)-N(1)	- 64.8(11)	
Mn(2)-C(10)-C(11)-C(12)	4.5(10)	
Mn(2)-C(10)-C(11)-Y	- 174.4(4)	
C(3)-Mn(1)-Mn(2)-C(6)	44.6(2)	
C(6)-Mn(2)-C(10)-C(11)	- 47.3(5)	
C(7)-Mn(2)-C(10)-C(11)	42.5(5)	

As can be seen from Figure 4.10, the nitrogen atom is orientated away from the adjacent carbonyl ligands. Steric hindrance is caused by the CH₂-group bonded to the nitrogen. Figure 4.12 illustrates the major component (C(15), H(15a), H(15b)) of the CH₂ of the disordered propylamine group in relation to the adjacent carbonyls (C(6),O(6) and C(7), O(7)) on Mn(2). The carbonyl (C(3), O(3)) is also shown space filled.

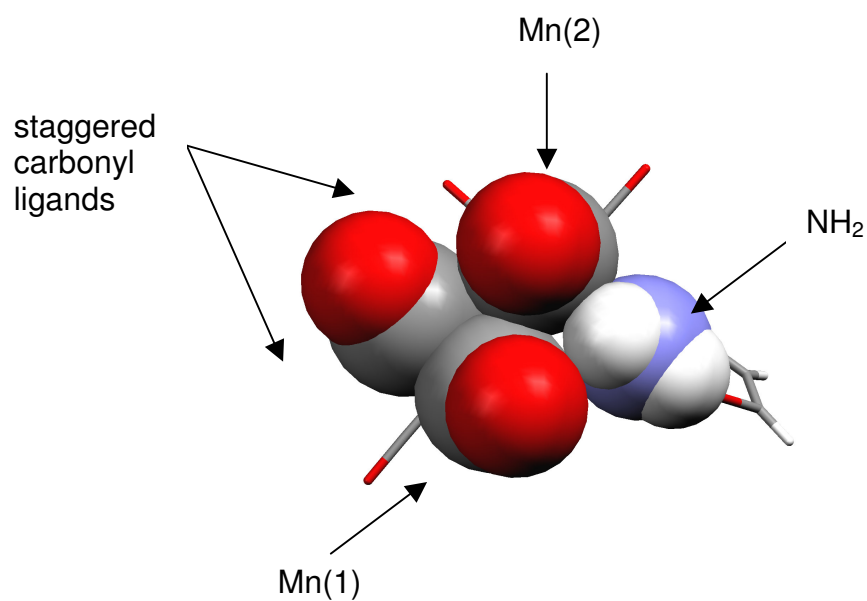


Figure 4.11 Space-filling model of **9** illustrating position of substituent NH₂-group on *eq*-carbene ligand

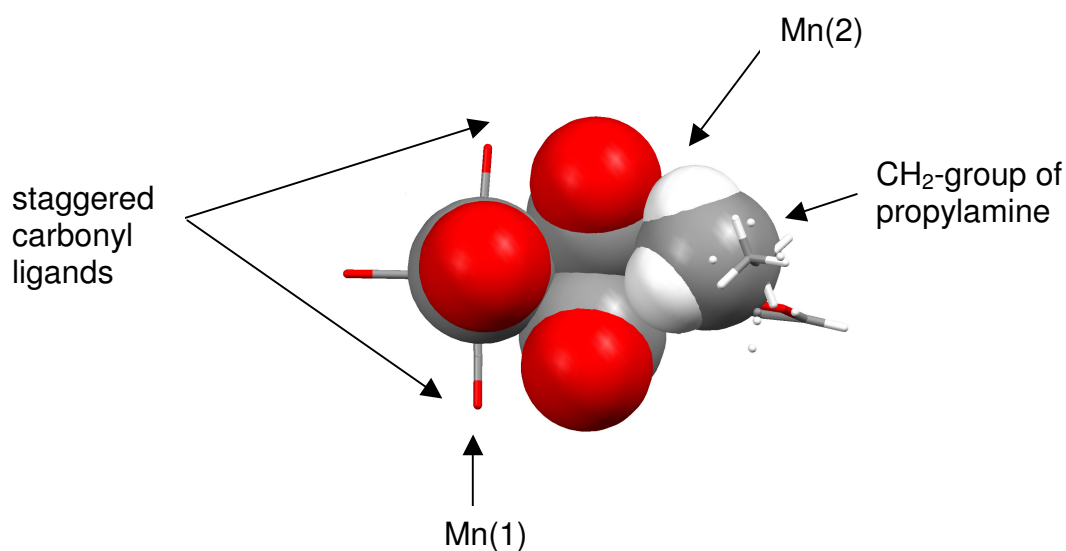


Figure 4.12 Space-filling model of **11** illustrating position of substituent propylamine on *ax*-carbene ligand

The torsion angles C(3)-Mn(1)-Mn(2)-C(6) for **11** is 44.6(2)°, similar to that of **2** and **3** (46.0(3)° and 45.97(10)°). For **8** and **9** the analogous C(8)-Mn(2)-

Mn(1)-C(5) torsion angles are $-40.16(16)^\circ$ and $-40.64(9)^\circ$ respectively. This indicates that the carbonyl ligands on adjacent manganese atoms are more staggered in **11**, the axially substituted binuclear carbene. **8** and **9** have a more eclipsed carbonyl conformation, but it is still significantly more staggered than the dirhenium monocarbene complex **5** (Chapter 2), with C(3)-Re(1)-Re(2)-C(8) $-30.93(19)^\circ$, due to the shorter Mn-Mn bond length.

When looking at the bonding geometry of the free thiophene and furan, and comparing it with the thienyl and furyl rings of **2**, **3**, **8**, **9** and **11**, it can be seen that the bond lengths of the aminocarbene complexes **8** and **9**, and especially **11**, more closely resemble that of the free heteroaryls (Table 2.8, 2.9 and 4.9). However, the bond angles of **2** and **3** are closer to the angles of the uncoordinated rings than **8**, **9** or **11** (Table 4.10). The high degree of electron donation from the nitrogen lone pair to the electrophilic carbene carbon means that there is less need for ring involvement in stabilizing the carbene carbon, so that the bonding lengths of the aminocarbene aryl rings are closer to that of the free rings. However, carbene ligands of these aminocarbene complexes are not coplanar with the plane of the bonding geometry about the carbene carbon, and the rings are twisted to fit in between the carbonyl ligands on the adjacent manganese atom. Presumably, that explains the unusually long C(11)-C(12) bond length ($1.496(4)\text{\AA}$) observed for **8**. This means that the bonding angles in these heteroaryl substituents will differ more significantly from the uncoordinated heteroaryls than the ethoxycarbene complexes.

4.4 Conclusions

Complexes **8** - **15** were synthesized and characterized spectroscopically, and final confirmation of the structures of these complexes in the solid state determined by X-ray diffraction. All the dirhenium aminocarbene complexes (**12** - **15**) were found to have the carbene ligand in an equatorial position, the Re-Re bond long enough to allow even bulky substituents on the carbene to be accommodated between the carbonyl ligands on the adjacent rhenium

atom. The dimanganese aminocarbenes (**8**, **9**) with an NH₂-group also have equatorial carbene ligands, but the bulky NH(C₃H₇)-substituted complexes (**10**, **11**) retain the axial configuration of their ethoxy precursors.

As proposed in Chapter 2, the position of the carbene ligand in [Mn₂(CO)₉(carbene)] complexes are determined by steric factors, due to the limitation of the short Mn-Mn bond. Bulky -OEt and -NH(C₃H₇) cannot be accommodated in an intermediate position between the adjacent carbonyl ligands, and therefore force the carbene ligand in an axial position.

The aminocarbene ligand is a weak π-acceptor with the electrophilic carbene carbon atom stabilized predominantly by electron donation from the nitrogen lone pair. The aminocarbene ligand would therefore preferentially occur at an equatorial position *trans* to a carbonyl ligand (a better π-acceptor ligand) in the electronically favourable position, unless forced by steric reasons into the axial position. On the other hand, the ethoxycarbene ligand is a better π-acceptor ligand in [Mn₂(CO)₉(carbene)] complexes, and can be better stabilized in an axial position. It is therefore possible to manipulate the position of the carbene ligand merely by varying the steric effects of the substituent on the carbene ligand. An attempt at aminolysis with an diethylamine and diisopropylamine did not prove successful, and it seems sterically not possible to accommodate a secondary amine substituent on the carbene ligand, even in the axial position.

4.5 References

1. A. Yamashita, *Tetrahedron Lett.* 27, **1986**, 5915.
2. C. Alvarez, A. Parlier, H. Rudler, R. Yefsah, J.C. Daran, C. Knobler, *Organometallics* 8, **1989**, 2253.
3. H. Rudler, A. Parlier, R. Yefsah, B. Denise, J.C. Daran, J. Vaissermann, C. Knobler, *J. Organomet. Chem.* 358, **1988**, 245.
4. C. Borel, L.S. Hegedus, S. Krebs, Y. Satoh, *J. Am. Chem. Soc.* 109, **1987**, 1101.
5. L.S. Hegedus, J.D.B. Miller, *J. Org. Chem.* 54, **1989**, 1249.
6. K.H. Dötz, H. Erben, K. Harms, *J. Chem. Soc., Chem. Commun.* **1989**, 692.
7. K.H. Dötz, T. Schaffer, K. Harms, *Angew. Chem. Int. Ed. Engl.* 29, **1990**, 176.
8. R. Aumann, P. Hinterding, *Chem. Ber.* 123, **1989**, 611.
9. W.D. Wulff, B.A. Anderson, L.D. Isaac, *Tetrahedron Lett.* 30, **1985**, 4061.
10. B.A. Anderson, W.D. Wulff, *J. Am. Chem. Soc.* 112, **1990**, 8615.
11. J.A. Connor, E.O. Fischer, *J. Chem. Soc. A* **1969**, 578.
12. U. Klabunde, E.O. Fischer, *J. Am. Chem. Soc.* 89, **1967**, 7141.
13. B. Crociani, *Reactions of Coordinated Ligands*, Plenum, New York **1986**, 553.
14. L. Canovese, F. Visente, P. Uguagliati, B. Crociani, *J. Organomet. Chem.* 535, **1997**, 69.
15. R. Imwinkelried, L.S. Hegedus, *Organometallics* 7, **1988**, 702.
16. F.R. Kreissl, W.J. Sieber, M. Wolfgruber, J. Riede, *Angew. Chem. Int. Ed. Engl.* 23, **1984**, 640.
17. F.R. Kreissl, W.J. Sieber, M. Wolfgrüber, *J. Organomet. Chem.* 270, **1984**, C45.
18. E.O. Fischer, E. Offhaus, *Chem. Ber.* 102, **1969**, 2449.

19. E.O. Fischer, E. Offhaus, J. Muller, D. Nöthe, *Chem. Ber.* 105, **1972**, 3027.
20. G. Huttner, D. Regler, *Chem. Ber.* 105, **1972**, 1230.
21. E.W. Post, K.L. Watters, *Inorg. Chim. Acta* 26, **1978**, 29.
22. H. Werner, E.O. Fischer, B. Heckl, C.G. Kreiter, *J. Organomet. Chem.* 28, **1971**, 367.
23. S. Lotz, M. Landman, D.I. Bezuidenhout, A.J. Olivier, D.C. Liles, P.H. van Rooyen, *J. Organomet. Chem.* 690, **2005**, 5929.
24. K. Nakamoto, *Infrared and Raman Spectra of Inorganic and Coordination Compounds. Part A: Theory and Applications in Inorganic Chemistry*, 5th ed. John Wiley & Sons, New York **1997**, 345.
25. E. van der Watt, *Synthesis of Fischer Carbene Complexes with Metal-containing Substituents*, University of Pretoria, **2006**.
26. M.Y. Darensbourg, D.J. Darensbourg, *Inorg. Chem.* 9, **1970**, 32.
27. J.A. Connor, J.P. Lloyd, *Chem. Rev.* **1970**, 3237.
28. L.J. Farrugia, *J. Appl. Crystallogr.* 30, **1997**, 565.
29. The POV-Ray Team, POV-Ray **2004**, URL: <http://www.pov-ray.org/download/>.
30. F.H. Allen, O. Kennard, D.G. Watson, L. Brammer, A.G. Orpen, R. Taylor, *J. Chem. Soc., Perkin Trans. II* **1987**, S1-S19.

5 Kinetic Investigation of Aminolysis Reaction

5.1 Background

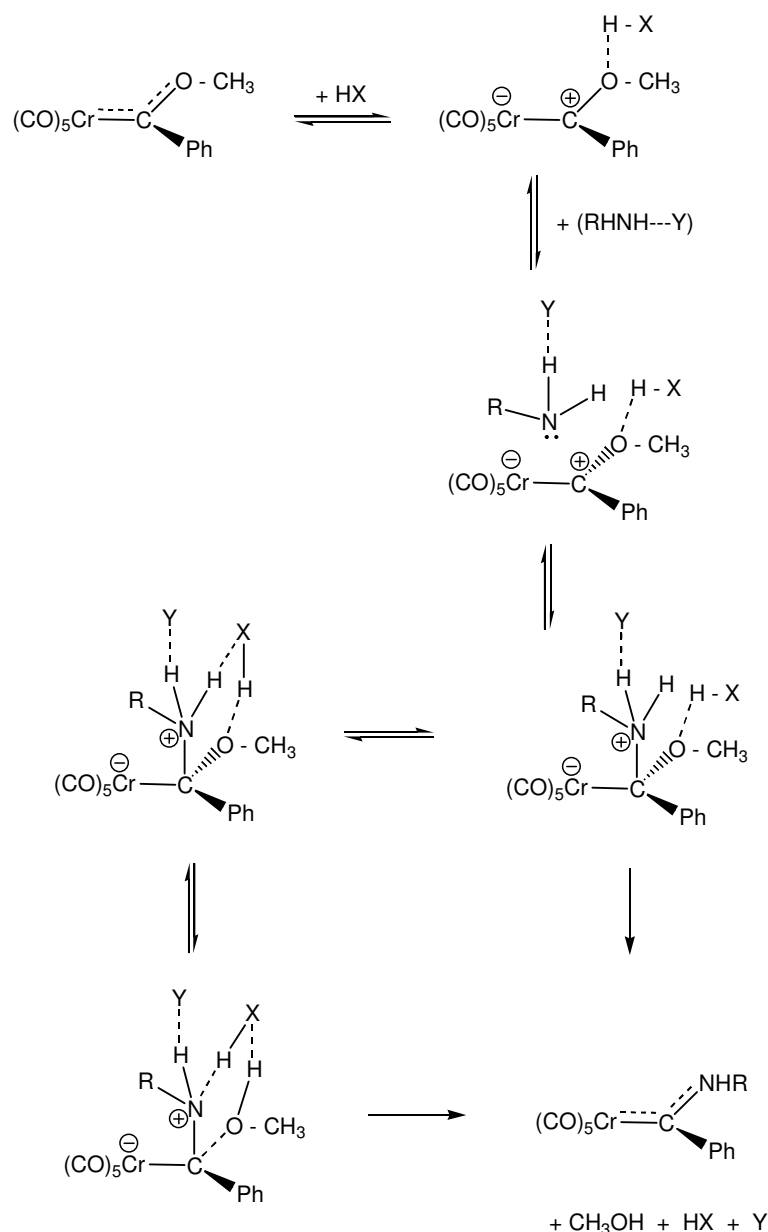
5.1.1 Overview

The carbene carbon of Fischer type carbene complexes is electrophilic in nature^[1] and undergoes facile substitution of the alkoxy group with nucleophiles such as OH⁻, water, MeO⁻, amines, thiolate ions, carbanion and others^[2-19].

The first extensive kinetic investigation of the aminolysis of alkoxy carbene complexes was carried out by Werner and Fischer^[9]. They studied the reaction of [Cr(CO)₅{C(OMe)Ph}] with the primary amines RNH₂ (R = *n*-C₄H₉, C₆H₁₁, CH₂Ph), and followed the reaction by UV-visible spectrophotometry in *n*-decane, dioxane, methanol and dioxane:methanol (1:1) solvent systems at various temperatures. They found that the formation of the aminocarbene complexes [Cr(CO)₅{C(NHR)Ph}] follows the fourth-order rate law:

$$\frac{d[\text{aminocarbene}]}{dt} = k_A [\text{alkoxy carbene}] [\text{RNH}_2] [\text{HX}] [\text{Y}]$$

where HX and Y represent proton-donating and accepting agents, respectively. The specific species HX and Y within a given solvent system, along with the postulated mechanism are shown in Scheme 5.1. The activation of the amine by way of an external proton accepting agent Y was assumed to be the cause of the negative entropy of activation.



Scheme 5.1 The mechanism of the aminolysis of $[\text{Cr}(\text{CO})_5\{\text{C}(\text{OMe})\text{Ph}\}]$ in polar and nonpolar solvents (*n*-decane, HX and Y = RNH_2 ; dioxane, HX = RNH_2 , Y = $\text{C}_4\text{H}_8\text{O}_2$ or RNH_2 ; methanol, HX = MeOH or RNH_2 , Y = RNH_2 or MeOH).

More recent kinetic studies on aminolysis of alkoxycarbene complexes are included in the work of Bernasconi and Ali^[3;20-22]. They found that the second-order rate constant (k_A , $m^{-1}s^{-1}$) increases with amine concentration, giving a linear dependence with a tendency towards levelling off at higher amine concentration. They proposed that the reaction undergoes base catalysis, with a mechanism very similar to those for ester reactions, involving a nucleophilic addition of amine to the substrate to yield a zwitterionic tetrahedral intermediate in the first step, followed by deprotonation. In the third step, the intermediate is converted to product by water and/or conjugate acid of the base.

5.1.2 Focus of this study

The aminolysis reaction of the ethoxycarbene complexes synthesized in Chapter 2, with the amines ammonia and propylamine, was investigated.

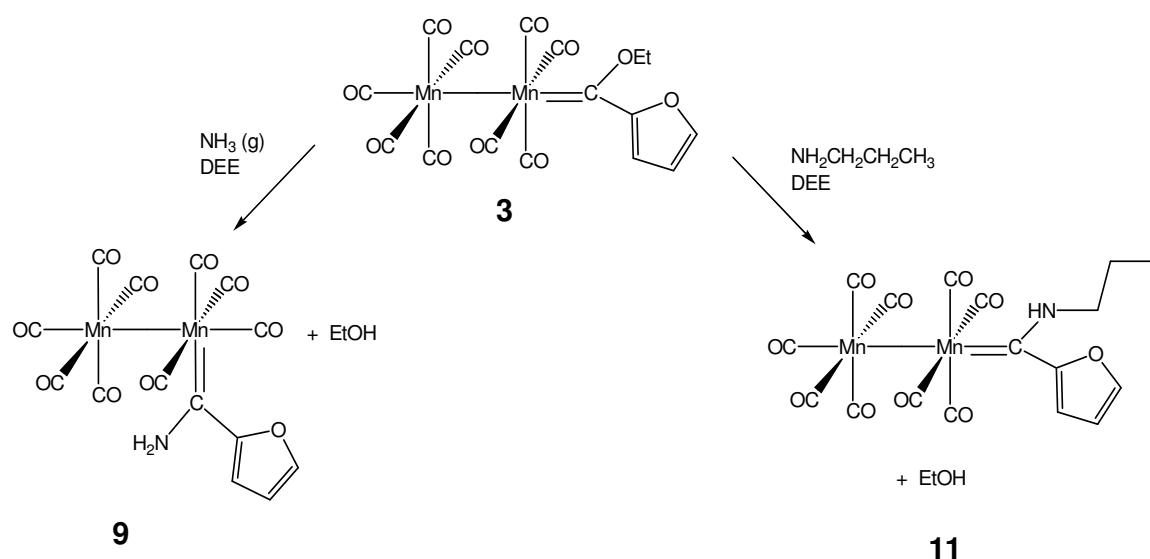


Figure 5.1 Reactions to be studied kinetically via UV-visible spectrophotometry

The aim was to elucidate the reaction mechanism of the nucleophilic substitution of -OEt by -NHR in the reaction solvent diethyl ether, as well as to identify intermediates formed, which could then possibly explain the axial-equatorial isomerization observed during reaction with the very small amine NH_3 .

5.2 Electronic Spectra

Three intense bands are present on the UV-spectrum of thiophene in the gas phase at 240 nm, 207 nm and 188 nm. Two bands, at 215 nm and 231 nm, are observed on the spectrum of thiophene in solution^[23]. Substituents on the ring have an influence on the position of these bands, depending on the ring position of the substituent. Furan also exhibits two bands in solvent dichloromethane (232 nm, 283 nm) and hexane (244 nm, 277 nm)^[24], but only one band is observed in ethanol (208 nm)^[25].

The UV-visible spectra of the complexes **2**, **3**, **8** - **11** were recorded in diethyl ether, the solvent employed in the aminolysis reaction. The electronic data of these complexes are summarized in Table 5.1, and the electronic spectrum of complex **3** is presented in Figure 5.2.

Table 5.1 UV-visible data of complexes **2**, **3**, **8** - **11** recorded in diethyl ether

Complex	Colour	Ligand π - π^* transition (λ , nm)	Metal-ligand transition (λ , nm)
2	orange-red	276, 350	414
3	orange-red	300, 350	396
8	yellow-orange	308, 346	436
9	yellow-orange	292, 346	442
10	yellow-orange	278, 354	436
11	yellow-orange	282, 354	442

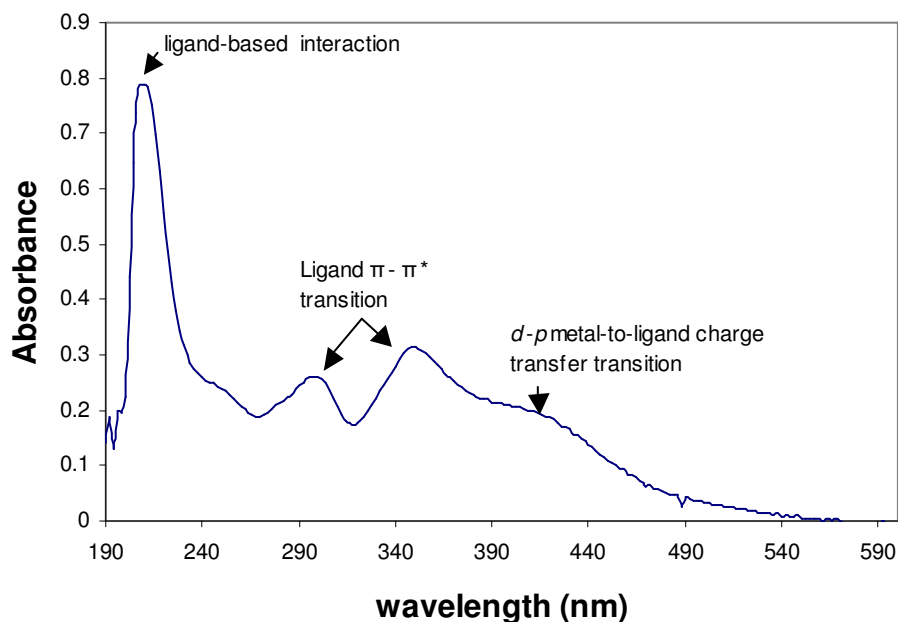


Figure 5.2 UV-spectrum of **3**

All complexes exhibit strong ligand-based absorption bands between 242 - 253 nm. Two intense characteristic absorption bands with λ_{max} in the range 276 - 354 nm are the thiophene/furan-based π - π^* transitions. Coordination to metal fragments shift these bands to higher wavelengths, indicating interaction of the metal carbene π -system with that of the heteroaryl substituent^[24;26]. The energies of the π - π^* transitions in the heteroarenes are reduced.

The absorption band at lower energy is assigned to a *d-p* metal-to-ligand charge transfer (MLCT) transition^[27]. The metal donates electrons to the empty *p*-orbital of the carbene carbon in the excited state whilst the heteroatom bonded to the carbene carbon atom acts as a π -donor towards the metal in the ground state (Figure 5.3). Since the colours of these complexes are characteristic to the number of metal moieties coordinated to the ligand the values of this transition are very similar for different monocarbene complexes of Cr, W and Mo of an orange-red colour^[24;26], with absorption energy ranging from 460 - 493 nm in these complexes. In the case of the dimanganese monocarbene complexes synthesized, these bands are

slightly overlapped by the π - π^* transition bands, but can be distinguished as distinct shoulders.

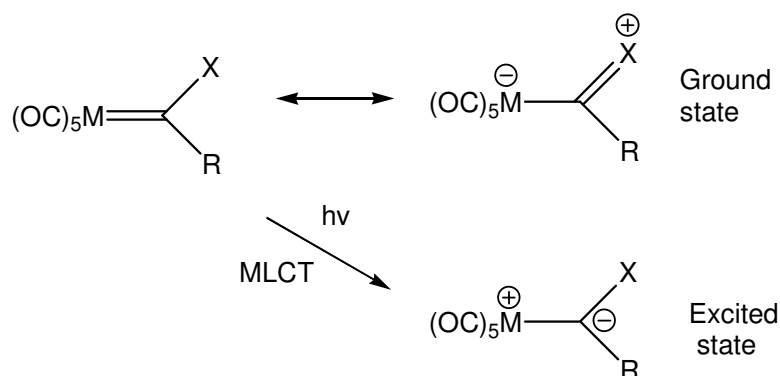


Figure 5.3 Ground and excited states in Fischer carbene complexes

5.3 Kinetic Investigation

The aminolysis reaction of **2** converted into **8**, **10** and **3** into **9**, **11** can be studied by spectroscopic techniques, as conversions are associated with major spectral changes. In essence, no differences in the general kinetic behaviour of **2** and **3** were observed. Since the same reaction occurs for both complexes **2** and **3**, our kinetic investigations focused on **3** and its converted products. Aminolysis reactions of **3** were studied, employing two different amines: ammonia, which yields equatorially substituted **9**, and propylamine, which yields **11**, an axially substituted complex.

The UV-vis spectrum of **3** in diethyl ether display maxima at 300, 350 and 396 nm, and minima at 270, 318 and 384 nm. For **9** and **11**, the maxima are 292, 346, 442 nm and 282, 354, 442 nm respectively, while the minima are 272, 318, 408 nm and 286, 320, 412 nm respectively. The nucleophilic substitution of the ethoxy group by an amine group during the conversion of **3** into **9**, **11** is accompanied by characteristic changes in the spectra, as indicated by a decrease in the intensity of the band at 350 nm, shift of the shoulder maximum at 396 nm to 442 nm, and the shift of the maximum at 300 nm to 292 nm and 282 nm for **9** and **11**, respectively.

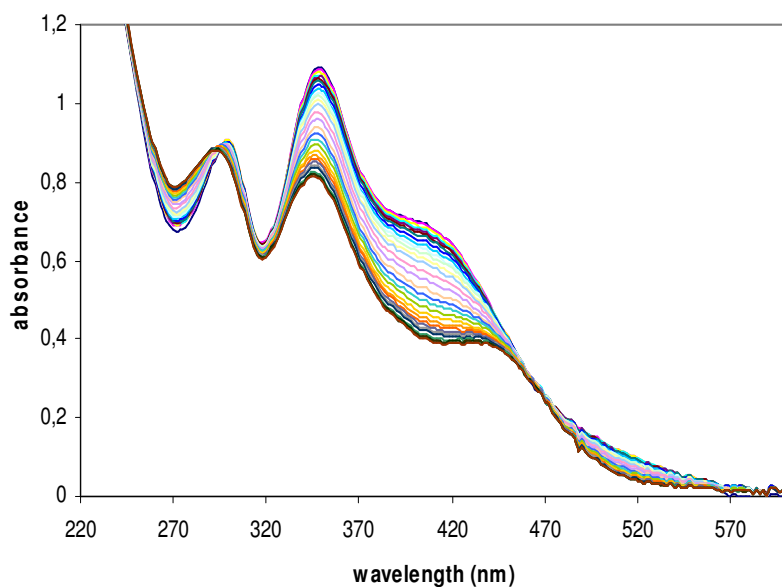


Figure 5.4 Repetitive scan spectra recorded for the conversion of **3** to **9** at 25°C, experimental conditions $[3] = 5.70 \times 10^{-5} \text{M}$, $t_{\text{total}} = 10200 \text{ s}$

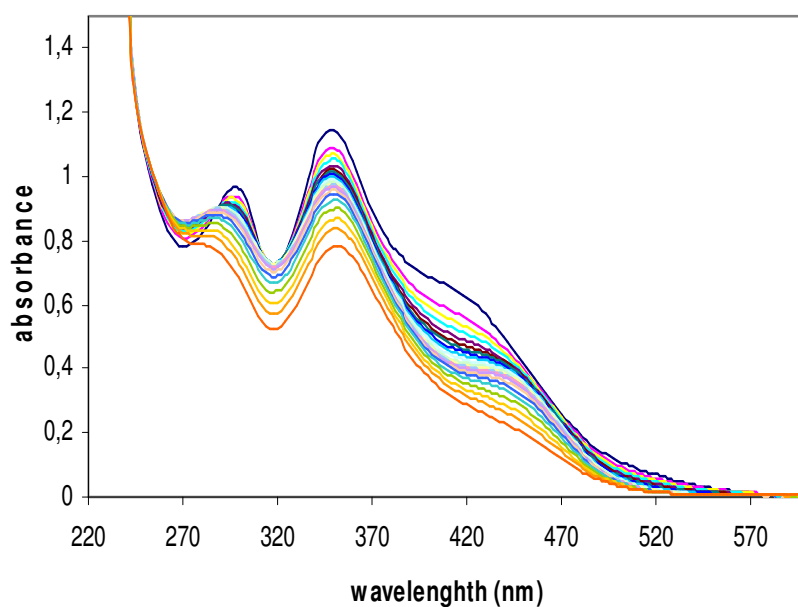


Figure 5.5 Repetitive scan spectra recorded for the conversion of **3** to **11** at 25°C, experimental conditions $[3] = 4.50 \times 10^{-5} \text{M}$, $t_{\text{total}} = 14400 \text{ s}$

The progress of the reaction was therefore monitored by the increase and decrease of the π - π^* ligand transitions and MLCT bands over the range 220 - 600 nm. The repetitive scan spectra recorded for the conversion of **3** to **9** is shown in Figure 5.4, and in Figure 5.5 for the propylamino-analogue **11**.

The spectra exhibit two initial isosbestic points at 288 nm and 452 nm, and 286 nm and 458 nm for **3** converted to **9** and **11** respectively. No calculations of the isosbestic points were done, due to the decomposition that occurred after approximately 4000 s, causing a drift of the isosbestic points.

For both reactions studied, the concentration of the amine reagent was always in great excess compared to that of the parent ethoxycarbene reagent, so that the kinetic experiments were conducted under pseudo-first order conditions, with the carbene complex as the minor component at 25 °C. Typical substrate concentrations were $(3.0 - 6.0) \times 10^{-5} \text{ mol.L}^{-1}$ while the amine concentrations varied for $[\text{NH}_3] = (1.08 - 10.8) \times 10^{-2} \text{ mol.L}^{-1}$ and $[\text{propylamine}] = (3.04 - 12.20) \times 10^{-2} \text{ mol.L}^{-1}$. The pseudo-first-order rate constants (k_{obs}, s^{-1}) were obtained by fitting the kinetic absorbance-time traces (measured at wavelengths 348 nm for **9** and 354 nm for **11**) with a suitable computer-fit program (See Section 6.2.6 in Chapter 6).

Table 5.2 lists data obtained for the reaction of **3** converted to **9** in ether at different concentrations of ammonia, and for the analogous conversion into **11** at different concentrations of propylamine. The values listed in Table 5.2 are the average values obtained of at least four kinetic traces, but the irreproducibility of these measurements, caused by the decomposition of the complexes, rendered fitting of the k_{obs} vs [amine] graphs difficult.

In both cases, the observed pseudo-first order rate constants, k_{obs} , showed a non-linear dependence on amine concentration (Figure 5.6 and 5.7), indicating a change in the order of the reaction from second- or mixed order to first-order in amine concentration^[20]. When plotting the values of k_{obs} obtained for these reactions against $[\text{amine}]^2$, a seemingly linear dependence was

obtained (Figure 5.8, 5.9). This indicated that k_{obs} is the second-order rate constant. In all graphs, a zero point was added for aiding the fitting of the plotted data points.

Table 5.2 Kinetic data for the influence of the concentration of the amines on the aminolysis reaction in diethyl ether at 25 °C.

Conversion of 3 to 9 [3] = $5.70 \times 10^{-5} \text{M}$		Conversion of 3 to 11 [3] = $4.50 \times 10^{-5} \text{M}$	
[NH ₃] (mol.L ⁻¹)	k_{obs} (s ⁻¹)	[propylamine] (mol.L ⁻¹)	k_{obs} (s ⁻¹)
1.08×10^{-2}	3.26×10^{-4}	3.04×10^{-2}	5.79×10^{-4}
2.16×10^{-2}	6.89×10^{-4}	6.08×10^{-2}	2.35×10^{-3}
5.40×10^{-2}	2.09×10^{-3}	9.12×10^{-2}	5.98×10^{-3}
7.20×10^{-2}	6.92×10^{-3}	1.22×10^{-1}	1.18×10^{-2}
8.64×10^{-2}	1.00×10^{-2}	-	-
1.08×10^{-1}	2.10×10^{-2}	-	-

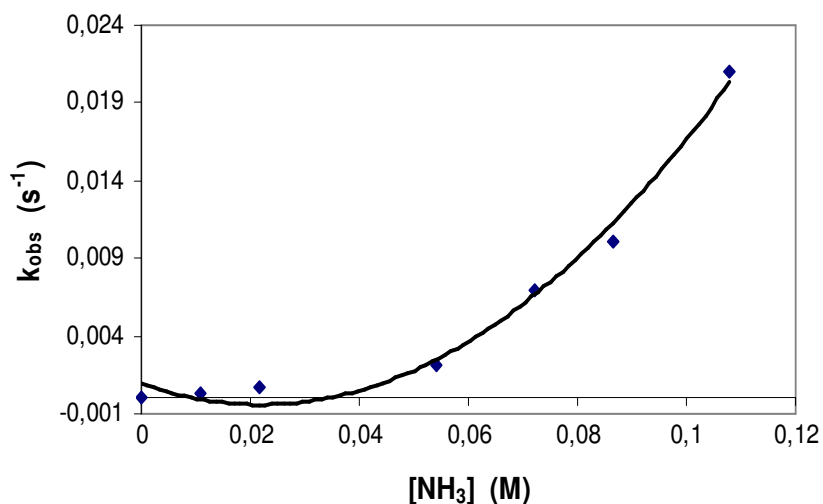


Figure 5.6 Plot of k_{obs} vs [NH₃] for the reaction between ammonia and **3** in diethyl ether at 25 °C

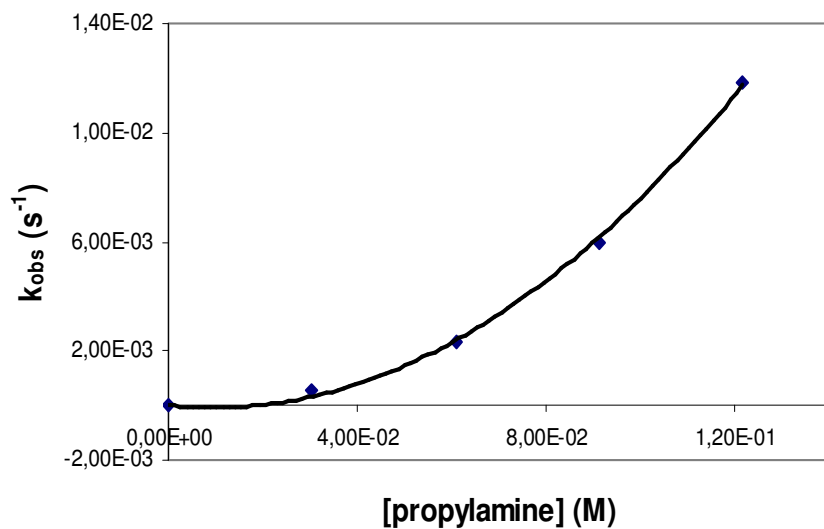


Figure 5.7 Plot of k_{obs} vs [propylamine] for the reaction between propylamine and **3** in diethyl ether at 25 °C

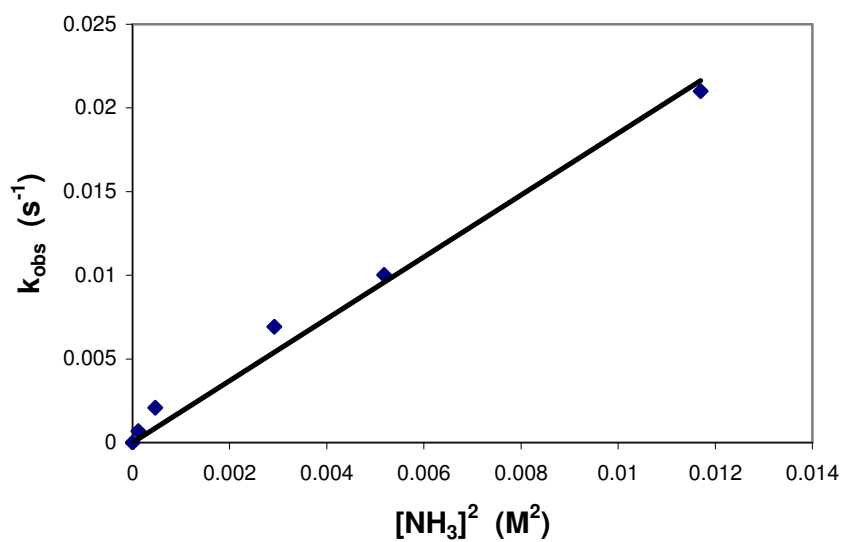


Figure 5.8 Plot of k_{obs} vs $[NH_3]^2$ for the reaction between ammonia and **3** in diethyl ether at 25 °C

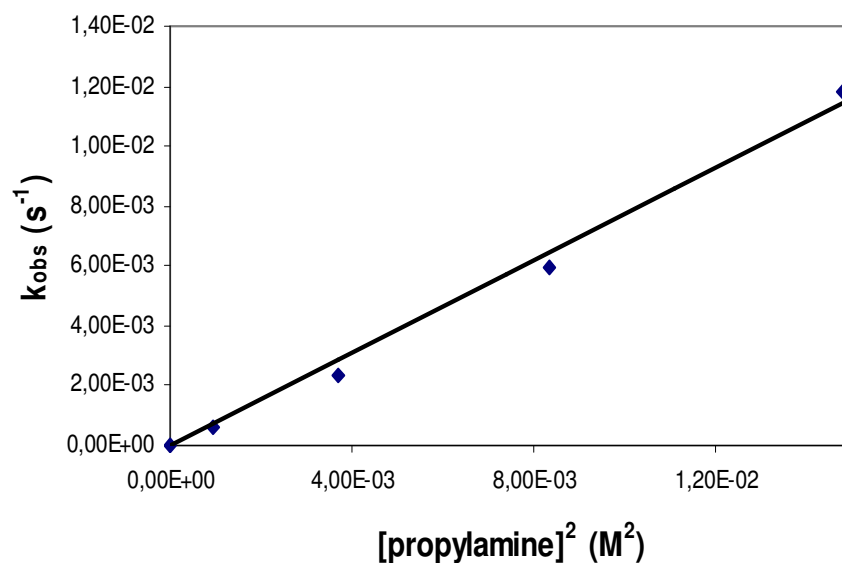


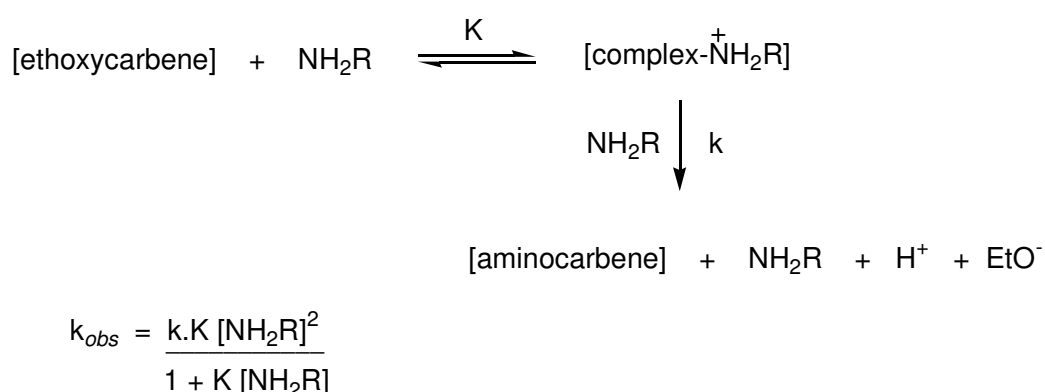
Figure 5.9 Plot of k_{obs} vs $[\text{propylamine}]^2$ for the reaction between propylamine and **3** in diethyl ether at 25 °C

5.4 Conclusions

These results would indicate a second-order reaction, involving at least two amine molecules during the aminolysis reaction. It was not possible to study the temperature or pressure dependence of these reactions, due to experimental difficulties associated with diethyl ether as solvent. The low boiling point and vapour pressure of ether, as well as its reaction with the plastic chambers within the high-pressure stopped-flow spectrophotometer, rendered the results obtained irreproducible. Another very important contributing factor to the irreproducibility of the results is the competing decomposition of the carbene complexes, as seen in Figure 5.4, 5.5. This meant that neither the Arrhenius activation energy, nor the reaction activation enthalpy or entropy could be calculated.

No significant differences were observed for the reactions of **3** with ammonia, compared with propylamine, except for the larger k_{obs} values determined for the reaction with ammonia. Therefore, no absolute information could be obtained about the axial-equatorial isomerisation. The two cases appear similar, which could mean that the axial-to-equatorial conversion only occurs later, to yield the thermodynamically favoured product, and not during the initial aminolysis reaction. Another indication that this might be a possibility is seen by the mixture of isomers seen in the NMR spectra of the manganese aminocarbene complexes (Chapter 4).

A probable reaction route could be postulated, as illustrated in Scheme 5.2, where at high concentrations of amine, $k_{obs} = k[\text{amine}]$, and at low concentrations of amine, $k_{obs} = k.K[\text{amine}]^2$.



Scheme 5.2 Postulated reaction mechanism

No further information about intermediates could be deduced, but the results obtained can be explained by the mechanisms proposed by Werner, and Bernasconi and Ali discussed in Section 5.1. The second-order rate constant determined agrees with the findings of Ali^[20] but not with the results of Werner^[9], where the aminolysis reaction of $[\text{Cr}(\text{CO})_5\{\text{C}(\text{OMe})\text{Ph}\}]$ follows the fourth-order rate law.

5.5 References

1. K.H. Dötz, H. Fischer, P. Hofmann, F.R. Kreissl, U. Schubert, K. Weiss, *Transition Metal Carbene Complexes*, VCH Verlag Chemie, Weinheim **1983**.
2. R. Aumann, P. Hinterding, C. Kruger, R. Goddard, *J. Organomet. Chem.* 459, **1993**, 145.
3. C.F. Bernasconi, F.X. Flores, K.W. Kittredge, *J. Am. Chem. Soc.* 119, **1997**, 2103.
4. C.F. Bernasconi, L. Garcia-Rio, *J. Am. Chem. Soc.* 122, **2000**, 3821.
5. U. Klabunde, E.O. Fischer, *J. Am. Chem. Soc.* 89, **1967**, 7141.
6. J.A. Connor, E.O. Fischer, *J. Chem. Soc. A*, **1969**, 578.
7. E.O. Fischer, B. Heckl, H. Werner, *J. Organomet. Chem.* 28, **1971**, 359.
8. C.F. Bernasconi, M.W. Stronach, *J. Am. Chem. Soc.* 115, **1993**, 1341.
9. H. Werner, E.O. Fischer, B. Heckl, C.G. Kreiter, *J. Organomet. Chem.* 28, **1971**, 367.
10. E.O. Fischer, M. Leupold, C.G. Kreiter, J. Müller, *Chem. Ber.* 105, **1972**, 150.
11. C.T. Lam, C.V. Senoff, J.E.H. Ward, *J. Organomet. Chem.* 70, **1974**, 273.
12. R. Aumann, J. Schröder, *Chem. Ber.* 123, **1990**, 2053.
13. C.F. Bernasconi, K.W. Kittredge, F.X. Flores, *J. Am. Chem. Soc.* 121, **1999**, 6630.
14. E.O. Fischer, S. Riedmüller, *Chem. Ber.* 109, **1976**, 3358.
15. T.J. Burkhardt, C.P. Casey, *J. Am. Chem. Soc.* 95, **1973**, 5833.
16. C.P. Casey, T.J. Burkhardt, C.A. Bunnell, J.C. Calabrese, *J. Am. Chem. Soc.* 99, **1977**, 2127.
17. E.O. Fischer, G. Kreis, F.R. Kreissl, C.G. Kreiter, J. Muller, *Chem. Ber.* 106, **1973**, 3910.
18. C.P. Casey, W.P. Brunsvold, *Inorg. Chem.* 16, **1977**, 391.

19. R.A. Bell, M.H. Chrisholm, D.A. Couch, L.A. Rankel, *Inorg. Chem.* 16, **1977**, 677.
20. M. Ali, *New J. Chem.* 27, **2003**, 349.
21. C.F. Bernasconi, M. Ali, *J. Am. Chem. Soc.* 121, **1999**, 11384.
22. M. Ali, D. Maiti, *J. Organomet. Chem.* 689, **2004**, 3520.
23. Y. Mazaki, K. Kobayashi, *Tetrahedron Lett.* 30, **1989**, 3315.
24. C. Crause, *Synthesis and Application of Carbene Complexes with Heteroaromatic Substituents*, University of Pretoria, **2004**.
25. R.P. Kreher, *Houben-Weyl Methoden Der Organischen Chemie*, 1st ed. Stuttgart, New York **1994**, 328.
26. M. Landman, *Synthesis of Metal Complexes with Thiophene Ligands*, University of Pretoria, **2000**.
27. D.F. Shriver, P.W. Atkins, *Inorganic Chemistry*, 3rd ed. Oxford University Press, Oxford **1999**, 437.

6 Experimental

6.1 Standard Operating Procedure

All operations were carried out under an inert atmosphere of nitrogen or argon gas using standard Schlenk techniques. Solvents were dried and distilled under an atmosphere of nitrogen. Ether and THF were distilled from sodium metal, with benzophenone as indicator. Dichloromethane and hexane were distilled from phosphorous pentoxide. Most chemicals were used without prior purification, unless stated otherwise. Column chromatography, using Kieselgel 60 (particle size 0.0063 - 0.200mm) or neutral aluminium oxide 90 was used as resin for all separations. The column was cooled with isopropanol (-30 °C) in the column jacket.

6.2 Characterization Techniques

6.2.1 Nuclear Magnetic Resonance Spectroscopy

NMR spectra were recorded on a Bruker ARX-300 spectrometer and on an AVANCE 500 spectrometer. ^1H NMR spectra were recorded at 300.135 and 500.139 MHz and ^{13}C NMR spectra at 75.469 and 125.75 MHz respectively. The signal of the deuterated solvent was used as reference: ^1H CDCl_3 7.24

ppm, acetone-d₆ 2.09 ppm and ¹³C CDCl₃ 77.00 ppm, acetone-d₆ 205.87 ppm. For resolution enhancement of the manganese complexes, longer acquisition times were achieved by manual shimming and manipulation of the sweep width.

6.2.2 Infrared Spectroscopy

IR spectra were recorded on a Perkin-Elmer Spectrum RXI FT-IR spectrophotometer with a NaCl cell. All spectra were recorded using either dichloromethane or hexane as solvent. The vibrational stretching bands in the carbonyl region (*ca.* 1500 - 2200 cm⁻¹) were recorded for all complexes, as well as the N-H vibrational frequencies in the range of 3300 - 3500 cm⁻¹ for the aminocarbene complexes in Chapter 4.

6.2.3 Fast Atom Bombardment Mass Spectrometry

FAB-MS spectra were recorded on a VG 70SEQ Mass Spectrometer, with the resolution for FAB = 1000 in a field of 8 kV. Nitrobenzyl alcohol was used as solvent and internal standard. The spectra were recorded by Mr T. van der Merwe at the University of the Witwatersrand.

6.2.4 X-Ray Crystallography

Data collection and structure determinations were done by Mr Dave Liles, University of Pretoria. X-ray crystal structure analysis was done from data collected at 20°C on a Siemens P4 Bruker 1K CCK diffractometer using graphite-monochromated, Mo-K α radiation. Data were corrected for Lorenz polarization effects and structures were solved by direct methods (SHELXS) and refined by full-matrix least squares techniques. In the structure

refinements all hydrogen atoms were added in calculated positions and treated as riding on the atom to which they are attached. All non-hydrogen atoms (except those refined as rigid groups) were refined with anisotropic displacement parameters, all isotropic displacement parameters for hydrogen atoms were calculated as $X \times U_{eq}$ of the atom to which they are attached, $X = 1.5$ for the methyl hydrogens and 1.2 for all other hydrogens. In structures **2**, **7** and **11** some disorder was observed. The parameters for the major orientations were refined freely. The minor orientations were refined as rigid bodies with geometries derived from those of the major orientations. Site occupation factors for the major and minor orientations were refined but constrained to sum to 1.0.

6.2.5 UV-Visible Spectroscopy

All the complexes were referenced to diethyl ether and spectra measured in a range of 200.0 - 800.0 nm in a quartz sample cell. A Hewlett-Packard 8452A Diode Array spectrophotometer and a Shimadzu UV-2101 PC UV-Vis scanning spectrophotometer were used.

6.2.6 Kinetic Measurements

The kinetics of the aminolysis reactions were followed at ambient pressure in the thermostated cell compartment (quartz sample cell) of a Shimadzu UV-2101 PC UV-Vis scanning spectrophotometer. Reported rate constants are the average of at least four kinetic runs. OLIS KINFIT^[1] software was employed to calculate k_{obs} values from absorbance vs time traces by fitting single- or double exponential functions through the data points.

6.3 Preparation of Compounds

6.3.1 Preparation of Starting Compounds

6.3.1.1 Triethyl oxonium tetrafluoroborate^[2]

Epichlorohydrin (140.0 g, 119 mL, 1.51 mol) was added dropwise to a solution of sodium-dried ether (500 mL) and freshly distilled boron fluoride etherate (284.0 g, 252 mL, 2.00 mol) at a rate sufficient to maintain vigorous boiling (about 1 hour is needed). The mixture was refluxed and allowed to stand at RT overnight. Supernatant ether was withdrawn from the crystalline mass of triethyloxonium tetrafluoroborate under an inert N₂ atmosphere. Crystals were washed with ether; yield 244 - 272 g (85 - 95%).

6.3.2 Preparation of Organometallic Complexes

6.3.2.1 General Method of Carbene Formation^[3-5]

An excess of 10% butyllithium was used in the syntheses. Complexes **1** - **5** were synthesized according to the general method given below:

Method:

The heteroarene (2.2 mmol) was stirred while adding *n*-BuLi (2.2 mmol, 1.6 M, 1.4 mL) in 40 mL THF at -20 °C under an inert N₂ atmosphere. Stirring was continued for 30 minutes. Yellow Mn₂(CO)₁₀ (2 mmol, 0.78 g) [white Re₂(CO)₁₀ (2 mmol, 1.31 g) in the case of the synthesis of **5**] was added to the reaction mixture at -70 °C, resulting in a colour change of the reaction mixture to orange-red while stirring for 1 h. Stirring was then continued for an additional 30 min at RT. THF solvent was evaporated under reduced pressure. Et₃OBF₄ (2.2 mmol, 0.42 g) in dichloromethane was added to the reaction mixture at -30 °C and stirred until reaction completion. LiBF₄ salts were removed by filtering and reaction products were purified via column

chromatography using hexane/dichloromethane (4:1) as eluent. Recrystallization of products was done by solvent layering of hexane/dichloromethane (1:1). Products **1** - **5** were obtained.

Table 6.1 Information of individual complexes synthesized

Complex	Heteroarene (2.2 mmol)	Product obtained				
		Colour	Molar mass (g/mol)	Mass (g)	mmol	Yield (%)
1	2,2'- bithiophene (0.366 g)	orange solid	584.30	0.760	1.30	65
2	thiophene (0.185 g, 0.175 mL)	orange solid	502.18	0.723	1.44	72
3	furan (0.150 g, 0.160 mL)	orange solid	486.11	0.661	1.36	68
4	N-methyl pyrrole (0.178 g, 0.196 mL)	orange solid	499.16	0.629	1.26	63
5	furan (0.150 g, 0.160 mL)	orange- red solid	748.66	1.108	1.48	74

6.3.2.2 Cleaving of Metal-Metal Bonds^[6;7]

Method:

To a minimum volume of hexane solvent was added the binuclear monocarbene precursor complex **1** (1 mmol, 0.58 g) and Br₂ (1.1 mmol, 0.176

g, 0.056 mL) while stirring at RT under an inert N₂ atmosphere until reaction was complete. The unreacted Br₂ was removed under reduced pressure. Products **6** and [Mn(CO)₅Br] were obtained. Complex **7** was prepared in a similar fashion from precursor **2** (1 mmol, 0.50 g) and I₂ (1 mmol, 0.26 g). Unreacted I₂ was separated on an aluminium oxide 90 column with a hexane eluent, and products **7** and [Mn(CO)₅I] were purified using silica gel column chromatography. The complexes were crystallized from a hexane/dichloromethane (3:1) solution by layering of the solvents.

Table 6.2 Information of cleavage products

Complex	Product obtained					Product [Mn(CO) ₅ X]		
	Colour	Molar mass (g/mol)	Mass (g)	mmol	Yield (%)	Mass (g)	mmol	Yield (%)
6 (X = Br)	dark red	516.21	0.108	0.21	21	0.113	0.41	41
7 (X = I)	red	434.09	0.187	0.43	43	0.154	0.48	48

6.3.2.3 Aminolysis of Ethoxycarbene Complexes^[8-10]

Method:

The binuclear ethoxycarbene precursor complex (2 mmol) (**2** (1.00 g), **3** (0.97 g), **5** (1.50 g) as well as [Re₂(CO)₉{C(OEt)(2-thienyl)}]^[11] (1.53 g), respectively) was dissolved in diethyl ether at RT, and a slow stream of NH₃(g) was bubbled through the reaction solutions until the colour of the reaction mixture changed from red to orange. After evaporation of the solvent under reduced pressure and purification on aluminium oxide (for the dimanganese complexes) or silica gel (for the dirhenium complexes), products **8**, **9**, **12** and **13** respectively, were obtained.

The reaction procedure was repeated using the same precursors, in the same amounts, but instead of bubbling ammonia through the solution, excess propylamine (5 mmol, 0.30 g, 0.41 mL) was added to the reaction mixture and products **10**, **11**, **14** and **15** were obtained from the individual reactions.

Recrystallization of products was done by solvent layering of hexane/dichloromethane (1:1).

Table 6.3 Information of aminolysis reaction products

Complex	Colour	Molar mass (g/mol)	Mass (g)	mmol	Yield (%)
8	orange	473.14	0.84	1.78	89
9	light orange	457.07	0.87	1.90	95
10	orange-yellow	515.22	0.77	1.50	75
11	orange-yellow	499.15	0.78	1.56	78
12	orange	735.68	1.25	1.70	85
13	orange	719.62	1.24	1.72	86
14	orange-yellow	777.76	1.26	1.62	81
15	orange-yellow	761.70	1.33	1.74	87

6.4 Analytical Data of Complexes 1 - 15

Melting points were recorded on a hot stage Gallenkamp melting apparatus and are uncorrected. Most complexes decomposed during heating, and only melting points for complexes **1 - 3**, **5 - 9** could be determined, as listed in Table 6.4, as well as the elemental analyses done for the carbon and hydrogen atoms of the complexes. The C and H elemental analyses were

performed by the analytical laboratories of ARC-LNR Institute for Soil, Climate and Water.

Table 6.4 Analytical data of **1 - 15**

Complex	Molecular formula	Mp (°C)	Calculated (%)		Found (%)	
			C	H	C	H
1	Mn ₂ C ₂₀ H ₁₀ O ₁₀ S ₂	103-106	41.11	1.73	41.56	1.81
2	Mn ₂ C ₁₆ H ₈ O ₁₀ S	85-87	38.27	1.61	38.51	1.74
3	Mn ₂ C ₁₆ H ₈ O ₁₁	123-125	39.53	1.66	40.23	1.65
4	Mn ₂ C ₁₇ H ₁₁ O ₁₀ N	-	40.91	2.22	40.90	2.32
5	Re ₂ C ₁₆ H ₈ O ₁₁	57-60	25.67	1.08	26.12	1.12
6	MnC ₁₅ H ₁₀ O ₅ S ₂ Br	103-106	34.90	1.96	35.08	2.08
7	MnC ₁₁ H ₈ O ₅ SI	103-106	30.43	1.86	30.81	1.98
8	Mn ₂ C ₁₄ H ₅ O ₉ SN	116-117	35.54	1.07	35.46	1.11
9	Mn ₂ C ₁₄ H ₅ O ₁₀ N	116-117	36.79	1.10	35.98	1.06
10	Mn ₂ C ₁₇ H ₁₁ O ₉ SN	-	39.63	2.15	40.24	2.20
11	Mn ₂ C ₁₇ H ₁₁ O ₁₀ N	-	40.91	2.22	41.35	2.43
12	Re ₂ C ₁₄ H ₅ O ₉ SN	-	22.86	0.69	23.12	1.01
13	Re ₂ C ₁₄ H ₅ O ₁₀ N	-	23.37	0.70	23.42	0.98
14	Re ₂ C ₁₇ H ₁₁ O ₉ SN	-	26.25	1.43	26.24	1.48
15	Re ₂ C ₁₇ H ₁₁ O ₁₀ N	-	26.81	1.46	27.07	1.48

6.5 References

1. OLIS KINFIT, Bogart, G.A.
2. H. Meerwein, *Org. Synth.* 46, **1966**, 113.
3. E.O. Fischer, E. Offhaus, *Chem. Ber.* 102, **1969**, 2449.
4. E.O. Fischer, P. Rustemeyer, *J. Organomet. Chem.* 225, **1982**, 265.
5. U. Schubert, K. Ackermann, P. Rustemeyer, *J. Organomet. Chem.* 231, **1982**, 323.
6. M.H. Quick, R.J. Angelici, *Inorg. Synth.* R.J. Angelici, USA, John Wiley & Sons, Inc. **1990**, 199.
7. C.M. Lukehart, G. Paull Torrence, *Inorg. Synth.* R.J. Angelici, USA, John Wiley & Sons, Inc. **1990**, 156.
8. E.W. Post, K.L. Watters, *Inorg. Chim. Acta* 26, **1978**, 29.
9. B. Denise, P. Dubost, A. Parlier, M. Rudler, H. Rudler, J.C. Daran, J. Vaissermann, F. Delgado, A.R. Arevalo, R.A. Toscano, C. Alvarez, *J. Organomet. Chem.* 418, **1991**, 377.
10. J.A. Connor, E.O. Fischer, *J. Chem. Soc. Chem. Commun.* **1967**, 1024.
11. S. Lotz, M. Landman, D.I. Bezuidenhout, A.J. Olivier, D.C. Liles, P.H. van Rooyen, *J. Organomet. Chem.* 690, **2005**, 5929.

Appendix 1

Crystallographic data of Complex 2

Table 1. Crystal data and structure refinement

Identification code	db15	
Empirical formula	$C_{16} H_8 Mn_2 O_{10} S$	
Formula weight	502.16	
Temperature	293(2) K	
Wavelength	0.71073 Å	
Crystal system	Monoclinic	
Space group	P 2 ₁ /c	
Unit cell dimensions	a = 7.920(4) Å	α = 90°
	b = 22.236(11) Å	β = 95.591(7)°
	c = 11.548(5) Å	γ = 90°
Volume	2024.0(16) Å ³	
Z	4	
Density (calculated)	1.648 Mg/m ³	
Absorption coefficient	1.400 mm ⁻¹	
F(000)	1000	
Crystal size	0.40 x 0.30 x 0.18 mm ³	
Theta range for data collection	2.55 to 26.30°	
Index ranges	-5 ≤ h ≤ 9, -24 ≤ k ≤ 27, -10 ≤ l ≤ 13	
Reflections collected	6741	
Independent reflections	3324 [R(int) = 0.0390]	
Completeness to theta = 25.00°	89.3 %	
Absorption correction	Semi-empirical from equivalents	
Max. and min. transmission	0.777 and 0.476	
Refinement method	Full-matrix least-squares on F ²	
Data / restraints / parameters	3324 / 0 / 271	
Goodness-of-fit on F ²	1.106	
Final R indices [I > 2σ(I)]	R1 = 0.0582, wR2 = 0.1338	
R indices (all data)	R1 = 0.0792, wR2 = 0.1431	
Extinction coefficient	0	
Largest diff. peak and hole	0.425 and -0.365 e.Å ⁻³	

Table 2. Atomic coordinates ($\times 10^4$) and equivalent isotropic displacement parameters ($\text{\AA}^2 \times 10^3$)U(eq) is defined as one third of the trace of the orthogonalized U^{ij} tensor.

	x	y	z	U(eq)
Mn(1)	3948(1)	6623(1)	4314(1)	56(1)
Mn(2)	1394(1)	6114(1)	2591(1)	44(1)
O(1)	6582(7)	7097(3)	6054(5)	131(3)
O(2)	1042(7)	7057(2)	5549(4)	78(1)
O(3)	3657(7)	7748(3)	2928(5)	96(2)
O(4)	6457(6)	6170(3)	2763(5)	108(2)
O(5)	3736(8)	5421(3)	5463(5)	102(2)
O(6)	-455(7)	7265(2)	2817(4)	89(2)
O(7)	3379(6)	6684(2)	826(4)	79(1)
O(8)	3674(7)	5048(2)	2541(5)	96(2)
O(9)	-364(6)	5699(2)	4616(4)	77(1)
C(1)	5552(9)	6907(4)	5384(7)	87(2)
C(2)	2144(8)	6883(3)	5072(5)	58(2)
C(3)	3767(9)	7313(3)	3430(6)	68(2)
C(4)	5466(9)	6340(4)	3353(6)	75(2)
C(5)	3824(9)	5876(4)	5023(6)	72(2)
C(6)	239(8)	6820(3)	2707(5)	55(2)
C(7)	2599(7)	6454(3)	1490(6)	54(2)
C(8)	2782(8)	5453(3)	2583(5)	61(2)
C(9)	338(7)	5847(3)	3846(5)	50(1)
C(10)	-307(12)	5734(5)	1518(8)	45(3)
O(10)	-1172(7)	5938(2)	573(5)	58(1)
C(11)	-968(17)	5122(6)	1641(10)	53(4)
S(1)	-2679(3)	4876(1)	741(2)	82(1)
C(12)	-474(19)	4673(6)	2432(9)	73(4)
C(13)	-1450(30)	4158(6)	2251(14)	102(6)
C(14)	-2691(14)	4208(4)	1418(9)	99(3)
C(15)	-1030(14)	6544(4)	107(10)	69(3)
C(16)	-2453(11)	6607(5)	-825(10)	97(4)
C(10A)	-240(90)	5660(30)	1540(60)	52(19)

O(10A)	-980(70)	5130(30)	1630(40)	52(19)
C(11A)	-1130(70)	5960(20)	530(50)	81(6)
S(1A)	-2810(20)	5591(7)	-283(15)	81(6)
C(12A)	-870(100)	6520(20)	50(70)	81(6)
C(13A)	-1990(80)	6649(17)	-940(60)	81(6)
C(14A)	-3110(40)	6183(13)	-1220(30)	81(6)
C(15A)	-440(100)	4700(40)	2550(60)	52(19)
C(16A)	-1560(100)	4160(30)	2360(70)	52(19)

Table 3. Bond lengths [Å] and angles [°]

Mn(1)-C(1)	1.798(7)	C(15)-C(16)	1.487(9)
Mn(1)-C(4)	1.825(8)	C(15)-H(15A)	0.97
Mn(1)-C(2)	1.840(7)	C(15)-H(15B)	0.97
Mn(1)-C(3)	1.841(8)	C(16)-H(16A)	0.96
Mn(1)-C(5)	1.858(9)	C(16)-H(16B)	0.96
Mn(1)-Mn(2)	2.9238(14)	C(16)-H(16C)	0.96
Mn(2)-C(7)	1.826(7)	C(11)-C(12)	1.384(10)
Mn(2)-C(6)	1.828(7)	C(11)-S(1)	1.715(10)
Mn(2)-C(8)	1.836(7)	S(1)-C(14)	1.679(10)
Mn(2)-C(9)	1.841(6)	C(12)-C(13)	1.386(12)
Mn(2)-C(10)	1.933(7)	C(12)-H(12)	0.93
Mn(2)-C(10A)	1.96(4)	C(13)-C(14)	1.313(19)
O(1)-C(1)	1.148(8)	C(13)-H(13)	0.93
O(2)-C(2)	1.144(7)	C(14)-H(14)	0.93
O(3)-C(3)	1.128(8)	C(10A)-O(10A)	1.332
O(4)-C(4)	1.153(8)	C(10A)-C(11A)	1.457
O(5)-C(5)	1.136(9)	O(10A)-C(15A)	1.450
O(6)-C(6)	1.145(7)	C(15A)-C(16A)	1.508
O(7)-C(7)	1.152(7)	C(15A)-H(15C)	0.97
O(8)-C(8)	1.147(7)	C(15A)-H(15D)	0.97
O(9)-C(9)	1.141(7)	C(16A)-H(16D)	0.96
C(10)-O(10)	1.312(7)	C(16A)-H(16E)	0.96
C(10)-C(11)	1.470(11)	C(16A)-H(16F)	0.96
O(10)-C(15)	1.457(8)	C(11A)-C(12A)	1.39

C(11A)-S(1A)	1.755	C(9)-Mn(2)-C(10A)	90(3)
S(1A)-C(14A)	1.704	C(10)-Mn(2)-C(10A)	5(2)
C(12A)-C(13A)	1.409	C(7)-Mn(2)-Mn(1)	86.54(18)
C(12A)-H(12A)	0.93	C(6)-Mn(2)-Mn(1)	86.33(18)
C(13A)-C(14A)	1.378	C(8)-Mn(2)-Mn(1)	86.45(19)
C(13A)-H(13A)	0.93	C(9)-Mn(2)-Mn(1)	85.76(18)
C(14A)-H(14A)	0.93	C(10)-Mn(2)-Mn(1)	176.3(3)
		C(10A)-Mn(2)-Mn(1)	171.9(17)
C(1)-Mn(1)-C(4)	94.4(3)	O(1)-C(1)-Mn(1)	178.8(9)
C(1)-Mn(1)-C(2)	95.3(3)	O(2)-C(2)-Mn(1)	178.4(6)
C(4)-Mn(1)-C(2)	170.2(3)	O(3)-C(3)-Mn(1)	177.3(7)
C(1)-Mn(1)-C(3)	95.7(3)	O(4)-C(4)-Mn(1)	178.3(6)
C(4)-Mn(1)-C(3)	88.3(4)	O(5)-C(5)-Mn(1)	179.3(7)
C(2)-Mn(1)-C(3)	88.8(3)	O(6)-C(6)-Mn(2)	177.6(5)
C(1)-Mn(1)-C(5)	94.4(4)	O(7)-C(7)-Mn(2)	177.5(6)
C(4)-Mn(1)-C(5)	91.5(3)	O(8)-C(8)-Mn(2)	177.4(6)
C(2)-Mn(1)-C(5)	89.7(3)	O(9)-C(9)-Mn(2)	177.3(6)
C(3)-Mn(1)-C(5)	169.9(3)	O(10)-C(10)-C(11)	103.8(5)
C(1)-Mn(1)-Mn(2)	177.8(3)	O(10)-C(10)-Mn(2)	131.1(6)
C(4)-Mn(1)-Mn(2)	84.6(2)	C(11)-C(10)-Mn(2)	125.1(6)
C(2)-Mn(1)-Mn(2)	85.85(19)	C(10)-O(10)-C(15)	125.0(5)
C(3)-Mn(1)-Mn(2)	86.2(2)	O(10)-C(15)-C(16)	105.9(6)
C(5)-Mn(1)-Mn(2)	83.7(2)	O(10)-C(15)-H(15A)	110.6
C(7)-Mn(2)-C(6)	89.7(3)	C(16)-C(15)-H(15A)	110.6
C(7)-Mn(2)-C(8)	88.5(3)	O(10)-C(15)-H(15B)	110.5
C(6)-Mn(2)-C(8)	172.7(3)	C(16)-C(15)-H(15B)	110.5
C(7)-Mn(2)-C(9)	171.8(3)	H(15A)-C(15)-H(15B)	108.7
C(6)-Mn(2)-C(9)	87.2(3)	C(15)-C(16)-H(16A)	109.5
C(8)-Mn(2)-C(9)	93.7(3)	C(15)-C(16)-H(16B)	109.5
C(7)-Mn(2)-C(10)	96.5(4)	H(16A)-C(16)-H(16B)	109.5
C(6)-Mn(2)-C(10)	95.7(4)	C(15)-C(16)-H(16C)	109.5
C(8)-Mn(2)-C(10)	91.6(4)	H(16A)-C(16)-H(16C)	109.5
C(9)-Mn(2)-C(10)	91.3(4)	H(16B)-C(16)-H(16C)	109.5
C(7)-Mn(2)-C(10A)	98(2)	C(12)-C(11)-C(10)	130.6(7)
C(6)-Mn(2)-C(10A)	100(3)	C(12)-C(11)-S(1)	109.0(6)
C(8)-Mn(2)-C(10A)	87(3)	C(10)-C(11)-S(1)	120.3(6)

C(14)-S(1)-C(11)	92.3(5)	C(15A)-C(16A)-H(16D)	109.5
C(11)-C(12)-C(13)	112.3(9)	C(15A)-C(16A)-H(16E)	109.5
C(11)-C(12)-H(12)	123.8	H(16D)-C(16A)-H(16E)	109.5
C(13)-C(12)-H(12)	123.9	C(15A)-C(16A)-H(16F)	109.5
C(14)-C(13)-C(12)	114.0(9)	H(16D)-C(16A)-H(16F)	109.5
C(14)-C(13)-H(13)	123.0	H(16E)-C(16A)-H(16F)	109.5
C(12)-C(13)-H(13)	123.0	C(12A)-C(11A)-C(10A)	130.5
C(13)-C(14)-S(1)	112.3(8)	C(12A)-C(11A)-S(1A)	109.4
C(13)-C(14)-H(14)	123.9	C(10A)-C(11A)-S(1A)	120.1
S(1)-C(14)-H(14)	123.9	C(14A)-S(1A)-C(11A)	91.9
O(10A)-C(10A)-C(11A)	106.3	C(11A)-C(12A)-C(13A)	114.1
O(10A)-C(10A)-Mn(2)	133(3)	C(11A)-C(12A)-H(12A)	123.0
C(11A)-C(10A)-Mn(2)	120(3)	C(13A)-C(12A)-H(12A)	123.0
C(10A)-O(10A)-C(15A)	122.5	C(14A)-C(13A)-C(12A)	111.8
O(10A)-C(15A)-C(16A)	107.3	C(14A)-C(13A)-H(13A)	124.1
O(10A)-C(15A)-H(15C)	110.3	C(12A)-C(13A)-H(13A)	124.1
C(16A)-C(15A)-H(15C)	110.3	C(13A)-C(14A)-S(1A)	112.8
O(10A)-C(15A)-H(15D)	110.3	C(13A)-C(14A)-H(14A)	123.6
C(16A)-C(15A)-H(15D)	110.3	S(1A)-C(14A)-H(14A)	123.6
H(15C)-C(15A)-H(15D)	108.5		

Table 4. Anisotropic displacement parameters ($\text{\AA}^2 \times 10^3$)

The anisotropic displacement factor exponent takes the form: $-2\pi^2 [h^2 a^2 U^{11} + \dots + 2 h k a^* b^* U^{12}]$

	U ¹¹	U ²²	U ³³	U ²³	U ¹³	U ¹²
Mn(1)	46(1)	76(1)	45(1)	-11(1)	-8(1)	1(1)
Mn(2)	39(1)	52(1)	39(1)	-5(1)	-4(1)	3(1)
O(1)	91(4)	211(7)	85(4)	-37(4)	-28(3)	-42(4)
O(2)	87(4)	82(3)	66(3)	-11(2)	18(3)	13(3)
O(3)	119(5)	82(4)	85(4)	4(3)	4(3)	-20(3)
O(4)	52(3)	175(6)	97(4)	-34(4)	11(3)	10(4)
O(5)	120(5)	96(4)	87(4)	19(3)	-1(3)	45(4)
O(6)	107(4)	77(3)	81(4)	-6(3)	-1(3)	46(3)

O(7)	72(3)	108(4)	57(3)	0(3)	11(2)	-18(3)
O(8)	90(4)	88(4)	107(4)	-15(3)	-5(3)	43(3)
O(9)	85(3)	89(3)	59(3)	4(2)	16(3)	-12(3)
C(1)	64(5)	121(7)	74(5)	-18(5)	-14(4)	-11(4)
C(2)	64(4)	62(4)	47(4)	-7(3)	-4(3)	-2(3)
C(3)	73(5)	74(5)	53(4)	-9(3)	-9(3)	-12(4)
C(4)	45(4)	117(6)	61(5)	-18(4)	-5(3)	-2(4)
C(5)	68(5)	89(5)	55(4)	-16(4)	-14(3)	28(4)
C(6)	60(4)	61(4)	43(4)	-4(3)	-3(3)	2(3)
C(7)	41(3)	69(4)	52(4)	-6(3)	-3(3)	-1(3)
C(8)	61(4)	70(4)	49(4)	-6(3)	-2(3)	7(3)
C(9)	51(4)	56(4)	43(4)	-4(3)	1(3)	2(3)
C(10)	38(4)	53(5)	42(4)	3(3)	6(3)	3(3)
O(10)	53(3)	67(3)	51(3)	3(2)	-16(2)	-9(2)
C(11)	59(6)	60(6)	42(5)	-14(3)	6(3)	-11(3)
S(1)	80(2)	92(2)	70(2)	-18(1)	-6(1)	-33(1)
C(12)	114(9)	59(6)	46(5)	0(4)	2(4)	-22(5)
C(13)	180(15)	59(6)	74(8)	-2(5)	44(8)	-32(7)
C(14)	133(9)	81(6)	85(8)	-22(5)	19(6)	-58(6)
C(15)	69(6)	79(5)	55(5)	22(4)	-18(4)	-6(4)
C(16)	75(7)	114(7)	93(8)	48(6)	-35(6)	-16(6)

Table 5. Hydrogen coordinates (x 10⁴) and isotropic displacement parameters (Å²x 10³)

	x	y	z	U(eq)
H(12)	410	4713	3019	88
H(13)	-1237	3807	2680	123
H(14)	-3488	3908	1226	119
H(15A)	51	6596	-209	83
H(15B)	-1123	6841	712	83
H(16A)	-2399	6995	-1182	145
H(16B)	-3513	6566	-493	145
H(16C)	-2366	6299	-1400	145
H(12A)	-40	6785	351	97

H(13A)	-1983	7006	-1364	97
H(14A)	-3939	6191	-1847	97
H(15C)	-554	4880	3302	63
H(15D)	736	4595	2505	63
H(16D)	-1238	3866	2956	79
H(16E)	-1440	3988	1612	79
H(16F)	-2724	4272	2407	79

Table 6. Torsion angles [°]

C(4)-Mn(1)-Mn(2)-C(7)	-44.7(3)	C(9)-Mn(2)-C(10)-O(10)	132.7(9)
C(2)-Mn(1)-Mn(2)-C(7)	133.0(3)	C(6)-Mn(2)-C(10)-C(11)	-132.0(6)
C(3)-Mn(1)-Mn(2)-C(7)	43.9(3)	C(7)-Mn(2)-C(10)-C(11)	137.6(6)
C(5)-Mn(1)-Mn(2)-C(7)	-136.8(3)	C(8)-Mn(2)-C(10)-C(11)	48.9(7)
C(4)-Mn(1)-Mn(2)-C(6)	-134.6(3)	C(9)-Mn(2)-C(10)-C(11)	-44.8(7)
C(2)-Mn(1)-Mn(2)-C(6)	43.1(3)	C(11)-C(10)-O(10)-C(15)	177.2(8)
C(3)-Mn(1)-Mn(2)-C(6)	-46.0(3)	Mn(2)-C(10)-O(10)-C(15)	-0.7(16)
C(5)-Mn(1)-Mn(2)-C(6)	133.3(3)	C(10)-O(10)-C(15)-C(16)	-169.7(7)
C(4)-Mn(1)-Mn(2)-C(8)	44.0(3)	O(10)-C(10)-C(11)-C(12)	175.5(9)
C(2)-Mn(1)-Mn(2)-C(8)	-138.3(3)	Mn(2)-C(10)-C(11)-C(12)	-6.4(11)
C(3)-Mn(1)-Mn(2)-C(8)	132.7(3)	O(10)-C(10)-C(11)-S(1)	-7.1(9)
C(5)-Mn(1)-Mn(2)-C(8)	-48.1(3)	Mn(2)-C(10)-C(11)-S(1)	171.0(10)
C(4)-Mn(1)-Mn(2)-C(9)	138.0(3)	C(12)-C(11)-S(1)-C(14)	0.1(7)
C(2)-Mn(1)-Mn(2)-C(9)	-44.3(3)	C(10)-C(11)-S(1)-C(14)	-177.8(8)
C(3)-Mn(1)-Mn(2)-C(9)	-133.4(3)	C(10)-C(11)-C(12)-C(13)	179.6(9)
C(5)-Mn(1)-Mn(2)-C(9)	45.9(3)	S(1)-C(11)-C(12)-C(13)	1.9(10)
C(7)-Mn(2)-C(10)-O(10)	-44.9(10)	C(11)-C(12)-C(13)-C(14)	-3.7(15)
C(6)-Mn(2)-C(10)-O(10)	45.5(10)	C(12)-C(13)-C(14)-S(1)	3.7(15)
C(8)-Mn(2)-C(10)-O(10)	-133.6(9)	C(11)-S(1)-C(14)-C(13)	-2.2(10)

Appendix 2

Crystallographic data of Complex 3

Table 1. Crystal data and structure refinement

Identification code	DBMCO2	
Empirical formula	C ₁₆ H ₈ Mn ₂ O ₁₁	
Formula weight	486.10	
Temperature	293(2) K	
Wavelength	0.71073 Å	
Crystal system	Monoclinic	
Space group	P 2 ₁ /c	
Unit cell dimensions	a = 12.4868(14) Å	α = 90°.
	b = 12.3976(14) Å	β = 92.723(2)°.
	c = 12.5593(14) Å	γ = 90°.
Volume	1942.1(4) Å ³	
Z	4	
Density (calculated)	1.663 Mg/m ³	
Absorption coefficient	1.357 mm ⁻¹	
F(000)	968	
Crystal size	0.36 x 0.23 x 0.18 mm ³	
Theta range for data collection	2.31 to 26.47°.	
Index ranges	-15 ≤ h ≤ 15, -15 ≤ k ≤ 14, -4 ≤ l ≤ 15	
Reflections collected	10177	
Independent reflections	3652 [R(int) = 0.0216]	
Completeness to theta = 25.00°	99.4 %	
Absorption correction	Semi-empirical from equivalents	
Max. and min. transmission	0.783 and 0.715	
Refinement method	Full-matrix least-squares on F ²	
Data / restraints / parameters	3652 / 0 / 294	
Goodness-of-fit on F ²	1.083	
Final R indices [I > 2σ(I)]	R1 = 0.0303, wR2 = 0.0771	
R indices (all data)	R1 = 0.0385, wR2 = 0.0846	
Extinction coefficient	0	
Largest diff. peak and hole	0.307 and -0.191 e.Å ⁻³	

Table 2. Atomic coordinates ($\times 10^4$) and equivalent isotropic displacement parameters ($\text{\AA}^2 \times 10^3$)U(eq) is defined as one third of the trace of the orthogonalized U^{ij} tensor.

	x	y	z	U(eq)
Mn(1)	1030(1)	1423(1)	3219(1)	48(1)
Mn(2)	2905(1)	371(1)	2358(1)	47(1)
C(1)	-62(2)	2125(2)	3822(2)	63(1)
O(1)	-728(2)	2571(2)	4217(2)	92(1)
C(2)	1238(2)	476(2)	4343(2)	56(1)
O(2)	1338(2)	-95(2)	5045(1)	78(1)
C(3)	2037(2)	2335(2)	3838(2)	60(1)
O(3)	2635(2)	2916(2)	4240(2)	91(1)
C(4)	993(2)	2266(2)	2008(2)	64(1)
O(4)	954(2)	2805(2)	1275(2)	99(1)
C(5)	165(2)	409(2)	2512(2)	65(1)
O(5)	-382(2)	-208(2)	2093(2)	98(1)
C(6)	3508(2)	479(2)	3718(2)	56(1)
O(6)	3850(2)	525(2)	4577(1)	77(1)
C(7)	3369(2)	1735(2)	2020(2)	60(1)
O(7)	3650(2)	2580(2)	1802(2)	86(1)
C(8)	2082(2)	321(2)	1088(2)	59(1)
O(8)	1564(2)	277(2)	326(1)	85(1)
C(9)	2254(2)	-900(2)	2725(2)	55(1)
O(9)	1844(2)	-1685(2)	2956(1)	75(1)
C(10)	4104(2)	-354(2)	1753(2)	55(1)
O(10)	5158(1)	-187(2)	1863(1)	74(1)
C(11)	4018(2)	-1257(2)	1025(2)	57(1)
O(11)	3019(1)	-1702(2)	812(1)	77(1)
C(12)	4723(2)	-1811(2)	450(2)	76(1)
C(13)	4157(2)	-2614(2)	-127(2)	81(1)
C(14)	3147(3)	-2525(2)	116(2)	81(1)
C(15)	5651(2)	634(4)	2539(4)	89(1)
C(16)	6825(3)	541(4)	2424(4)	100(1)

Table 3. Bond lengths [Å] and angles [°]

Mn(1)-C(1)	1.813(2)	C(16)-H(16A)	0.82(4)
Mn(1)-C(3)	1.836(3)	C(16)-H(16B)	0.92(4)
Mn(1)-C(4)	1.844(2)	C(16)-H(16C)	0.92(5)
Mn(1)-C(2)	1.845(2)		
Mn(1)-C(5)	1.857(3)	C(1)-Mn(1)-C(3)	92.36(11)
Mn(1)-Mn(2)	2.9316(5)	C(1)-Mn(1)-C(4)	94.76(10)
Mn(2)-C(6)	1.839(2)	C(3)-Mn(1)-C(4)	89.46(11)
Mn(2)-C(9)	1.842(2)	C(1)-Mn(1)-C(2)	93.81(10)
Mn(2)-C(7)	1.844(3)	C(3)-Mn(1)-C(2)	89.98(10)
Mn(2)-C(8)	1.857(2)	C(4)-Mn(1)-C(2)	171.43(10)
Mn(2)-C(10)	1.932(2)	C(1)-Mn(1)-C(5)	95.33(11)
C(1)-O(1)	1.133(3)	C(3)-Mn(1)-C(5)	172.32(10)
C(2)-O(2)	1.133(3)	C(4)-Mn(1)-C(5)	89.87(11)
C(3)-O(3)	1.138(3)	C(2)-Mn(1)-C(5)	89.54(11)
C(4)-O(4)	1.136(3)	C(1)-Mn(1)-Mn(2)	175.74(8)
C(5)-O(5)	1.137(3)	C(3)-Mn(1)-Mn(2)	83.55(7)
C(6)-O(6)	1.142(3)	C(4)-Mn(1)-Mn(2)	86.40(8)
C(7)-O(7)	1.142(3)	C(2)-Mn(1)-Mn(2)	85.04(7)
C(8)-O(8)	1.130(3)	C(5)-Mn(1)-Mn(2)	88.77(8)
C(9)-O(9)	1.144(3)	C(6)-Mn(2)-C(9)	89.74(9)
C(10)-O(10)	1.332(3)	C(6)-Mn(2)-C(7)	91.61(10)
C(10)-C(11)	1.446(3)	C(9)-Mn(2)-C(7)	171.74(10)
O(10)-C(15)	1.444(3)	C(6)-Mn(2)-C(8)	170.35(10)
C(11)-C(12)	1.352(3)	C(9)-Mn(2)-C(8)	87.33(9)
C(11)-O(11)	1.379(3)	C(7)-Mn(2)-C(8)	90.02(10)
O(11)-C(14)	1.358(3)	C(6)-Mn(2)-C(10)	96.22(9)
C(12)-C(13)	1.403(4)	C(9)-Mn(2)-C(10)	93.42(9)
C(12)-H(12)	0.94(3)	C(7)-Mn(2)-C(10)	94.53(10)
C(13)-C(14)	1.317(4)	C(8)-Mn(2)-C(10)	93.14(9)
C(13)-H(13)	1.01(4)	C(6)-Mn(2)-Mn(1)	85.62(7)
C(14)-H(14)	1.03(3)	C(9)-Mn(2)-Mn(1)	85.33(7)
C(15)-C(16)	1.484(5)	C(7)-Mn(2)-Mn(1)	86.64(7)
C(15)-H(15A)	0.86(3)	C(8)-Mn(2)-Mn(1)	84.98(7)
C(15)-H(15B)	0.86(3)	C(10)-Mn(2)-Mn(1)	177.78(7)

O(1)-C(1)-Mn(1)	178.4(2)	C(13)-C(12)-H(12)	125.0(19)
O(2)-C(2)-Mn(1)	178.0(2)	C(14)-C(13)-C(12)	106.6(2)
O(3)-C(3)-Mn(1)	177.7(2)	C(14)-C(13)-H(13)	129.7(19)
O(4)-C(4)-Mn(1)	178.2(2)	C(12)-C(13)-H(13)	123.7(19)
O(5)-C(5)-Mn(1)	178.5(2)	C(13)-C(14)-O(11)	110.8(3)
O(6)-C(6)-Mn(2)	177.4(2)	C(13)-C(14)-H(14)	135.2(18)
O(7)-C(7)-Mn(2)	179.3(2)	O(11)-C(14)-H(14)	113.5(18)
O(8)-C(8)-Mn(2)	178.5(2)	O(10)-C(15)-C(16)	106.5(3)
O(9)-C(9)-Mn(2)	179.5(2)	O(10)-C(15)-H(15A)	114(2)
O(10)-C(10)-C(11)	103.25(18)	C(16)-C(15)-H(15A)	118(2)
O(10)-C(10)-Mn(2)	131.79(16)	O(10)-C(15)-H(15B)	111(2)
C(11)-C(10)-Mn(2)	124.96(15)	C(16)-C(15)-H(15B)	115(2)
C(10)-O(10)-C(15)	124.2(2)	H(15A)-C(15)-H(15B)	93(3)
C(12)-C(11)-O(11)	107.4(2)	C(15)-C(16)-H(16A)	112(3)
C(12)-C(11)-C(10)	134.4(2)	C(15)-C(16)-H(16B)	108(3)
O(11)-C(11)-C(10)	118.13(18)	H(16A)-C(16)-H(16B)	119(4)
C(14)-O(11)-C(11)	107.0(2)	C(15)-C(16)-H(16C)	115(3)
C(11)-C(12)-C(13)	108.2(2)	H(16A)-C(16)-H(16C)	101(4)
C(11)-C(12)-H(12)	126.7(19)	H(16B)-C(16)-H(16C)	103(4)

Table 4. Anisotropic displacement parameters ($\text{\AA}^2 \times 10^3$)

The anisotropic displacement factor exponent takes the form: $-2p^2 [h^2 a^{*2} U^{11} + \dots + 2 h k a^* b^* U^{12}]$

	U ¹¹	U ²²	U ³³	U ²³	U ¹³	U ¹²
Mn(1)	43(1)	55(1)	46(1)	5(1)	7(1)	4(1)
Mn(2)	45(1)	52(1)	46(1)	-2(1)	6(1)	1(1)
C(1)	53(1)	74(2)	63(1)	13(1)	10(1)	11(1)
O(1)	70(1)	107(2)	103(1)	13(1)	30(1)	37(1)
C(2)	48(1)	63(1)	57(1)	5(1)	11(1)	5(1)
O(2)	81(1)	87(1)	68(1)	29(1)	14(1)	12(1)
C(3)	52(1)	65(1)	63(1)	-4(1)	15(1)	5(1)
O(3)	68(1)	95(1)	109(1)	-39(1)	12(1)	-14(1)
C(4)	69(2)	66(1)	58(1)	7(1)	10(1)	6(1)
O(4)	131(2)	97(1)	70(1)	35(1)	13(1)	21(1)
C(5)	52(1)	77(2)	67(1)	6(1)	2(1)	0(1)

O(5)	77(1)	107(2)	108(2)	-9(1)	-15(1)	-26(1)
C(6)	48(1)	61(1)	60(1)	-2(1)	6(1)	2(1)
O(6)	69(1)	101(1)	60(1)	-3(1)	-8(1)	2(1)
C(7)	55(1)	63(1)	62(1)	-5(1)	16(1)	2(1)
O(7)	89(1)	64(1)	107(1)	6(1)	30(1)	-8(1)
C(8)	61(1)	64(1)	52(1)	5(1)	8(1)	0(1)
O(8)	94(1)	100(2)	59(1)	7(1)	-16(1)	-5(1)
C(9)	56(1)	62(1)	46(1)	-2(1)	2(1)	4(1)
O(9)	91(1)	65(1)	69(1)	6(1)	6(1)	-14(1)
C(10)	47(1)	61(1)	57(1)	-4(1)	4(1)	-2(1)
O(10)	46(1)	88(1)	88(1)	-28(1)	4(1)	-3(1)
C(11)	48(1)	64(1)	60(1)	-10(1)	7(1)	2(1)
O(11)	59(1)	89(1)	84(1)	-37(1)	14(1)	-13(1)
C(12)	57(2)	82(2)	91(2)	-21(2)	11(1)	6(1)
C(13)	82(2)	76(2)	86(2)	-27(2)	12(2)	5(1)
C(14)	80(2)	86(2)	79(2)	-34(2)	16(1)	-14(2)
C(15)	55(2)	105(3)	108(3)	-42(2)	3(2)	-13(2)
C(16)	54(2)	111(3)	133(3)	-31(3)	-3(2)	-12(2)

Table 5. Hydrogen coordinates (x 10⁴) and isotropic displacement parameters (Å²x 10³)

	x	y	z	U(eq)
H(12)	5460(30)	-1670(20)	410(20)	94(9)
H(13)	4510(30)	-3150(30)	-610(30)	110(11)
H(14)	2440(30)	-2870(30)	-150(20)	101(10)
H(15A)	5360(20)	1260(30)	2450(20)	78(10)
H(15B)	5450(30)	580(30)	3180(30)	96(11)
H(16A)	7160(30)	1000(30)	2780(30)	112(13)
H(16B)	6950(30)	480(30)	1710(30)	119(14)
H(16C)	7130(40)	-80(50)	2700(40)	170(20)

Table 6. Torsion angles [°]

C(3)-Mn(1)-Mn(2)-C(6)	45.97(10)	C(4)-Mn(1)-Mn(2)-C(6)	135.84(11)
-----------------------	-----------	-----------------------	------------

C(2)-Mn(1)-Mn(2)-C(6)	-44.57(10)	C(2)-Mn(1)-Mn(2)-C(8)	133.24(10)
C(5)-Mn(1)-Mn(2)-C(6)	-134.21(10)	C(5)-Mn(1)-Mn(2)-C(8)	43.60(10)
C(3)-Mn(1)-Mn(2)-C(9)	136.07(10)	C(6)-Mn(2)-C(10)-O(10)	-43.4(2)
C(4)-Mn(1)-Mn(2)-C(9)	-134.07(10)	C(9)-Mn(2)-C(10)-O(10)	-133.5(2)
C(2)-Mn(1)-Mn(2)-C(9)	45.52(9)	C(7)-Mn(2)-C(10)-O(10)	48.7(2)
C(5)-Mn(1)-Mn(2)-C(9)	-44.12(10)	C(8)-Mn(2)-C(10)-O(10)	139.0(2)
C(3)-Mn(1)-Mn(2)-C(7)	-45.90(11)	C(6)-Mn(2)-C(10)-C(11)	137.1(2)
C(4)-Mn(1)-Mn(2)-C(7)	43.97(11)	C(9)-Mn(2)-C(10)-C(11)	47.0(2)
C(2)-Mn(1)-Mn(2)-C(7)	-136.44(10)	C(7)-Mn(2)-C(10)-C(11)	-130.8(2)
C(5)-Mn(1)-Mn(2)-C(7)	133.91(11)	C(8)-Mn(2)-C(10)-C(11)	-40.5(2)
C(3)-Mn(1)-Mn(2)-C(8)	-136.21(10)	C(11)-C(10)-O(10)-C(15)	-178.9(3)
C(4)-Mn(1)-Mn(2)-C(8)	-46.35(11)		

Appendix 3

Crystallographic data of Complex 5

Table 1. Crystal data and structure refinement

Identification code	dbmc12_abs	
Empirical formula	C ₁₆ H ₈ O ₁₁ Re ₂	
Formula weight	748.62	
Temperature	293(2) K	
Wavelength	0.71073 Å	
Crystal system	Orthorhombic	
Space group	P b c a	
Unit cell dimensions	a = 12.9646(8) Å	α = 90°.
	b = 15.6580(9) Å	β = 90°.
	c = 19.3844(11) Å	γ = 90°.
Volume	3935.0(4) Å ³	
Z	8	
Density (calculated)	2.527 Mg/m ³	
Absorption coefficient	12.350 mm ⁻¹	
F(000)	2736	
Crystal size	0.34 x 0.22 x 0.20 mm ³	
Theta range for data collection	2.60 to 26.58°.	
Index ranges	-16 ≤ h ≤ 16, -14 ≤ k ≤ 18, -24 ≤ l ≤ 12	
Reflections collected	20120	
Independent reflections	3784 [R(int) = 0.0346]	
Completeness to theta = 25.00°	99.9 %	
Absorption correction	Semi-empirical from equivalents	
Max. and min. transmission	0.085 and 0.045	
Refinement method	Full-matrix least-squares on F ²	
Data / restraints / parameters	3784 / 0 / 263	
Goodness-of-fit on F ²	1.134	
Final R indices [I > 2σ(I)]	R1 = 0.0205, wR2 = 0.0506	
R indices (all data)	R1 = 0.0229, wR2 = 0.0520	
Extinction coefficient	0.00093(4)	
Largest diff. peak and hole	0.927 and -0.651 e.Å ⁻³	

Table 2. Atomic coordinates ($\times 10^4$) and equivalent isotropic displacement parameters ($\text{\AA}^2 \times 10^3$)
 $U(\text{eq})$ is defined as one third of the trace of the orthogonalized U^{ij} tensor.

	x	y	z	U(eq)
Re(1)	4861(1)	2119(1)	6807(1)	35(1)
Re(2)	4325(1)	1913(1)	5268(1)	37(1)
C(1)	5279(3)	2230(3)	7755(2)	51(1)
O(1)	5535(3)	2252(3)	8314(2)	73(1)
C(2)	6290(3)	2254(2)	6454(2)	41(1)
O(2)	7119(2)	2207(2)	6257(2)	60(1)
C(3)	5220(4)	883(3)	6841(2)	49(1)
O(3)	5434(4)	194(2)	6877(2)	84(1)
C(4)	3463(3)	1722(3)	7087(2)	48(1)
O(4)	2729(2)	1401(2)	7259(2)	68(1)
C(5)	4015(3)	1667(3)	4312(2)	48(1)
O(5)	3848(3)	1509(2)	3753(2)	66(1)
C(6)	3282(4)	2844(3)	5347(2)	49(1)
O(6)	2694(3)	3372(3)	5370(2)	78(1)
C(7)	5399(4)	2777(3)	5027(2)	47(1)
O(7)	5994(3)	3271(3)	4880(2)	76(1)
C(8)	5414(3)	1027(3)	5312(2)	48(1)
O(8)	6039(3)	514(2)	5328(2)	67(1)
C(9)	3282(3)	1082(3)	5600(2)	47(1)
O(9)	2664(3)	607(2)	5770(2)	73(1)
C(10)	4491(3)	3432(2)	6664(2)	37(1)
O(10)	3616(2)	3846(2)	6771(1)	48(1)
C(11)	5188(3)	4102(3)	6431(2)	44(1)
O(11)	6210(2)	3927(2)	6334(2)	60(1)
C(12)	5017(4)	4937(3)	6285(3)	67(1)
C(13)	5978(4)	5302(4)	6097(3)	83(2)
C(14)	6664(4)	4671(3)	6137(3)	77(2)
C(15)	2693(3)	3457(3)	7043(2)	50(1)
C(16)	1883(4)	4144(3)	7027(3)	80(2)

Table 3. Bond lengths [Å] and angles [°]

Re(1)-C(1)	1.923(5)	C(16)-H(16B)	0.9600
Re(1)-C(2)	1.987(4)	C(16)-H(16C)	0.9600
Re(1)-C(4)	1.992(4)		
Re(1)-C(3)	1.992(5)	C(1)-Re(1)-C(2)	93.26(18)
Re(1)-C(10)	2.129(4)	C(1)-Re(1)-C(4)	91.36(19)
Re(1)-Re(2)	3.0809(3)	C(2)-Re(1)-C(4)	167.42(16)
Re(2)-C(5)	1.934(4)	C(1)-Re(1)-C(3)	89.42(19)
Re(2)-C(8)	1.981(5)	C(2)-Re(1)-C(3)	84.07(17)
Re(2)-C(9)	1.984(4)	C(4)-Re(1)-C(3)	84.28(17)
Re(2)-C(6)	1.995(5)	C(1)-Re(1)-C(10)	95.82(17)
Re(2)-C(7)	1.997(4)	C(2)-Re(1)-C(10)	93.60(15)
C(1)-O(1)	1.135(5)	C(4)-Re(1)-C(10)	97.58(15)
C(2)-O(2)	1.143(5)	C(3)-Re(1)-C(10)	174.38(15)
C(3)-O(3)	1.117(6)	C(1)-Re(1)-Re(2)	176.58(13)
C(4)-O(4)	1.127(5)	C(2)-Re(1)-Re(2)	83.56(11)
C(5)-O(5)	1.132(5)	C(4)-Re(1)-Re(2)	91.50(13)
C(6)-O(6)	1.126(5)	C(3)-Re(1)-Re(2)	89.00(12)
C(7)-O(7)	1.128(6)	C(10)-Re(1)-Re(2)	85.66(9)
C(8)-O(8)	1.141(5)	C(5)-Re(2)-C(8)	92.90(17)
C(9)-O(9)	1.142(5)	C(5)-Re(2)-C(9)	92.26(17)
C(10)-O(10)	1.323(5)	C(8)-Re(2)-C(9)	90.72(18)
C(10)-C(11)	1.457(5)	C(5)-Re(2)-C(6)	94.52(17)
O(10)-C(15)	1.443(5)	C(8)-Re(2)-C(6)	172.56(17)
C(11)-C(12)	1.355(6)	C(9)-Re(2)-C(6)	89.60(18)
C(11)-O(11)	1.367(5)	C(5)-Re(2)-C(7)	93.18(17)
O(11)-C(14)	1.360(5)	C(8)-Re(2)-C(7)	89.3(2)
C(12)-C(13)	1.418(7)	C(9)-Re(2)-C(7)	174.55(17)
C(12)-H(12)	0.9300	C(6)-Re(2)-C(7)	89.7(2)
C(13)-C(14)	1.331(8)	C(5)-Re(2)-Re(1)	174.48(13)
C(13)-H(13)	0.9300	C(8)-Re(2)-Re(1)	82.54(12)
C(14)-H(14)	0.9300	C(9)-Re(2)-Re(1)	84.71(12)
C(15)-C(16)	1.504(6)	C(6)-Re(2)-Re(1)	90.08(12)
C(15)-H(15A)	0.9700	C(7)-Re(2)-Re(1)	89.89(12)
C(15)-H(15B)	0.9700	O(1)-C(1)-Re(1)	176.6(4)
C(16)-H(16A)	0.9600	O(2)-C(2)-Re(1)	170.1(3)

O(3)-C(3)-Re(1)	178.1(5)	C(14)-C(13)-C(12)	105.9(5)
O(4)-C(4)-Re(1)	171.4(4)	C(14)-C(13)-H(13)	127.1
O(5)-C(5)-Re(2)	178.6(4)	C(12)-C(13)-H(13)	127.1
O(6)-C(6)-Re(2)	177.9(4)	C(13)-C(14)-O(11)	111.2(4)
O(7)-C(7)-Re(2)	178.7(4)	C(13)-C(14)-H(14)	124.4
O(8)-C(8)-Re(2)	179.0(4)	O(11)-C(14)-H(14)	124.4
O(9)-C(9)-Re(2)	177.5(4)	O(10)-C(15)-C(16)	105.6(3)
O(10)-C(10)-C(11)	103.1(3)	O(10)-C(15)-H(15A)	110.6
O(10)-C(10)-Re(1)	130.2(3)	C(16)-C(15)-H(15A)	110.6
C(11)-C(10)-Re(1)	126.6(3)	O(10)-C(15)-H(15B)	110.6
C(10)-O(10)-C(15)	124.1(3)	C(16)-C(15)-H(15B)	110.6
C(12)-C(11)-O(11)	108.9(4)	H(15A)-C(15)-H(15B)	108.7
C(12)-C(11)-C(10)	131.2(4)	C(15)-C(16)-H(16A)	109.5
O(11)-C(11)-C(10)	119.9(3)	C(15)-C(16)-H(16B)	109.5
C(14)-O(11)-C(11)	106.6(4)	H(16A)-C(16)-H(16B)	109.5
C(11)-C(12)-C(13)	107.4(5)	C(15)-C(16)-H(16C)	109.5
C(11)-C(12)-H(12)	126.3	H(16A)-C(16)-H(16C)	109.5
C(13)-C(12)-H(12)	126.3	H(16B)-C(16)-H(16C)	109.5

Table 4. Anisotropic displacement parameters ($\text{\AA}^2 \times 10^3$)

The anisotropic displacement factor exponent takes the form:

$$-2p^2 [h^2 a^* 2U^{11} + \dots + 2 h k a^* b^* U^{12}]$$

	U ¹¹	U ²²	U ³³	U ²³	U ¹³	U ¹²
Re(1)	38(1)	31(1)	35(1)	0(1)	2(1)	0(1)
Re(2)	38(1)	35(1)	37(1)	1(1)	-2(1)	-1(1)
C(1)	52(3)	55(3)	45(2)	-1(2)	2(2)	3(2)
O(1)	84(3)	95(3)	41(2)	-3(2)	-9(2)	6(2)
C(2)	41(2)	37(2)	44(2)	-2(2)	1(2)	0(2)
O(2)	42(2)	63(2)	75(2)	0(2)	7(2)	1(1)
C(3)	55(3)	43(3)	50(3)	1(2)	9(2)	4(2)
O(3)	106(3)	36(2)	109(3)	10(2)	19(2)	18(2)
C(4)	51(2)	35(2)	58(2)	-1(2)	12(2)	5(2)
O(4)	54(2)	48(2)	101(2)	9(2)	27(2)	-6(2)
C(5)	45(2)	44(2)	55(3)	-4(2)	-3(2)	-2(2)
O(5)	78(2)	73(2)	47(2)	-16(2)	-12(2)	-2(2)

C(6)	54(3)	50(2)	45(2)	0(2)	-7(2)	5(2)
O(6)	84(3)	74(2)	75(2)	-10(2)	-16(2)	35(2)
C(7)	56(2)	47(2)	39(2)	1(2)	-2(2)	-9(2)
O(7)	84(2)	75(2)	68(2)	8(2)	9(2)	-35(2)
C(8)	44(2)	45(2)	53(2)	-3(2)	-4(2)	-2(2)
O(8)	56(2)	55(2)	89(3)	-8(2)	2(2)	14(2)
C(9)	45(2)	47(2)	49(2)	8(2)	-1(2)	3(2)
O(9)	63(2)	67(2)	89(3)	23(2)	2(2)	-17(2)
C(10)	43(2)	32(2)	35(2)	-2(1)	-1(2)	-2(2)
O(10)	47(2)	35(2)	62(2)	3(1)	11(1)	2(1)
C(11)	42(2)	36(2)	55(2)	-5(2)	2(2)	-4(2)
O(11)	46(2)	42(2)	92(2)	-3(2)	13(2)	-7(1)
C(12)	62(3)	43(3)	96(4)	21(3)	4(3)	0(2)
C(13)	75(3)	56(3)	120(5)	24(3)	13(3)	-21(3)
C(14)	62(3)	49(3)	119(5)	5(3)	24(3)	-21(2)
C(15)	49(2)	41(2)	61(2)	10(2)	16(2)	5(2)
C(16)	64(3)	52(3)	123(5)	25(3)	42(3)	18(2)

Table 5. Hydrogen coordinates ($\times 10^4$) and isotropic displacement parameters ($\text{\AA}^2 \times 10^3$)

	x	y	z	U(eq)
H(12)	4386	5218	6305	80
H(13)	6103	5866	5972	100
H(14)	7363	4732	6041	92
H(15A)	2805	3260	7512	60
H(15B)	2486	2974	6761	60
H(16A)	2014	4522	6647	120
H(16B)	1902	4461	7451	120
H(16C)	1215	3888	6972	120

Table 6. Torsion angles [°]

C(2)-Re(1)-Re(2)-C(8)	53.22(17)	C(10)-Re(1)-Re(2)-C(8)	147.34(16)
C(4)-Re(1)-Re(2)-C(8)	-115.18(17)	C(2)-Re(1)-Re(2)-C(9)	144.64(16)
C(3)-Re(1)-Re(2)-C(8)	-30.93(19)	C(4)-Re(1)-Re(2)-C(9)	-23.76(16)

C(3)-Re(1)-Re(2)-C(9)	60.49(17)		
C(10)-Re(1)-Re(2)-C(9)	-121.24(16)	Re(1)-C(10)-O(10)-C(15)	1.9(5)
C(2)-Re(1)-Re(2)-C(6)	-125.77(18)	O(10)-C(10)-C(11)-C(12)	-5.7(6)
C(4)-Re(1)-Re(2)-C(6)	65.83(18)	Re(1)-C(10)-C(11)-C(12)	175.6(4)
C(3)-Re(1)-Re(2)-C(6)	150.08(19)	O(10)-C(10)-C(11)-O(11)	173.3(4)
C(10)-Re(1)-Re(2)-C(6)	-31.65(17)	Re(1)-C(10)-C(11)-O(11)	-5.4(5)
C(2)-Re(1)-Re(2)-C(7)	-36.09(18)	C(12)-C(11)-O(11)-C(14)	0.8(5)
C(4)-Re(1)-Re(2)-C(7)	155.52(18)	C(10)-C(11)-O(11)-C(14)	-178.4(4)
C(3)-Re(1)-Re(2)-C(7)	-120.24(19)	O(11)-C(11)-C(12)-C(13)	-0.6(6)
C(10)-Re(1)-Re(2)-C(7)	58.03(17)	C(10)-C(11)-C(12)-C(13)	178.5(5)
C(1)-Re(1)-C(10)-O(10)	-88.6(4)	C(11)-C(12)-C(13)-C(14)	0.3(7)
C(2)-Re(1)-C(10)-O(10)	177.7(3)	C(12)-C(13)-C(14)-O(11)	0.2(7)
C(4)-Re(1)-C(10)-O(10)	3.5(4)	C(11)-O(11)-C(14)-C(13)	-0.6(6)
Re(2)-Re(1)-C(10)-O(10)	94.5(3)	C(10)-O(10)-C(15)-C(16)	-175.9(4)
C(1)-Re(1)-C(10)-C(11)	89.7(3)		
C(2)-Re(1)-C(10)-C(11)	-3.9(3)		
C(4)-Re(1)-C(10)-C(11)	-178.1(3)		
Re(2)-Re(1)-C(10)-C(11)	-87.2(3)		
C(11)-C(10)-O(10)-C(15)	-176.7(4)		

Appendix 4

Crystallographic data of Complex 7

Table 1. Crystal data and structure refinement

Identification code	db14d_absd	
Empirical formula	C ₁₁ H ₈ I Mn O ₅ S	
Formula weight	434.07	
Temperature	293(2) K	
Wavelength	0.71073 Å	
Crystal system	Tetragonal	
Space group	I 4 ₁ /a	
Unit cell dimensions	a = 21.438(8) Å	α = 90°
	b = 21.438(8) Å	β = 90°
	c = 12.895(10) Å	γ = 90°
Volume	5926(5) Å ³	
Z	16	
Density (calculated)	1.946 Mg/m ³	
Absorption coefficient	3.125 mm ⁻¹	
F(000)	3328	
Crystal size	0.58 x 0.54 x 0.42 mm ³	
Theta range for data collection	2.65 to 26.43°	
Index ranges	-25 ≤ h ≤ 21, -20 ≤ k ≤ 25, -15 ≤ l ≤ 10	
Reflections collected	11926	
Independent reflections	2678 [R(int) = 0.0339]	
Completeness to theta = 25.00°	93.1 %	
Absorption correction	Semi-empirical from equivalents	
Max. and min. transmission	0.269 and 0.188	
Refinement method	Full-matrix least-squares on F ²	
Data / restraints / parameters	2678 / 0 / 181	
Goodness-of-fit on F ²	1.170	
Final R indices [I > 2σ(I)]	R1 = 0.0409, wR2 = 0.1039	
R indices (all data)	R1 = 0.0537, wR2 = 0.1147	
Extinction coefficient	0	
Largest diff. peak and hole	0.821 and -0.596 e.Å ⁻³	

Table 2. Atomic coordinates ($\times 10^4$) and equivalent isotropic displacement parameters ($\text{\AA}^2 \times 10^3$)U(eq) is defined as one third of the trace of the orthogonalized U^{ij} tensor.

	x	y	z	U(eq)
Mn(1)	6829(1)	6773(1)	10431(1)	47(1)
I(1)	8084(1)	6827(1)	10659(1)	66(1)
C(1)	6839(3)	6712(3)	11939(7)	67(2)
O(1)	6805(3)	6678(3)	12661(5)	86(2)
C(2)	6870(3)	5910(3)	10398(5)	53(1)
O(2)	6892(2)	5387(2)	10460(5)	75(1)
C(3)	5997(3)	6758(3)	10432(5)	52(1)
O(3)	5463(2)	6747(2)	10465(4)	75(1)
C(4)	6905(3)	7636(3)	10517(6)	60(2)
O(4)	6963(3)	8159(2)	10584(5)	85(2)
C(5)	6840(4)	6845(4)	8895(6)	45(2)
O(5)	7144(2)	6540(2)	8165(4)	54(1)
C(6)	6472(5)	7301(4)	8355(8)	52(2)
S(1)	6577(1)	7397(1)	7002(2)	70(1)
C(7)	6004(5)	7710(5)	8716(9)	68(3)
C(8)	5750(5)	8051(6)	7878(11)	84(4)
C(9)	6010(4)	7940(4)	6930(9)	78(3)
C(10)	7531(4)	5994(3)	8338(7)	60(2)
C(11)	7834(5)	5855(5)	7331(8)	76(2)
C(5A)	6810(20)	6950(20)	8783(13)	42(9)
O(5A)	6479(15)	7313(14)	8144(19)	42(9)
C(6A)	7208(17)	6568(15)	8129(11)	73(4)
S(1A)	7186(6)	6652(6)	6776(11)	73(4)
C(7A)	7640(20)	6110(20)	8391(19)	73(4)
C(8A)	7945(18)	5841(17)	7530(30)	73(4)
C(9A)	7741(10)	6092(10)	6610(20)	73(4)
C(10A)	6020(20)	7761(19)	8510(30)	42(9)
C(11A)	5753(19)	8081(19)	7580(40)	42(9)

Table 3. Bond lengths [Å] and angles [°]

Mn(1)-C(3)	1.784(6)	C(11A)-H(11D)	0.96
Mn(1)-C(2)	1.851(6)	C(11A)-H(11E)	0.96
Mn(1)-C(4)	1.862(6)	C(11A)-H(11F)	0.96
Mn(1)-C(1)	1.949(10)	C(6A)-C(7A)	1.390
Mn(1)-C(5)	1.986(8)	C(6A)-S(1A)	1.755
Mn(1)-C(5A)	2.159(19)	S(1A)-C(9A)	1.704
Mn(1)-I(1)	2.7090(13)	C(7A)-C(8A)	1.409
C(1)-O(1)	0.937(9)	C(7A)-H(7A)	0.93
C(2)-O(2)	1.126(7)	C(8A)-C(9A)	1.378
C(3)-O(3)	1.145(7)	C(8A)-H(8A)	0.93
C(4)-O(4)	1.131(7)	C(9A)-H(9A)	0.93
C(5)-O(5)	1.318(8)		
C(5)-C(6)	1.437(9)	C(3)-Mn(1)-C(2)	91.7(2)
O(5)-C(10)	1.452(8)	C(3)-Mn(1)-C(4)	96.0(3)
C(10)-C(11)	1.482(11)	C(2)-Mn(1)-C(4)	172.0(3)
C(10)-H(10A)	0.97	C(3)-Mn(1)-C(1)	90.5(3)
C(10)-H(10B)	0.97	C(2)-Mn(1)-C(1)	87.5(3)
C(11)-H(11A)	0.96	C(4)-Mn(1)-C(1)	90.3(3)
C(11)-H(11B)	0.96	C(3)-Mn(1)-C(5)	90.8(3)
C(11)-H(11C)	0.96	C(2)-Mn(1)-C(5)	93.1(3)
C(6)-C(7)	1.411(10)	C(4)-Mn(1)-C(5)	88.9(3)
C(6)-S(1)	1.770(11)	C(1)-Mn(1)-C(5)	178.5(4)
S(1)-C(9)	1.685(8)	C(3)-Mn(1)-C(5A)	88.9(13)
C(7)-C(8)	1.414(13)	C(2)-Mn(1)-C(5A)	98.9(11)
C(7)-H(7)	0.93	C(4)-Mn(1)-C(5A)	83.5(12)
C(8)-C(9)	1.364(15)	C(1)-Mn(1)-C(5A)	173.6(11)
C(8)-H(8)	0.93	C(5)-Mn(1)-C(5A)	6.0(10)
C(9)-H(9)	0.93	C(3)-Mn(1)-I(1)	173.5(2)
C(5A)-O(5A)	1.333	C(2)-Mn(1)-I(1)	89.92(18)
C(5A)-C(6A)	1.457	C(4)-Mn(1)-I(1)	82.19(19)
O(5A)-C(10A)	1.450	C(1)-Mn(1)-I(1)	83.3(2)
C(10A)-C(11A)	1.500	C(5)-Mn(1)-I(1)	95.4(3)
C(10A)-H(10C)	0.97	C(5A)-Mn(1)-I(1)	97.0(13)
C(10A)-H(10D)	0.97	O(1)-C(1)-Mn(1)	174.8(9)

O(2)-C(2)-Mn(1)	174.6(6)	S(1)-C(9)-H(9)	124.3
O(3)-C(3)-Mn(1)	177.9(6)	O(5A)-C(5A)-C(6A)	106.2
O(4)-C(4)-Mn(1)	178.4(6)	O(5A)-C(5A)-Mn(1)	136.4(14)
O(5)-C(5)-C(6)	105.2(6)	C(6A)-C(5A)-Mn(1)	117.2(14)
O(5)-C(5)-Mn(1)	132.8(6)	C(5A)-O(5A)-C(10A)	122.4
C(6)-C(5)-Mn(1)	122.0(6)	O(5A)-C(10A)-C(11A)	107.3
C(5)-O(5)-C(10)	124.9(6)	O(5A)-C(10A)-H(10C)	110.3
O(5)-C(10)-C(11)	106.2(7)	C(11A)-C(10A)-H(10C)	110.3
O(5)-C(10)-H(10A)	110.5	O(5A)-C(10A)-H(10D)	110.3
C(11)-C(10)-H(10A)	110.5	C(11A)-C(10A)-H(10D)	110.3
O(5)-C(10)-H(10B)	110.5	H(10C)-C(10A)-H(10D)	108.5
C(11)-C(10)-H(10B)	110.5	C(10A)-C(11A)-H(11D)	109.5
H(10A)-C(10)-H(10B)	108.7	C(10A)-C(11A)-H(11E)	109.5
C(10)-C(11)-H(11A)	109.5	H(11D)-C(11A)-H(11E)	109.5
C(10)-C(11)-H(11B)	109.5	C(10A)-C(11A)-H(11F)	109.5
H(11A)-C(11)-H(11B)	109.5	H(11D)-C(11A)-H(11F)	109.5
C(10)-C(11)-H(11C)	109.5	H(11E)-C(11A)-H(11F)	109.5
H(11A)-C(11)-H(11C)	109.5	C(7A)-C(6A)-C(5A)	130.5
H(11B)-C(11)-H(11C)	109.5	C(7A)-C(6A)-S(1A)	109.4
C(7)-C(6)-C(5)	130.7(7)	C(5A)-C(6A)-S(1A)	120.1
C(7)-C(6)-S(1)	110.1(6)	C(9A)-S(1A)-C(6A)	91.9
C(5)-C(6)-S(1)	119.2(6)	C(6A)-C(7A)-C(8A)	114.1
C(9)-S(1)-C(6)	92.5(5)	C(6A)-C(7A)-H(7A)	123.0
C(6)-C(7)-C(8)	110.0(9)	C(8A)-C(7A)-H(7A)	123.0
C(6)-C(7)-H(7)	125.0	C(9A)-C(8A)-C(7A)	111.8
C(8)-C(7)-H(7)	125.0	C(9A)-C(8A)-H(8A)	124.1
C(9)-C(8)-C(7)	116.0(9)	C(7A)-C(8A)-H(8A)	124.1
C(9)-C(8)-H(8)	122.0	C(8A)-C(9A)-S(1A)	112.8
C(7)-C(8)-H(8)	122.0	C(8A)-C(9A)-H(9A)	123.6
C(8)-C(9)-S(1)	111.4(7)	S(1A)-C(9A)-H(9A)	123.6
C(8)-C(9)-H(9)	124.3		

Table 4. Anisotropic displacement parameters ($\text{\AA}^2 \times 10^3$).The anisotropic displacement factor exponent takes the form: $-2\pi^2 [h^2 a^{*2} U^{11} + \dots + 2 h k a^* b^* U^{12}]$

	U ¹¹	U ²²	U ³³	U ²³	U ¹³	U ¹²
Mn(1)	45(1)	40(1)	57(1)	-2(1)	1(1)	1(1)
I(1)	50(1)	65(1)	83(1)	0(1)	-8(1)	-3(1)
C(1)	67(4)	46(3)	86(5)	-5(4)	30(4)	6(3)
O(1)	98(4)	83(4)	76(4)	-17(3)	-19(4)	11(3)
C(2)	47(3)	48(3)	65(4)	2(3)	2(3)	4(2)
O(2)	78(3)	44(2)	104(4)	8(2)	8(3)	0(2)
C(3)	53(3)	45(3)	59(3)	-1(3)	9(3)	1(2)
O(3)	45(2)	79(3)	101(4)	5(3)	12(2)	-4(2)
C(4)	54(3)	55(4)	71(4)	-2(3)	-1(3)	4(3)
O(4)	96(4)	47(3)	112(5)	-11(3)	-1(3)	2(2)
C(5)	46(4)	31(3)	58(4)	-1(3)	-2(3)	-5(3)
O(5)	58(3)	46(2)	58(3)	-3(2)	2(2)	1(2)
C(6)	53(4)	48(4)	54(5)	9(4)	-4(4)	-2(3)
S(1)	73(1)	70(1)	67(1)	9(1)	-12(1)	1(1)
C(7)	64(5)	55(4)	83(7)	20(5)	-10(5)	7(4)
C(8)	68(6)	81(6)	103(10)	27(6)	-10(6)	14(4)
C(9)	64(5)	73(5)	98(7)	20(5)	-25(5)	8(4)
C(10)	61(5)	48(4)	72(5)	-11(3)	-4(4)	13(4)
C(11)	74(5)	72(5)	80(6)	-24(5)	14(5)	2(4)

Table 5. Hydrogen coordinates ($\times 10^4$) and isotropic displacement parameters ($\text{\AA}^2 \times 10^3$).

	x	y	z	U(eq)
H(7)	5881	7750	9405	81
H(8)	5426	8334	7967	101
H(9)	5890	8139	6321	94
H(10A)	7277	5643	8561	72
H(10B)	7842	6077	8866	72

H(11A)	8099	5496	7405	114
H(11B)	8081	6207	7119	114
H(11C)	7521	5772	6818	114
H(7A)	7724	5997	9073	88
H(8A)	8246	5531	7585	88
H(9A)	7890	5968	5965	88
H(10C)	6223	8064	8965	50
H(10D)	5698	7551	8901	50
H(11D)	5449	8383	7794	63
H(11E)	5558	7778	7136	63
H(11F)	6080	8288	7200	63

Table 6. Torsion angles [°].

C(3)-Mn(1)-C(5)-O(5)	-130.6(7)	C(5)-O(5)-C(10)-C(11)	-173.7(7)
C(2)-Mn(1)-C(5)-O(5)	-38.9(7)	O(5)-C(5)-C(6)-C(7)	172.0(8)
C(4)-Mn(1)-C(5)-O(5)	133.4(7)	Mn(1)-C(5)-C(6)-C(7)	-8.6(11)
C(5A)-Mn(1)-C(5)-O(5)	158(17)	O(5)-C(5)-C(6)-S(1)	-6.8(8)
I(1)-Mn(1)-C(5)-O(5)	51.4(7)	Mn(1)-C(5)-C(6)-S(1)	172.6(6)
C(3)-Mn(1)-C(5)-C(6)	50.1(6)	C(7)-C(6)-S(1)-C(9)	-1.4(6)
C(2)-Mn(1)-C(5)-C(6)	141.9(6)	C(5)-C(6)-S(1)-C(9)	177.6(7)
C(4)-Mn(1)-C(5)-C(6)	-45.8(6)	C(5)-C(6)-C(7)-C(8)	-176.7(8)
C(5A)-Mn(1)-C(5)-C(6)	-22(16)	S(1)-C(6)-C(7)-C(8)	2.2(9)
I(1)-Mn(1)-C(5)-C(6)	-127.9(5)	C(6)-C(7)-C(8)-C(9)	-2.2(13)
C(6)-C(5)-O(5)-C(10)	-173.8(6)	C(7)-C(8)-C(9)-S(1)	1.1(13)
Mn(1)-C(5)-O(5)-C(10)	6.8(11)	C(6)-S(1)-C(9)-C(8)	0.2(8)

Appendix 5

Crystallographic data of Complex 8

Table 1. Crystal data and structure refinement

Identification code	dbamco2	
Empirical formula	C ₁₄ H ₅ Mn ₂ N O ₉ S	
Formula weight	473.13	
Temperature	293(2) K	
Wavelength	0.71073 Å	
Crystal system	Monoclinic	
Space group	P 2 ₁ /n	
Unit cell dimensions	a = 14.4298(8) Å	α = 90°.
	b = 9.1653(5) Å	β = 113.7790(10)°.
	c = 14.7785(8) Å	γ = 90°.
Volume	1788.58(17) Å ³	
Z	4	
Density (calculated)	1.757 Mg/m ³	
Absorption coefficient	1.576 mm ⁻¹	
F(000)	936	
Crystal size	0.32 x 0.28 x 0.20 mm ³	
Theta range for data collection	2.68 to 26.54°.	
Index ranges	-13 ≤ h ≤ 17, -11 ≤ k ≤ 11, -14 ≤ l ≤ 17	
Reflections collected	9351	
Independent reflections	3345 [R(int) = 0.0260]	
Completeness to theta = 25.00°	99.2 %	
Absorption correction	Semi-empirical from equivalents	
Max. and min. transmission	0.730 and 0.549	
Refinement method	Full-matrix least-squares on F ²	
Data / restraints / parameters	3345 / 0 / 256	
Goodness-of-fit on F ²	1.060	
Final R indices [I > 2σ(I)]	R1 = 0.0397, wR2 = 0.1198	
R indices (all data)	R1 = 0.0440, wR2 = 0.1263	
Extinction coefficient	0	
Largest diff. peak and hole	0.840 and -0.806 e.Å ⁻³	

Table 2. Atomic coordinates ($\times 10^4$) and equivalent isotropic displacement parameters ($\text{\AA}^2 \times 10^3$)U(eq) is defined as one third of the trace of the orthogonalized U^{ij} tensor.

	x	y	z	U(eq)
Mn(1)	7960(1)	9395(1)	-328(1)	47(1)
Mn(2)	7392(1)	6434(1)	-8(1)	37(1)
C(1)	8320(3)	11250(4)	-483(3)	67(1)
O(1)	8545(3)	12403(3)	-581(3)	99(1)
C(2)	9077(3)	9072(4)	823(3)	59(1)
O(2)	9783(2)	8890(4)	1528(2)	82(1)
C(3)	7223(3)	9914(4)	392(2)	54(1)
O(3)	6775(2)	10274(3)	838(2)	74(1)
C(4)	6799(3)	9452(4)	-1477(3)	62(1)
O(4)	6074(3)	9498(4)	-2178(2)	100(1)
C(5)	8637(3)	8528(4)	-1015(3)	59(1)
O(5)	9067(3)	8013(4)	-1424(3)	88(1)
C(6)	7007(2)	4602(3)	83(2)	47(1)
O(6)	6757(2)	3422(3)	115(2)	70(1)
C(7)	6107(2)	7221(3)	-475(2)	47(1)
O(7)	5296(2)	7661(3)	-827(2)	70(1)
C(8)	7214(2)	6103(4)	-1293(2)	52(1)
O(8)	7102(2)	5825(4)	-2081(2)	83(1)
C(9)	8738(2)	5934(4)	398(2)	49(1)
O(9)	9558(2)	5581(3)	657(2)	73(1)
C(10)	7620(2)	6780(3)	1415(2)	40(1)
N(1)	8506(2)	6826(4)	2170(2)	59(1)
S(1)	5742(1)	5918(2)	1319(1)	81(1)
C(11)	6810(2)	6932(3)	1766(2)	42(1)
C(12)	6818(2)	7950(3)	2560(2)	45(1)
C(13)	5887(4)	7684(6)	2661(3)	77(1)
C(14)	5278(3)	6691(6)	2069(3)	78(1)

Table 3. Bond lengths [\AA] and angles [$^\circ$]

Mn(1)-C(1)	1.820(4)	Mn(1)-C(4)	1.843(4)
Mn(1)-C(2)	1.836(4)	Mn(1)-C(3)	1.845(3)

Mn(1)-C(5)	1.849(4)	C(2)-Mn(1)-C(4)	172.15(16)
Mn(1)-Mn(2)	2.9280(6)	C(1)-Mn(1)-C(3)	95.26(16)
Mn(2)-C(6)	1.790(3)	C(2)-Mn(1)-C(3)	90.08(16)
Mn(2)-C(8)	1.836(3)	C(4)-Mn(1)-C(3)	90.20(16)
Mn(2)-C(7)	1.845(3)	C(1)-Mn(1)-C(5)	95.24(16)
Mn(2)-C(9)	1.845(3)	C(2)-Mn(1)-C(5)	88.77(17)
Mn(2)-C(10)	2.019(3)	C(4)-Mn(1)-C(5)	89.52(17)
C(1)-O(1)	1.132(5)	C(3)-Mn(1)-C(5)	169.49(15)
C(2)-O(2)	1.138(5)	C(1)-Mn(1)-Mn(2)	177.99(13)
C(3)-O(3)	1.141(4)	C(2)-Mn(1)-Mn(2)	84.21(11)
C(4)-O(4)	1.138(5)	C(4)-Mn(1)-Mn(2)	88.03(12)
C(5)-O(5)	1.128(4)	C(3)-Mn(1)-Mn(2)	83.22(10)
C(6)-O(6)	1.147(4)	C(5)-Mn(1)-Mn(2)	86.27(11)
C(7)-O(7)	1.145(4)	C(6)-Mn(2)-C(8)	90.28(15)
C(8)-O(8)	1.137(4)	C(6)-Mn(2)-C(7)	95.70(13)
C(9)-O(9)	1.133(4)	C(8)-Mn(2)-C(7)	88.73(14)
C(10)-N(1)	1.315(4)	C(6)-Mn(2)-C(9)	93.48(14)
C(10)-C(11)	1.464(4)	C(8)-Mn(2)-C(9)	89.14(14)
N(1)-H(1A)	0.77(5)	C(7)-Mn(2)-C(9)	170.58(14)
N(1)-H(1B)	0.85(5)	C(6)-Mn(2)-C(10)	89.69(13)
S(1)-C(14)	1.667(5)	C(8)-Mn(2)-C(10)	178.68(13)
S(1)-C(11)	1.690(3)	C(7)-Mn(2)-C(10)	92.59(12)
C(11)-C(12)	1.496(4)	C(9)-Mn(2)-C(10)	89.55(12)
C(12)-C(13)	1.431(5)	C(6)-Mn(2)-Mn(1)	175.42(10)
C(12)-H(12)	0.93(5)	C(8)-Mn(2)-Mn(1)	85.25(11)
C(13)-C(14)	1.321(7)	C(7)-Mn(2)-Mn(1)	83.20(9)
C(13)-H(13)	0.84(5)	C(9)-Mn(2)-Mn(1)	87.48(10)
C(14)-H(14)	0.94(5)	C(10)-Mn(2)-Mn(1)	94.80(8)
C(1)-Mn(1)-C(2)	94.48(18)	O(1)-C(1)-Mn(1)	179.8(4)
C(1)-Mn(1)-C(4)	93.31(19)	O(2)-C(2)-Mn(1)	178.3(3)

O(3)-C(3)-Mn(1)	178.1(3)	C(14)-S(1)-C(11)	93.09(19)
O(4)-C(4)-Mn(1)	178.8(4)	C(10)-C(11)-C(12)	125.6(2)
O(5)-C(5)-Mn(1)	178.7(4)	C(10)-C(11)-S(1)	122.8(2)
O(6)-C(6)-Mn(2)	178.1(3)	C(12)-C(11)-S(1)	111.5(2)
O(7)-C(7)-Mn(2)	175.1(3)	C(13)-C(12)-C(11)	105.4(3)
O(8)-C(8)-Mn(2)	176.5(3)	C(13)-C(12)-H(12)	127(3)
O(9)-C(9)-Mn(2)	177.6(3)	C(11)-C(12)-H(12)	127(3)
N(1)-C(10)-C(11)	109.8(3)	C(14)-C(13)-C(12)	116.8(4)
N(1)-C(10)-Mn(2)	125.7(2)	C(14)-C(13)-H(13)	130(4)
C(11)-C(10)-Mn(2)	124.43(19)	C(12)-C(13)-H(13)	112(4)
C(10)-N(1)-H(1A)	124(4)	C(13)-C(14)-S(1)	113.2(3)
C(10)-N(1)-H(1B)	124(3)	C(13)-C(14)-H(14)	121(3)
H(1A)-N(1)-H(1B)	111(5)	S(1)-C(14)-H(14)	126(3)

Table 4. Anisotropic displacement parameters ($\text{\AA}^2 \times 10^3$)

The anisotropic displacement factor exponent takes the form: $-2\sum [h^2 a^{*2} U^{11} + \dots + 2 h k a^* b^* U^{12}]$

	U^{11}	U^{22}	U^{33}	U^{23}	U^{13}	U^{12}
Mn(1)	53(1)	44(1)	51(1)	2(1)	29(1)	-3(1)
Mn(2)	37(1)	40(1)	34(1)	-2(1)	13(1)	-2(1)
C(1)	78(2)	56(2)	87(3)	3(2)	52(2)	-4(2)
O(1)	127(3)	50(2)	157(3)	5(2)	94(3)	-16(2)
C(2)	55(2)	57(2)	65(2)	-6(2)	26(2)	-12(2)
O(2)	66(2)	87(2)	77(2)	-5(2)	13(2)	-15(2)
C(3)	64(2)	45(2)	58(2)	1(1)	32(2)	-6(1)
O(3)	103(2)	56(1)	92(2)	-3(1)	69(2)	0(1)
C(4)	69(2)	67(2)	57(2)	13(2)	30(2)	5(2)
O(4)	91(2)	126(3)	64(2)	26(2)	13(2)	13(2)
C(5)	64(2)	60(2)	65(2)	6(2)	37(2)	-4(2)
O(5)	104(2)	89(2)	106(2)	0(2)	79(2)	4(2)
C(6)	44(2)	47(2)	45(2)	-2(1)	11(1)	0(1)
O(6)	75(2)	41(1)	87(2)	2(1)	26(1)	-8(1)

C(7)	48(2)	49(2)	40(1)	1(1)	14(1)	-4(1)
O(7)	41(1)	80(2)	75(2)	15(1)	9(1)	7(1)
C(8)	52(2)	58(2)	46(2)	-7(1)	19(1)	-3(1)
O(8)	94(2)	112(2)	46(1)	-22(1)	33(1)	-7(2)
C(9)	46(2)	53(2)	47(2)	-4(1)	19(1)	1(1)
O(9)	52(1)	90(2)	76(2)	-4(1)	25(1)	14(1)
C(10)	41(1)	40(1)	37(1)	2(1)	13(1)	-6(1)
N(1)	43(1)	88(2)	39(1)	2(1)	11(1)	-11(1)
S(1)	63(1)	113(1)	75(1)	-29(1)	38(1)	-28(1)
C(11)	47(1)	43(1)	36(1)	1(1)	16(1)	-4(1)
C(12)	57(2)	47(2)	41(1)	-3(1)	30(1)	-7(1)
C(13)	93(3)	90(3)	63(2)	-8(2)	47(2)	7(2)
C(14)	60(2)	116(4)	67(2)	-2(2)	35(2)	-6(2)

Table 5. Hydrogen coordinates (x 10⁴) and isotropic displacement parameters (Å²x 10³)

	x	y	z	U(eq)
H(1A)	9020(40)	6930(60)	2120(40)	88
H(1B)	8580(40)	6900(60)	2770(40)	88
H(12)	7320(40)	8610(60)	2910(40)	54
H(13)	5870(40)	8110(60)	3160(40)	92
H(14)	4650(40)	6460(50)	2100(40)	94

Table 6. Torsion angles [°]

C(2)-Mn(1)-Mn(2)-C(8)	-129.31(15)	C(5)-Mn(1)-Mn(2)-C(7)	-129.45(15)
C(4)-Mn(1)-Mn(2)-C(8)	49.48(16)	C(2)-Mn(1)-Mn(2)-C(9)	-39.96(15)
C(3)-Mn(1)-Mn(2)-C(8)	139.92(15)	C(4)-Mn(1)-Mn(2)-C(9)	138.83(15)
C(5)-Mn(1)-Mn(2)-C(8)	-40.16(16)	C(3)-Mn(1)-Mn(2)-C(9)	-130.74(15)
C(2)-Mn(1)-Mn(2)-C(7)	141.41(15)	C(5)-Mn(1)-Mn(2)-C(9)	49.18(15)
C(4)-Mn(1)-Mn(2)-C(7)	-39.80(15)	C(2)-Mn(1)-Mn(2)-C(10)	49.37(14)
C(3)-Mn(1)-Mn(2)-C(7)	50.64(14)	C(4)-Mn(1)-Mn(2)-C(10)	-131.84(14)

C(3)-Mn(1)-Mn(2)-C(10)	-41.40(14)		
C(5)-Mn(1)-Mn(2)-C(10)	138.51(14)	Mn(2)-C(10)-C(11)-C(12)	-142.7(2)
C(6)-Mn(2)-C(10)-N(1)	103.9(3)	N(1)-C(10)-C(11)-S(1)	-137.9(3)
C(7)-Mn(2)-C(10)-N(1)	-160.4(3)	Mn(2)-C(10)-C(11)-S(1)	38.8(3)
C(9)-Mn(2)-C(10)-N(1)	10.4(3)	C(14)-S(1)-C(11)-C(10)	178.9(3)
Mn(1)-Mn(2)-C(10)-N(1)	-77.1(3)	C(14)-S(1)-C(11)-C(12)	0.2(3)
C(6)-Mn(2)-C(10)-C(11)	-72.3(3)	C(10)-C(11)-C(12)-C(13)	-178.5(3)
C(7)-Mn(2)-C(10)-C(11)	23.4(3)	S(1)-C(11)-C(12)-C(13)	0.2(3)
C(9)-Mn(2)-C(10)-C(11)	-165.8(3)	C(11)-C(12)-C(13)-C(14)	-0.6(5)
Mn(1)-Mn(2)-C(10)-C(11)	106.7(2)	C(12)-C(13)-C(14)-S(1)	0.8(6)
N(1)-C(10)-C(11)-C(12)	40.6(4)	C(11)-S(1)-C(14)-C(13)	-0.6(4)

Appendix 6

Crystallographic data of Complex 9

Table 1. Crystal data and structure refinement

Identification code	dbamco3a_abs	
Empirical formula	C ₁₄ H ₅ Mn ₂ N O ₁₀	
Formula weight	457.07	
Temperature	293(2) K	
Wavelength	0.71073 Å	
Crystal system	Monoclinic	
Space group	P 21/c	
Unit cell dimensions	a = 12.0713(9) Å	α = 90°.
	b = 9.0817(7) Å	β = 92.5930(10)°.
	c = 15.8406(12) Å	γ = 90°.
Volume	1734.8(2) Å ³	
Z	4	
Density (calculated)	1.750 Mg/m ³	
Absorption coefficient	1.510 mm ⁻¹	
F(000)	904	
Crystal size	0.36 x 0.34 x 0.24 mm ³	
Theta range for data collection	2.57 to 26.49°.	
Index ranges	-14 ≤ h ≤ 11, -11 ≤ k ≤ 5, -19 ≤ l ≤ 19	
Reflections collected	9176	
Independent reflections	3301 [R(int) = 0.0224]	
Completeness to theta = 25.00°	99.8 %	
Absorption correction	Semi-empirical from equivalents	
Max. and min. transmission	0.696 and 0.587	
Refinement method	Full-matrix least-squares on F ²	
Data / restraints / parameters	3301 / 0 / 265	
Goodness-of-fit on F ²	1.091	
Final R indices [I > 2σ(I)]	R1 = 0.0274, wR2 = 0.0727	
R indices (all data)	R1 = 0.0299, wR2 = 0.0760	
Extinction coefficient	0.0014(5)	
Largest diff. peak and hole	0.258 and -0.233 e.Å ⁻³	

Table 2. Atomic coordinates ($\times 10^4$) and equivalent isotropic displacement parameters ($\text{\AA}^2 \times 10^3$)U(eq) is defined as one third of the trace of the orthogonalized U^{ij} tensor.

	x	y	z	U(eq)
Mn(1)	8297(1)	4141(1)	8790(1)	45(1)
Mn(2)	7333(1)	1182(1)	8648(1)	38(1)
C(1)	8815(2)	6012(2)	8839(1)	62(1)
O(1)	9128(2)	7193(2)	8872(1)	93(1)
C(2)	8200(2)	3952(2)	9942(1)	58(1)
O(2)	8159(2)	3873(2)	10655(1)	84(1)
C(3)	6809(2)	4644(2)	8706(1)	51(1)
O(3)	5912(1)	4986(2)	8658(1)	72(1)
C(4)	8358(2)	4048(2)	7628(1)	57(1)
O(4)	8412(2)	4009(2)	6917(1)	86(1)
C(5)	9672(2)	3255(2)	8875(1)	61(1)
O(5)	10524(1)	2737(2)	8928(1)	92(1)
C(6)	6749(2)	-622(2)	8512(1)	53(1)
O(6)	6374(2)	-1763(2)	8415(1)	84(1)
C(7)	6594(1)	1934(2)	7706(1)	49(1)
O(7)	6189(1)	2349(2)	7085(1)	75(1)
C(8)	8478(2)	730(2)	7970(1)	54(1)
O(8)	9165(1)	389(2)	7546(1)	86(1)
C(9)	8256(2)	682(2)	9569(1)	49(1)
O(9)	8826(1)	328(2)	10120(1)	73(1)
C(10)	6100(1)	1643(2)	9435(1)	41(1)
N(1)	6227(2)	1718(2)	10260(1)	60(1)
O(10)	4243(1)	2348(2)	9753(1)	71(1)
C(11)	4946(1)	1838(2)	9159(1)	45(1)
C(12)	4340(2)	1582(3)	8442(1)	62(1)
C(13)	3232(2)	1979(3)	8585(2)	77(1)
C(14)	3213(2)	2416(3)	9368(2)	81(1)

Table 3. Bond lengths [Å] and angles [°]

Mn(1)-C(1)	1.8106(19)	C(1)-Mn(1)-C(5)	95.61(9)
Mn(1)-C(2)	1.841(2)	C(2)-Mn(1)-C(5)	89.12(9)
Mn(1)-C(5)	1.844(2)	C(1)-Mn(1)-C(4)	93.19(9)
Mn(1)-C(4)	1.849(2)	C(2)-Mn(1)-C(4)	171.91(9)
Mn(1)-C(3)	1.8518(19)	C(5)-Mn(1)-C(4)	88.60(9)
Mn(1)-Mn(2)	2.9331(4)	C(1)-Mn(1)-C(3)	95.98(9)
Mn(2)-C(6)	1.7928(19)	C(2)-Mn(1)-C(3)	89.43(9)
Mn(2)-C(8)	1.8355(19)	C(5)-Mn(1)-C(3)	168.40(8)
Mn(2)-C(7)	1.8364(17)	C(4)-Mn(1)-C(3)	91.25(9)
Mn(2)-C(9)	1.8506(18)	C(1)-Mn(1)-Mn(2)	176.33(7)
Mn(2)-C(10)	2.0275(16)	C(2)-Mn(1)-Mn(2)	87.01(6)
C(1)-O(1)	1.138(2)	C(5)-Mn(1)-Mn(2)	87.62(6)
C(2)-O(2)	1.135(2)	C(4)-Mn(1)-Mn(2)	85.14(6)
C(3)-O(3)	1.126(2)	C(3)-Mn(1)-Mn(2)	80.81(5)
C(4)-O(4)	1.131(2)	C(6)-Mn(2)-C(8)	91.59(9)
C(5)-O(5)	1.131(2)	C(6)-Mn(2)-C(7)	93.94(8)
C(6)-O(6)	1.138(2)	C(8)-Mn(2)-C(7)	87.61(8)
C(7)-O(7)	1.141(2)	C(6)-Mn(2)-C(9)	95.15(8)
C(8)-O(8)	1.133(2)	C(8)-Mn(2)-C(9)	87.92(8)
C(9)-O(9)	1.134(2)	C(7)-Mn(2)-C(9)	169.98(8)
C(10)-N(1)	1.310(2)	C(6)-Mn(2)-C(10)	88.10(8)
C(10)-C(11)	1.452(2)	C(8)-Mn(2)-C(10)	177.79(7)
N(1)-H(1A)	0.90(2)	C(7)-Mn(2)-C(10)	94.60(7)
N(1)-H(1B)	0.77(2)	C(9)-Mn(2)-C(10)	89.92(7)
O(10)-C(14)	1.361(3)	C(6)-Mn(2)-Mn(1)	177.51(6)
O(10)-C(11)	1.376(2)	C(8)-Mn(2)-Mn(1)	86.75(6)
C(11)-C(12)	1.344(3)	C(7)-Mn(2)-Mn(1)	84.14(6)
C(12)-C(13)	1.414(3)	C(9)-Mn(2)-Mn(1)	86.66(6)
C(12)-H(12)	0.87(2)	C(10)-Mn(2)-Mn(1)	93.63(4)
C(13)-C(14)	1.304(4)	O(1)-C(1)-Mn(1)	179.1(2)
C(13)-H(13)	0.85(3)	O(2)-C(2)-Mn(1)	177.92(19)
C(14)-H(14)	0.95(3)	O(3)-C(3)-Mn(1)	178.20(17)
		O(4)-C(4)-Mn(1)	178.7(2)
C(1)-Mn(1)-C(2)	94.75(9)	O(5)-C(5)-Mn(1)	178.8(2)

O(6)-C(6)-Mn(2)	179.03(19)	C(12)-C(11)-C(10)	135.38(16)
O(7)-C(7)-Mn(2)	175.00(16)	O(10)-C(11)-C(10)	116.64(15)
O(8)-C(8)-Mn(2)	176.9(2)	C(11)-C(12)-C(13)	107.7(2)
O(9)-C(9)-Mn(2)	177.56(17)	C(11)-C(12)-H(12)	128.0(16)
N(1)-C(10)-C(11)	111.20(15)	C(13)-C(12)-H(12)	124.3(16)
N(1)-C(10)-Mn(2)	124.59(14)	C(14)-C(13)-C(12)	106.7(2)
C(11)-C(10)-Mn(2)	124.10(11)	C(14)-C(13)-H(13)	129(2)
C(10)-N(1)-H(1A)	121.2(13)	C(12)-C(13)-H(13)	124(2)
C(10)-N(1)-H(1B)	124.3(17)	C(13)-C(14)-O(10)	111.0(2)
H(1A)-N(1)-H(1B)	114(2)	C(13)-C(14)-H(14)	135.2(18)
C(14)-O(10)-C(11)	106.72(17)	O(10)-C(14)-H(14)	113.7(18)
C(12)-C(11)-O(10)	107.91(16)		

Table 4. Anisotropic displacement parameters ($\text{\AA}^2 \times 10^3$)

The anisotropic displacement factor exponent takes the form: $-2p^2[h^2a^*2U^{11} + \dots + 2hk a^* b^* U^{12}]$

	U ¹¹	U ²²	U ³³	U ²³	U ¹³	U ¹²
Mn(1)	42(1)	42(1)	50(1)	4(1)	3(1)	-3(1)
Mn(2)	41(1)	39(1)	34(1)	0(1)	5(1)	0(1)
C(1)	56(1)	52(1)	76(1)	3(1)	5(1)	-5(1)
O(1)	93(1)	52(1)	133(2)	0(1)	9(1)	-22(1)
C(2)	62(1)	52(1)	58(1)	1(1)	0(1)	-6(1)
O(2)	110(1)	92(1)	50(1)	-1(1)	-2(1)	-16(1)
C(3)	51(1)	42(1)	59(1)	5(1)	5(1)	0(1)
O(3)	51(1)	58(1)	108(1)	9(1)	5(1)	7(1)
C(4)	58(1)	56(1)	59(1)	11(1)	10(1)	-2(1)
O(4)	106(1)	98(1)	56(1)	12(1)	19(1)	-10(1)
C(5)	51(1)	59(1)	72(1)	9(1)	2(1)	-5(1)
O(5)	48(1)	97(1)	132(2)	21(1)	3(1)	12(1)
C(6)	64(1)	51(1)	44(1)	-3(1)	5(1)	-3(1)
O(6)	118(1)	53(1)	81(1)	-9(1)	0(1)	-28(1)
C(7)	46(1)	62(1)	39(1)	2(1)	8(1)	-3(1)
O(7)	67(1)	114(1)	43(1)	21(1)	-6(1)	-6(1)
C(8)	56(1)	56(1)	52(1)	3(1)	8(1)	9(1)
O(8)	75(1)	104(1)	81(1)	-5(1)	35(1)	25(1)
C(9)	50(1)	49(1)	49(1)	3(1)	4(1)	5(1)

O(9)	69(1)	89(1)	60(1)	11(1)	-11(1)	18(1)
C(10)	48(1)	40(1)	36(1)	1(1)	7(1)	-7(1)
N(1)	53(1)	90(1)	36(1)	-4(1)	6(1)	-8(1)
O(10)	56(1)	96(1)	63(1)	-17(1)	16(1)	9(1)
C(11)	45(1)	47(1)	44(1)	0(1)	12(1)	-4(1)
C(12)	50(1)	85(1)	51(1)	-6(1)	6(1)	-9(1)
C(13)	46(1)	101(2)	83(2)	9(1)	-1(1)	-4(1)
C(14)	50(1)	99(2)	96(2)	-5(1)	18(1)	14(1)

Table 5. Hydrogen coordinates (x 10⁴) and isotropic displacement parameters (Å²x 10³)

	x	y	z	U(eq)
H(1A)	5654(19)	1920(20)	10580(14)	62(6)
H(1B)	6785(19)	1600(30)	10510(14)	60(7)
H(12)	4560(20)	1220(30)	7968(15)	74(7)
H(13)	2710(20)	1980(30)	8206(18)	97(9)
H(14)	2660(20)	2800(30)	9717(18)	103(9)

Table 6. Torsion angles [°]

C(2)-Mn(1)-Mn(2)-C(8)	-129.88(9)	C(3)-Mn(1)-Mn(2)-C(10)	-41.97(7)
C(5)-Mn(1)-Mn(2)-C(8)	-40.64(9)	C(6)-Mn(2)-C(10)-N(1)	105.07(16)
C(4)-Mn(1)-Mn(2)-C(8)	48.15(9)	C(7)-Mn(2)-C(10)-N(1)	-161.13(16)
C(3)-Mn(1)-Mn(2)-C(8)	140.21(8)	C(9)-Mn(2)-C(10)-N(1)	9.92(16)
C(2)-Mn(1)-Mn(2)-C(7)	142.19(8)	Mn(1)-Mn(2)-C(10)-N(1)	-76.73(15)
C(5)-Mn(1)-Mn(2)-C(7)	-128.57(9)	C(6)-Mn(2)-C(10)-C(11)	-70.79(14)
C(4)-Mn(1)-Mn(2)-C(7)	-39.77(8)	C(7)-Mn(2)-C(10)-C(11)	23.00(14)
C(3)-Mn(1)-Mn(2)-C(7)	52.29(8)	C(9)-Mn(2)-C(10)-C(11)	-165.95(14)
C(2)-Mn(1)-Mn(2)-C(9)	-41.77(9)	Mn(1)-Mn(2)-C(10)-C(11)	107.41(13)
C(5)-Mn(1)-Mn(2)-C(9)	47.46(9)	C(14)-O(10)-C(11)-C(12)	-1.2(2)
C(4)-Mn(1)-Mn(2)-C(9)	136.26(9)	C(14)-O(10)-C(11)-C(10)	-178.64(18)
C(3)-Mn(1)-Mn(2)-C(9)	-131.68(8)	N(1)-C(10)-C(11)-C(12)	-164.1(2)
C(2)-Mn(1)-Mn(2)-C(10)	47.93(8)	Mn(2)-C(10)-C(11)-C(12)	12.3(3)
C(5)-Mn(1)-Mn(2)-C(10)	137.17(8)	N(1)-C(10)-C(11)-O(10)	12.5(2)
C(4)-Mn(1)-Mn(2)-C(10)	-134.03(8)	Mn(2)-C(10)-C(11)-O(10)	-171.13(12)

O(10)-C(11)-C(12)-C(13)	1.5(2)	C(12)-C(13)-C(14)-O(10)	0.6(3)
C(10)-C(11)-C(12)-C(13)	178.3(2)	C(11)-O(10)-C(14)-C(13)	0.3(3)
C(11)-C(12)-C(13)-C(14)	-1.3(3)		

Appendix 7

Crystallographic data of Complex 11

Table 1. Crystal data and structure refinement

Identification code	dbamc08a1_abs3	
Empirical formula	C ₁₇ H ₁₁ Mn ₂ NO ₁₀	
Formula weight	499.15	
Temperature	293(2) K	
Wavelength	0.71073 Å	
Crystal system	monoclinic	
Space group	P2 ₁ /c	
Unit cell dimensions	a = 12.7412(13) Å	α = 90°.
	b = 12.9836(13) Å	β = 90.0000(10)°.
	c = 12.6967(12) Å	γ = 90°.
Volume	2100.4(4) Å ³	
Z	4	
Density (calculated)	1.578 Mg/m ³	
Absorption coefficient	1.254 mm ⁻¹	
F(000)	1000	
Crystal size	0.46 x 0.24 x 0.16 mm ³	
Theta range for data collection	2.76 to 26.44°.	
Index ranges	-15 ≤ h ≤ 15, -15 ≤ k ≤ 16, -15 ≤ l ≤ 5	
Reflections collected	10635	
Independent reflections	3943 [R(int) = 0.0272]	
Completeness to theta = 25.00°	99.5 %	
Refinement method	Full-matrix least-squares on F ²	
Data / restraints / parameters	3943 / 0 / 311	
Goodness-of-fit on F ²	1.073	
Final R indices [I > 2σ(I)]	R1 = 0.0522, wR2 = 0.1418	
R indices (all data)	R1 = 0.0703, wR2 = 0.1592	
Largest diff. peak and hole	0.505 and -0.337 e.Å ⁻³	

Table 2. Atomic coordinates ($\times 10^4$) and equivalent isotropic displacement parameters ($\text{\AA}^2 \times 10^3$)
 U(eq) is defined as one third of the trace of the orthogonalized U^{ij} tensor.

	x	y	z	U(eq)
Mn(1)	1194(1)	1515(1)	8294(1)	68(1)
Mn(2)	2875(1)	347(1)	7287(1)	67(1)
C(1)	198(4)	2246(5)	8962(4)	94(2)
O(1)	-421(3)	2714(4)	9406(4)	131(2)
C(2)	1244(4)	2369(5)	7135(4)	91(2)
O(2)	1261(4)	2922(4)	6436(3)	132(2)
C(3)	294(4)	657(5)	7557(4)	94(2)
O(3)	-272(3)	140(5)	7116(4)	139(2)
C(4)	1266(3)	539(4)	9344(3)	76(1)
O(4)	1287(3)	-45(3)	10008(3)	104(1)
C(5)	2278(4)	2237(4)	8903(3)	74(1)
O(5)	2945(3)	2682(3)	9281(3)	102(1)
C(6)	2127(4)	453(4)	6047(4)	80(1)
O(6)	1661(3)	517(4)	5283(3)	110(1)
C(7)	2105(3)	-790(4)	7642(3)	76(1)
O(7)	1610(3)	-1500(3)	7861(3)	101(1)
C(8)	3484(3)	313(3)	8591(4)	74(1)
O(8)	3866(3)	279(3)	9400(3)	102(1)
C(9)	3496(4)	1589(5)	6998(4)	87(1)
O(9)	3855(4)	2372(4)	6822(3)	125(2)
C(10)	4015(3)	-498(4)	6645(4)	88(2)
C(11)	3796(3)	-1383(4)	5979(4)	80(1)
O(10)	4630(3)	-1972(3)	5646(3)	106(1)
C(12)	2920(5)	-1796(5)	5598(5)	92(2)
C(13)	3199(6)	-2694(5)	5017(5)	108(2)
C(14)	4224(6)	-2771(5)	5074(5)	111(2)
N(1)	5023(8)	-187(14)	6561(12)	93(4)
C(15)	5596(9)	665(16)	7044(15)	115(5)
C(16)	6677(8)	401(11)	7014(14)	95(4)
C(17)	7220(10)	1037(13)	7481(11)	257(7)
N(1A)	5041(11)	-611(12)	6991(14)	75(3)
C(15A)	5636(10)	108(13)	7633(16)	86(5)
C(16A)	6784(19)	-80(20)	7730(30)	160(11)
C(17A)	7220(10)	1037(13)	7481(11)	257(7)

Table 3. Bond lengths [Å] and angles [°]

Mn(1)-C(1)	1.798(5)	C(16)-H(16B)	0.9700
Mn(1)-C(5)	1.840(5)	C(17)-H(17A)	0.9600
Mn(1)-C(4)	1.842(5)	C(17)-H(17B)	0.9600
Mn(1)-C(2)	1.843(6)	C(17)-H(17C)	0.9600
Mn(1)-C(3)	1.852(6)	N(1A)-C(15A)	1.453(19)
Mn(1)-Mn(2)	2.9190(9)	N(1A)-H(1A)	0.8600
Mn(2)-C(8)	1.828(5)	C(15A)-C(16A)	1.49(3)
Mn(2)-C(7)	1.828(6)	C(15A)-H(15C)	0.9700
Mn(2)-C(9)	1.834(6)	C(15A)-H(15D)	0.9700
Mn(2)-C(6)	1.845(5)	C(16A)-C(17A)	1.58(3)
Mn(2)-C(10)	1.994(5)	C(16A)-H(16C)	0.9700
C(1)-O(1)	1.144(6)	C(16A)-H(16D)	0.9700
C(2)-O(2)	1.142(6)	C(17A)-H(17D)	0.9600
C(3)-O(3)	1.133(7)	C(17A)-H(17E)	0.9600
C(4)-O(4)	1.133(5)	C(17A)-H(17F)	0.9600
C(5)-O(5)	1.134(5)		
C(6)-O(6)	1.141(6)	C(1)-Mn(1)-C(5)	93.6(2)
C(7)-O(7)	1.150(6)	C(1)-Mn(1)-C(4)	93.3(2)
C(8)-O(8)	1.139(5)	C(5)-Mn(1)-C(4)	90.5(2)
C(9)-O(9)	1.137(6)	C(1)-Mn(1)-C(2)	94.8(2)
C(10)-N(1)	1.351(12)	C(5)-Mn(1)-C(2)	90.2(2)
C(10)-N(1A)	1.387(15)	C(4)-Mn(1)-C(2)	171.9(2)
C(10)-C(11)	1.454(6)	C(1)-Mn(1)-C(3)	96.8(3)
C(11)-C(12)	1.329(7)	C(5)-Mn(1)-C(3)	169.6(2)
C(11)-O(10)	1.376(6)	C(4)-Mn(1)-C(3)	89.0(2)
O(10)-C(14)	1.369(7)	C(2)-Mn(1)-C(3)	88.9(3)
C(12)-C(13)	1.424(8)	C(1)-Mn(1)-Mn(2)	177.45(17)
C(12)-H(12)	0.74(4)	C(5)-Mn(1)-Mn(2)	84.13(13)
C(13)-C(14)	1.312(9)	C(4)-Mn(1)-Mn(2)	85.58(14)
C(13)-H(13)	0.97(7)	C(2)-Mn(1)-Mn(2)	86.44(17)
C(14)-H(14)	0.93(7)	C(3)-Mn(1)-Mn(2)	85.45(17)
N(1)-C(15)	1.460(16)	C(8)-Mn(2)-C(7)	89.2(2)
N(1)-H(1)	0.8600	C(8)-Mn(2)-C(9)	91.1(2)
C(15)-C(16)	1.420(16)	C(7)-Mn(2)-C(9)	172.2(2)
C(15)-H(15A)	0.9700	C(8)-Mn(2)-C(6)	173.3(2)
C(15)-H(15B)	0.9700	C(7)-Mn(2)-C(6)	89.7(2)
C(16)-C(17)	1.230(17)	C(9)-Mn(2)-C(6)	89.2(2)
C(16)-H(16A)	0.9700	C(8)-Mn(2)-C(10)	92.8(2)

C(7)-Mn(2)-C(10)	92.7(2)	C(16)-C(15)-N(1)	106.9(11)
C(9)-Mn(2)-C(10)	95.0(2)	C(16)-C(15)-H(15A)	110.3
C(6)-Mn(2)-C(10)	93.9(2)	N(1)-C(15)-H(15A)	110.3
C(8)-Mn(2)-Mn(1)	85.83(14)	C(16)-C(15)-H(15B)	110.3
C(7)-Mn(2)-Mn(1)	85.30(14)	N(1)-C(15)-H(15B)	110.3
C(9)-Mn(2)-Mn(1)	86.97(16)	H(15A)-C(15)-H(15B)	108.6
C(6)-Mn(2)-Mn(1)	87.47(15)	C(17)-C(16)-C(15)	111.8(12)
C(10)-Mn(2)-Mn(1)	177.59(18)	C(17)-C(16)-H(16A)	109.3
O(1)-C(1)-Mn(1)	178.4(5)	C(15)-C(16)-H(16A)	109.3
O(2)-C(2)-Mn(1)	177.8(5)	C(17)-C(16)-H(16B)	109.3
O(3)-C(3)-Mn(1)	178.8(5)	C(15)-C(16)-H(16B)	109.3
O(4)-C(4)-Mn(1)	177.8(4)	H(16A)-C(16)-H(16B)	107.9
O(5)-C(5)-Mn(1)	179.8(4)	C(16)-C(17)-H(17A)	109.5
O(6)-C(6)-Mn(2)	179.7(5)	C(16)-C(17)-H(17B)	109.5
O(7)-C(7)-Mn(2)	179.2(5)	H(17A)-C(17)-H(17B)	109.5
O(8)-C(8)-Mn(2)	179.1(4)	C(16)-C(17)-H(17C)	109.5
O(9)-C(9)-Mn(2)	178.1(5)	H(17A)-C(17)-H(17C)	109.5
N(1)-C(10)-N(1A)	32.9(5)	H(17B)-C(17)-H(17C)	109.5
N(1)-C(10)-C(11)	111.9(6)	C(10)-N(1A)-C(15A)	127.0(12)
N(1A)-C(10)-C(11)	106.3(7)	C(10)-N(1A)-H(1A)	116.5
N(1)-C(10)-Mn(2)	124.1(7)	C(15A)-N(1A)-H(1A)	116.5
N(1A)-C(10)-Mn(2)	128.0(7)	N(1A)-C(15A)-C(16A)	117.1(13)
C(11)-C(10)-Mn(2)	122.2(3)	N(1A)-C(15A)-H(15C)	108.0
C(12)-C(11)-O(10)	108.2(4)	C(16A)-C(15A)-H(15C)	108.0
C(12)-C(11)-C(10)	133.8(5)	N(1A)-C(15A)-H(15D)	108.0
O(10)-C(11)-C(10)	118.0(4)	C(16A)-C(15A)-H(15D)	108.0
C(14)-O(10)-C(11)	107.0(5)	H(15C)-C(15A)-H(15D)	107.3
C(11)-C(12)-C(13)	108.0(5)	C(15A)-C(16A)-C(17A)	100(2)
C(11)-C(12)-H(12)	127(3)	C(15A)-C(16A)-H(16C)	111.7
C(13)-C(12)-H(12)	125(3)	C(17A)-C(16A)-H(16C)	111.7
C(14)-C(13)-C(12)	106.4(6)	C(15A)-C(16A)-H(16D)	111.7
C(14)-C(13)-H(13)	127(4)	C(17A)-C(16A)-H(16D)	111.7
C(12)-C(13)-H(13)	125(4)	H(16C)-C(16A)-H(16D)	109.5
C(13)-C(14)-O(10)	110.3(6)	C(16A)-C(17A)-H(17D)	109.5
C(13)-C(14)-H(14)	132(4)	C(16A)-C(17A)-H(17E)	109.5
O(10)-C(14)-H(14)	117(4)	H(17D)-C(17A)-H(17E)	109.5
C(10)-N(1)-C(15)	131.9(10)	C(16A)-C(17A)-H(17F)	109.5
C(10)-N(1)-H(1)	114.0	H(17D)-C(17A)-H(17F)	109.5
C(15)-N(1)-H(1)	114.0	H(17E)-C(17A)-H(17F)	109.5

Table 4. Anisotropic displacement parameters ($\text{\AA}^2 \times 10^3$)The anisotropic displacement factor exponent takes the form: $-2p^2 [h^2 a^* 2U^{11} + \dots + 2 h k a^* b^* U^{12}]$

	U ¹¹	U ²²	U ³³	U ²³	U ¹³	U ¹²
Mn(1)	56(1)	93(1)	56(1)	3(1)	6(1)	7(1)
Mn(2)	54(1)	83(1)	64(1)	-12(1)	6(1)	-4(1)
C(1)	66(3)	136(5)	80(3)	6(3)	5(2)	24(3)
O(1)	88(3)	181(4)	124(3)	-10(3)	18(2)	58(3)
C(2)	91(3)	116(4)	68(3)	4(3)	0(2)	14(3)
O(2)	165(4)	147(4)	83(2)	39(3)	5(3)	20(3)
C(3)	62(3)	136(5)	85(3)	1(3)	-1(2)	1(3)
O(3)	85(3)	197(5)	134(4)	-32(3)	-18(3)	-23(3)
C(4)	64(3)	98(3)	65(2)	-1(2)	9(2)	0(2)
O(4)	112(3)	120(3)	80(2)	28(2)	12(2)	3(2)
C(5)	66(3)	86(3)	70(2)	-3(2)	13(2)	8(2)
O(5)	81(2)	117(3)	107(3)	-29(2)	2(2)	-9(2)
C(6)	75(3)	94(3)	70(3)	-10(2)	10(2)	-6(2)
O(6)	120(3)	140(4)	70(2)	-1(2)	-13(2)	-1(3)
C(7)	68(3)	95(3)	66(2)	-13(2)	0(2)	0(3)
O(7)	104(3)	101(3)	98(3)	0(2)	10(2)	-24(2)
C(8)	65(2)	74(3)	83(3)	-13(2)	-6(2)	0(2)
O(8)	100(3)	111(3)	94(2)	-1(2)	-30(2)	1(2)
C(9)	73(3)	111(4)	78(3)	-15(3)	22(2)	-18(3)
O(9)	131(4)	126(3)	116(3)	-2(3)	39(3)	-47(3)
C(10)	57(2)	110(4)	98(3)	-37(3)	4(2)	-7(2)
C(11)	63(3)	95(3)	82(3)	-21(2)	7(2)	-1(2)
O(10)	79(2)	118(3)	120(3)	-32(2)	9(2)	16(2)
C(12)	67(3)	112(4)	98(4)	-31(3)	5(3)	-6(3)
C(13)	107(5)	115(5)	101(4)	-36(4)	3(3)	-18(4)
C(14)	121(5)	98(4)	113(4)	-33(4)	22(4)	2(4)
N(1)	56(4)	118(11)	104(8)	-35(7)	1(5)	-2(6)
C(15)	72(6)	148(13)	127(11)	-32(10)	-7(6)	-26(7)
C(16)	60(5)	99(8)	125(9)	-23(7)	3(5)	-31(5)
C(17)	207(13)	258(17)	307(19)	-22(15)	91(13)	36(12)
N(1A)	54(5)	68(7)	102(10)	-3(6)	-5(6)	1(5)
C(15A)	63(7)	82(9)	113(11)	-9(8)	-6(7)	-12(6)
C(16A)	170(20)	150(20)	170(20)	-65(18)	-4(16)	-71(16)
C(17A)	207(13)	258(17)	307(19)	-22(15)	91(13)	36(12)

Table 5. Hydrogen coordinates (x 10⁴) and isotropic displacement parameters (Å²x 10³)

	x	y	z	U(eq)
H(12)	2380(30)	-1610(30)	5680(30)	57(13)
H(13)	2730(60)	-3070(50)	4550(50)	140(20)
H(14)	4700(50)	-3260(50)	4820(50)	130(20)
H(1)	5397	-560	6145	111
H(15A)	5473	1297	6656	139
H(15B)	5368	764	7765	139
H(16A)	6774	-271	7333	114
H(16B)	6905	358	6286	114
H(17A)	7945	841	7434	386
H(17B)	7013	1063	8208	386
H(17C)	7125	1703	7167	386
H(1A)	5360	-1166	6804	90
H(15C)	5336	106	8336	103
H(15D)	5537	793	7346	103
H(16C)	7029	-583	7224	192
H(16D)	6973	-302	8437	192
H(17D)	7973	1019	7461	386
H(17E)	6995	1507	8020	386
H(17F)	6956	1262	6812	386

Table 6. Torsion angles [°]

C(5)-Mn(1)-Mn(2)-C(8)	45.6(2)	C(2)-Mn(1)-Mn(2)-C(6)	-44.5(2)
C(4)-Mn(1)-Mn(2)-C(8)	-45.4(2)	C(3)-Mn(1)-Mn(2)-C(6)	44.6(2)
C(2)-Mn(1)-Mn(2)-C(8)	136.1(2)	C(8)-Mn(2)-C(10)-N(1)	-64.8(11)
C(3)-Mn(1)-Mn(2)-C(8)	-134.7(2)	C(7)-Mn(2)-C(10)-N(1)	-154.2(11)
C(5)-Mn(1)-Mn(2)-C(7)	135.1(2)	C(9)-Mn(2)-C(10)-N(1)	26.5(11)
C(4)-Mn(1)-Mn(2)-C(7)	44.1(2)	C(6)-Mn(2)-C(10)-N(1)	116.0(11)
C(2)-Mn(1)-Mn(2)-C(7)	-134.3(2)	C(8)-Mn(2)-C(10)-N(1A)	-24.1(11)
C(3)-Mn(1)-Mn(2)-C(7)	-45.2(2)	C(7)-Mn(2)-C(10)-N(1A)	-113.5(10)
C(5)-Mn(1)-Mn(2)-C(9)	-45.8(2)	C(9)-Mn(2)-C(10)-N(1A)	67.2(11)
C(4)-Mn(1)-Mn(2)-C(9)	-136.7(2)	C(6)-Mn(2)-C(10)-N(1A)	156.7(10)
C(2)-Mn(1)-Mn(2)-C(9)	44.8(2)	C(8)-Mn(2)-C(10)-C(11)	131.8(5)
C(3)-Mn(1)-Mn(2)-C(9)	133.9(3)	C(7)-Mn(2)-C(10)-C(11)	42.5(5)
C(5)-Mn(1)-Mn(2)-C(6)	-135.1(2)	C(9)-Mn(2)-C(10)-C(11)	-136.8(5)
C(4)-Mn(1)-Mn(2)-C(6)	134.0(2)	C(6)-Mn(2)-C(10)-C(11)	-47.3(5)

N(1)-C(10)-C(11)-C(12)	-160.6(11)	C(12)-C(13)-C(14)-O(10)	-0.7(8)
N(1A)-C(10)-C(11)-C(12)	165.0(10)	C(11)-O(10)-C(14)-C(13)	1.4(8)
Mn(2)-C(10)-C(11)-C(12)	4.5(10)	C(11)-C(10)-N(1)-C(15)	178.3(13)
N(1)-C(10)-C(11)-O(10)	20.4(12)	Mn(2)-C(10)-N(1)-C(15)	13(2)
N(1A)-C(10)-C(11)-O(10)	-14.0(10)	C(10)-N(1)-C(15)-C(16)	157.6(17)
Mn(2)-C(10)-C(11)-O(10)	-174.4(4)	N(1)-C(15)-C(16)-C(17)	-174.5(16)
C(12)-C(11)-O(10)-C(14)	-1.6(7)	N(1)-C(10)-N(1A)-C(15A)	71.4(17)
C(10)-C(11)-O(10)-C(14)	177.6(5)	C(11)-C(10)-N(1A)-C(15A)	176.6(12)
O(10)-C(11)-C(12)-C(13)	1.2(7)	Mn(2)-C(10)-N(1A)-C(15A)	-24.5(18)
C(10)-C(11)-C(12)-C(13)	-177.9(6)	C(10)-N(1A)-C(15A)-C(16A)	-168.4(15)
C(11)-C(12)-C(13)-C(14)	-0.3(8)	N(1A)-C(15A)-C(16A)-C(17A)	131.1(15)

